

PROSPECTIVE STUDY ON GEOMETRICAL PARAMETERS OF HIP PROSTHESES

Teză destinată obținerii
titlului științific de doctor inginer
la
Universitatea Politehnica Timișoara
în domeniul INGINERIE MECANICĂ
de către

ing. Mircea Krepelka

Conducător științific: prof.univ.dr.ing. Liviu Marșavina
prof.univ.dr.ing. Mirela Toth-Tașcău
Referenți științifici: prof.univ.dr.ing. Mircea Cristian DUDESCU
conf.univ.dr.med. Jenel-Marian PĂTRAȘCU
prof.univ.dr.ing. Nicolae FAUR

Ziua susținerii tezei: 20.03.2015

Seriile Teze de doctorat ale UPT sunt:

- | | |
|---|--|
| 1. Automatică | 9. Inginerie Mecanică |
| 2. Chimie | 10. Știința Calculatoarelor |
| 3. Energetică | 11. Știința și Ingineria Materialelor |
| 4. Ingineria Chimică | 12. Ingineria sistemelor |
| 5. Inginerie Civilă | 13. Inginerie energetică |
| 6. Inginerie Electrică | 14. Calculatoare și tehnologia informației |
| 7. Inginerie Electronică și Telecomunicații | 15. Ingineria materialelor |
| 8. Inginerie Industrială | 16. Inginerie și Management |

Universitatea Politehnica Timișoara a inițiat seriile de mai sus în scopul diseminării expertizei, cunoștințelor și rezultatelor cercetărilor întreprinse în cadrul Școlii doctorale a universității. Seriile conțin, potrivit H.B.Ex.S Nr. 14 / 14.07.2006, tezele de doctorat susținute în universitate începând cu 1 octombrie 2006.

Copyright © Editura Politehnica – Timișoara, 2015

Această publicație este supusă prevederilor legii dreptului de autor. Multiplicarea acestei publicații, în mod integral sau în parte, traducerea, tipărirea, reutilizarea ilustrațiilor, expunerea, radiodifuzarea, reproducerea pe microfilme sau în orice altă formă este permisă numai cu respectarea prevederilor Legii române a dreptului de autor în vigoare și permisiunea pentru utilizare obținută în scris din partea Universității Politehnica Timișoara. Toate încălcările acestor drepturi vor fi penalizate potrivit Legii române a drepturilor de autor.

România, 300159 Timișoara, Bd. Republicii 9,
Tel./fax 0256 403823
e-mail: editura@edipol.upt.ro

Cuvânt înainte

Teza de doctorat a fost elaborată pe parcursul activității mele în cadrul Departamentului de Mecanică și Rezistența Materialelor al Universității Politehnica Timișoara.

Mulțumiri deosebite se cuvin conducătorului de doctorat, domnul prof.dr.ing. Liviu MARȘAVINA pentru încrederea pe care mi-a acordat-o în demersul cercetărilor asociate prezentei teze, reușind, în același timp, să mă ghideze corect și eficient, spre finalizarea tezei de doctorat.

Doresc să mulțumesc membrilor comisiei de îndrumare, prof.dr.ing. Liviu BERETEU, ș.l.dr.ing. Lucian RUSU și as.dr.ing. Dan Ioan STOIA pentru sugestiile competente care au dus la rezolvarea problemelor apărute pe parcursul studiilor și cercetărilor efectuate în vederea elaborării tezei de doctorat.

De asemenea, mulțumesc colegilor din colectivul Centrului de Cercetare în Inginerie Medicală, pentru nenumăratele discuții și consultări, cât și pentru atmosfera prietenoasă creată. Deasemenea, doresc să-i mulțumesc domnului Ing. Marinel COJOCAR pentru promptitudinea și profesionalismul cu care m-a ajutat în realizarea nenumăratelor componente necesare testărilor experimentale.

Adresez sincere mulțumiri membrilor comisiei de doctorat, domnului prof.dr.ing. Mircea Cristian DUDESCU, domnului conf.dr.med. Jenel-Marian PĂTRAȘCU și domnului prof.dr.ing. Nicolae FAUR pentru răbdarea cu care au analizat lucrarea de față precum și pentru sugestiile formulate.

Un cuvânt de suflet adresez în amintirea doamnei prof.dr.ing. Mirela TOTH-TAȘCĂU care, cu mult tact pedagogic, competență profesională și înțelegere, și-a adus un aport esențial în formarea mea de-a lungul acestor ani atât pe plan profesional cât și pe plan uman.

În mod categoric, finalizarea tezei de doctorat nu ar fi fost posibilă fără ajutorul și sprijinul familiei mele, căreia îi mulțumesc pentru înțelegerea, sprijinul moral și răbdarea manifestate constant, ajutându-mă să duc la bun sfârșit această teză.

Timișoara, martie 2014

Mircea KREPELKA

Familiei

Krepelka, Mircea

Prospective study on geometrical parameters of hip prostheses

Teze de doctorat ale UPT, Seria 9, Nr. 159, Editura Politehnica, 2015, 129 pagini, 94 figuri, 19 tabele.

Cuvinte cheie: hip replacement, acetabular implant, gait analysis, finite element, DOE, impaction.

Rezumat,

Artroplastia de șold este o intervenție chirurgicală ortopedică ce are drept scop restabilirea funcționalității articulației coxofemorale deteriorate. Mai mulți factori pot fi implicați în eșecul protezei, inclusiv o dimensionare necorespunzătoare a protezei, orientare spațială și fixare inițială nesatisfăcătoare, uzură excesivă, cât și remodelarea osoasă. Pornind de la aceste considerente, teza de doctorat propune atât cercetări teoretice cât și aplicative în domeniul protezelor coxofemorale, îmbinând specificul proiectării asistate de calculator cu specificul utilizării calculatorului în domeniul medical pentru prelucrarea de informații și imagini. Studiile prezintă un spectru larg de parametrii geometrici, fiind concentrate pe proiectarea de modele de elemente finite și metode de încercare mecanice pentru evaluarea influenței acestor factori, ca un instrument preoperator de predicție a performanței componentelor acetabulare necimentate.

TABLE OF CONTENTS

INTRODUCTION	14
1. ASPECTS OF HIP JOINT STRUCTURE, PATHOLOGY AND FUNCTION.....	20
1.1. Bony structure.....	21
1.1.1. Pelvic bone	21
1.1.2. Femur	23
1.2. Capsule, ligaments and muscles	25
1.3. Hip joint disorders.....	27
1.3.1. Joint pathology.....	27
1.3.2. Hip fractures.....	31
1.4. Hip joint biomechanics.....	34
1.4.1. Hip joint mobility.....	34
1.4.2. Gait cycle.....	36
2. TOTAL HIP REPLACEMENT OVERVIEW	38
2.1. Bearing surface	39
2.2. Fixation.....	41
2.2.1. Cemented THP	41
2.2.2. Cementless THP	45
2.3. THR failure.....	53
3. RELIABILITY OF GAIT PARAMETERS IN GAIT ANALYSIS	55
3.1. Methods.....	56
3.2. Data analysis.....	59
3.3. Results and discussions	59
3.4. Concluding remarks	63
4. COMPUTATIONAL STUDIES ON THE EFFECT OF GEOMETRICAL PARAMETERS ON IMPLANT PERFORMANCE.....	65
4.1. Development of the hip joint model.....	67
4.1.1. Three-dimensional model reconstruction	67
4.1.2. Finite element model	71
4.2. Optimization of acetabular component orientation	73

4.2.1. Methods.....	73
4.2.2. Experimental design	77
4.2.3. Results.....	78
4.2.4. Concluding remarks	81
4.3. Influence of acetabular liner design.....	83
4.3.1. Methods.....	83
4.3.2. Results.....	88
4.3.3. Concluding remarks	91
5. MECHANICAL TESTING OF ACETABULAR IMPLANTS.....	92
5.1. Introduction.....	92
5.2. Validation of polyurethane foams for implant testing	93
5.2.1. Methods.....	94
5.2.2. Determination of foam density.....	95
5.2.3. Determination of Compressive Strength	96
5.2.4. Determination of Screw Pullout Strength	99
5.2.5. Concluding remarks	104
5.3. Mechanical testing of an oversized acetabular component.....	104
5.3.1. Materials and methods	105
5.3.2. Impaction	106
5.3.3. Primary stability	108
5.3.4. Results and discussions	109
5.3.5. Concluding remarks	112
6. CONCLUSIONS AND FUTURE RESEARCH.....	114
6.1. Conclusions and personal contributions.....	115
6.2. Future development.....	119
6.3. Valorisation of research results	120
REFERENCES.....	127

List of figures

Figure 1. Romanian hip arthroplasty annual statistics 2001-2014.....	14
Figure 2. National hip joint surgery statistics by fixation type	15
Figure 3. Anatomy of the hip joint.....	20
Figure 4. Bony structure of the pelvis	21
Figure 5. Acetabular bony anatomy	22
Figure 6. Anatomy of the femur, anterior view.....	24
Figure 7. Angle of femoral neck inclination	25
Figure 8. Comparison of normal hip joint and a joint with osteoarthritis	28
Figure 9. Geometry of the normal hip, cam, pincer and mixed impingement.....	29
Figure 10. Types of misalignments of femur head into the socket in hip dysplasia .	30
Figure 11. Avascular necrosis of the femoral head.....	31
Figure 12. Most common proximal femur fracture types.....	32
Figure 13. Elementary fracture Letournel classification	33
Figure 14. Anatomical planes definition.....	34
Figure 15. Lower limb hip movements	35
Figure 16. Human normal gait and phase duration	36
Figure 17. Range of motion during one cycle of normal walking	37
Figure 18. Components of THP	38
Figure 19. Most common THR bearing combinations.....	40
Figure 20. Method of thermal processing of Oxinium femoral heads	40
Figure 21. Charnley cemented THP	41
Figure 22. Section view representing a cemented stem and cement penetration ...	42
Figure 23. Cemented cup designs.	43
Figure 24. Examples of taper stems	43
Figure 25. Charnley Elite Plus stem with centralizer.....	44
Figure 26. Biomet Olympia anatomical stem.....	44
Figure 27. Biomet femoral pressurizer and OptiPlug distal plug.....	45
Figure 28. Microscopic view of several osseointegration surface treatments.....	46
Figure 29. Hydroxyapatite nanoparticles	46
Figure 30. Tapered stems	47
Figure 31. DePuy anatomic medullary locking distal fixation stem	48
Figure 32. Most commonly used metaphyseal fixation stems	48
Figure 33. Cementless acetabular shells with supplementary fixation	49
Figure 34. Modular acetabular component.....	50
Figure 35. Zimmer elliptical Trabecular Metal Modular Acetabular System	51
Figure 36. Components of hip resurfacing prosthesis	52
Figure 37. Unipolar and bipolar hemiarthroplasty implants	52
Figure 38. Zebris CMS-HS Gait analysis system	57
Figure 39. Geometrical model and movement graphs in Zebris WinGait software ..	57
Figure 40. Detail of the radiographic method.	58
Figure 41. Initial angular variation profiles for hip flexion-extension	60
Figure 42. Initial angular variation profiles for hip rotation	60

Figure 43. Initial angular variation profiles for hip adduction-abduction.....	60
Figure 44. Angular flexion-extension variation profiles for processed data series...	62
Figure 45. Angular rotation variation profiles for processed data series.....	62
Figure 46. Angular adduction-abduction variation profiles for processed data series	62
Figure 47. Selection of areas of interest in Mimics Software	68
Figure 48. Manual contour and cavity fill.....	68
Figure 49. Segmentation of the femur	69
Figure 50. Segmentation of the hemipelvis.....	69
Figure 51. Hemipelvic 3D model before and after smoothing and triangle reduction	70
Figure 52. Completed 3D reconstruction model of the hemipelvis.....	71
Figure 53. Necessary steps for FEA	72
Figure 54. Meshing detail.....	74
Figure 55. Definition of boundary conditions of the hemi-pelvis.....	75
Figure 56. Lateral view of the prosthetic hip model geometry and section view of the cup/liner assembly.....	76
Figure 57. Force application position and its component coordinates	76
Figure 58. Anteroposterior pelvic view showing the inclination/abduction angle and axial view revealing the anterior rotation/anteversion angle	77
Figure 59. Single block experimental matrix. Caption from StatGraphics software.	78
Figure 60. Normal probability plot.....	79
Figure 61. The main effect plot.....	80
Figure 62. Graphical representation of the Response surface	81
Figure 63. Geometric profile details of the proposed liner models: 170° design and 165° design.....	84
Figure 64. AP view of the orientation plane and exploded view of the hip-implant assembly	85
Figure 65. Bergmann's et al. graphical representation of hip joint peak loads during daily activities.....	86
Figure 66. Force application on the finite element model.....	87
Figure 67. Boundary areas of the fully constrained hemipelvic model.....	87
Figure 68. Contact pressure distributions in the acetabulum under loads corresponding to normal walking, walking upstairs and stair descending	88
Figure 69. Equivalent von Mises stress distribution in the prosthetic joint	89
Figure 70. Graphical representation of the FE simulation results	90
Figure 71. Average peak pressures for the investigated designs.....	90
Figure 73. Microstructures of cancellous bone and polyurethane foam.	93
Figure 74. PU foam blocks prepared for density testing.....	95
Figure 75. Kern PRJ620-3M Laboratory balance	95
Figure 79. Foam block preparation using a milling machine	97
Figure 76. Experimental setup for compression testing	97
Figure 77. Load-deflection curve for Grade 15 PU foam	98
Figure 78. Load-deflection curve for Grade 20 PU foam	99

Figure 80. Orthopedic screws used in mechanical testing	100
Figure 81. 2D drawing of the designed screw pullout fixture	100
Figure 82. Test apparatus for screw pullout.....	101
Figure 83. Screw pullout load-displacement curves for grade 15 foam	102
Figure 84. Screw pullout load-displacement curves for grade 20 foam	103
Figure 85. Mode of failure for the medical screws.....	103
Figure 86. The Atlas acetabular shell	105
Figure 87. Radiographic image of an Atlas acetabular component	105
Figure 88. Test block specimen with prepared acetabular cavity	106
Figure 89. Experimental setup for impaction testing	107
Figure 90. Test setup for rim edge loading	108
Figure 91. Representation of cup failure.....	109
Figure 92. Response surface plot for Impaction	110
Figure 93. Response surface plot for failure.....	111
Figure 94. The estimated response surface plot	111

List of tables

Table 1. Primary muscle groups and their action	27
Table 2. AO classification of acetabular fractures	33
Table 3. Hip motions average amplitudes	35
Table 4. Main advantages and disadvantages of common hip prosthesis bearing materials	40
Table 5. Hip gait abnormalities and their underlying cause	56
Table 6. Analysis results: Pearson's correlation, ICC and Bland-Altman statistics ..	61
Table 7. Analysis results: Pearson's correlation, ICC and Bland-Altman statistics ..	63
Table 8. Anatomic position and characteristic of restraining areas	75
Table 9. Material properties of the assembly bone-implant	77
Table 10. Simulation results for the specified scenarios	79
Table 11. Correlation matrix for the selected variables showing Correlations, Sample Size and P-Value	80
Table 12. Meshing and mass details of the assembly components	85
Table 13. Details of the loading forces	86
Table 14. Technical properties of the two selected PU foams.	94
Table 15. ASTM grade designation with nominal densities	94
Table 16. Results of the apparent density measurements	96
Table 17. Compressive strength and modulus results for the tested specimens	99
Table 18. Screw pullout strength test results	102
Table 19. Mean peak impaction and failure loads for the different tested combinations	109

List of abbreviations

3D	Three Dimensional
ANOVA	Analysis Of Variance
ASTM	American Society for Testing and Materials
CAD	Computer Aided Design
CT	Computed Tomography
DOE	Design Of Experiments
FEA	Finite Element Analysis
FEM	Finite Element Method
GT	Greater Trochanter
HJC	Hip Joint Center
ICC	Intraclass Correlation Coefficient
OA	Osteoarthritis
PE	Polyethylene
PU	Polyurethane
ROM	Range Of Motion
THA	Total hip arthroplasty
THP	Total hip prosthesis
THR	Total hip replacement
TI	Titanium

Abstract

The hip joint represents the primary connection between the lower limbs and the upper body, and is designed to be a stable, weight bearing joint, and plays an extremely important role in locomotion. The hip joint is a ball and socket joint, the femoral head articulates with the acetabulum, allowing smooth range of motion in multiple planes. During daily activities the human hip joint undergoes cyclic loadings that develop forces three to five times body weight. This repetitive loading of the hip joint may lead to degeneration of the surrounding articular cartilage and cortical bone resulting in bone defects and osteoarthritis.

Total hip arthroplasty involves an artificial hip joint that mediates the issue of joint degeneration by completely replacing the femoral and acetabular components of the deteriorated hip joint, relieving pain and restoring normal hip function, therefore improving the quality of life.

The hip joint center is a fundamental landmark in the identification of lower limb mechanical axis therefore the thesis describes the methods used for determination of hip joint center, the apparatus and methodology employed in the three-dimensional kinematical analysis. Further data analysis consisted of descriptive statistics were used as estimates of reliability of hip joint center estimation methods. A statistical method was developed to correct the initial gait data in order to allow for a better estimation using non-invasive methods.

Considering the incidence of aseptic loosening caused by stress shielding, a 3D finite element model suitable for patient-specific analysis was developed and used for computational simulations in order to help quantify the effect of factors such as component orientation and liner design on the magnitude and pattern of contact stresses at the cup-bone interface. In addition to 3D reconstruction and FE simulation, the study employs experimental design in order to identify the most significant factors for acetabular component behavior and generate a novel mathematical method of implant orientation optimization allowing for ideal acetabular cup positioning.

Furthermore, the biomechanical role of the acetabular liner chamfer was described using three-dimensional mathematical models loaded to simulate daily activities. The results of these studies suggest the risk of adaptive periprosthetic bone remodeling can be reduced with improved component positioning and use of chamfered design liners.

Finally, an experimental study was developed to evaluate the amount of impaction force needed and degree of primary stability achieved by press-fitting of the acetabular component during total hip replacement surgery considering the variability of bone quality. Polyurethane foams were tested in order to validate them as bone substitutes for mechanical testing.

The forces necessary for impaction of the cup to a complete seating were investigated under uniaxial compression test and analyzed to define the effects of degree of underreaming and bone quality. Subsequently, primary stability of each of the previously fitted implants was investigated by measuring the peak failure load in a tangential lever-out test method as a measure of stability against loads that cause out of plane rotations. The results suggest that the amount of oversizing of the acetabular component is beneficial for the primary stability as long as the quality of

the bony substrate is not optimal and the increase of primary fixation overcomes the risk of fractures caused by high impaction forces necessary for proper seating. Thus, the amount of underreaming should be adjusted according to the bone quality of each individual patient.

Additionally, using DOE response surface plots, an optimization design was created that would aid in the choice of optimal setting to minimize the impaction load while maximizing the edge resistance load.

The research presents methodologies to evaluate implant performance when various geometrical parameters are subjected to uncertainties. The results obtained provide details for application in the preoperative planning and also design considerations for an optimal acetabular implant to improve biomechanical performance, with the aim of achieving more stable fixations and increased survivorship.

INTRODUCTION

A Total Hip Prosthesis (THP) is an artificial hip joint that mediates the issue of joint degeneration by completely replacing the femoral and acetabular components of the deteriorated hip joint.

The overall goal of prosthetic reconstruction is to replace a degenerated joint and restore patient's mobility. In order to achieve it, the physiological hip center of rotation must be restored and implants must provide good initial and long-term stability.

Total hip replacement gives reasonably good results in elderly inactive people, but the long-term results appear to be less promising in active young people.

The current trend of performing Total Hip Replacements (THR) on younger patients will contribute to higher demands on hip replacements. The implants will have to endure forces of greater magnitude over longer periods of time causing an increasing chance of revision surgery. Extensive surgery is required for a hip replacement causing considerable strain to the patients, therefore the longevity of the implant is very important. Therefore, prolonging the life of THP is represents the motivation and main goal of this study.

Advances in design, prosthesis materials and surgical technique have improved the wear performance of implants. However, an ageing population combined with younger more active patients undergoing joint replacement surgery suggests that osteolysis and subsequent prosthesis loosening will continue to be the major complication of THR.

Studying the status of hip replacement in Romania, in relation with the ageing of the society, we found that, according to the Romanian Arthroplasty Register, the number of replacement surgeries grows significantly every year [1].

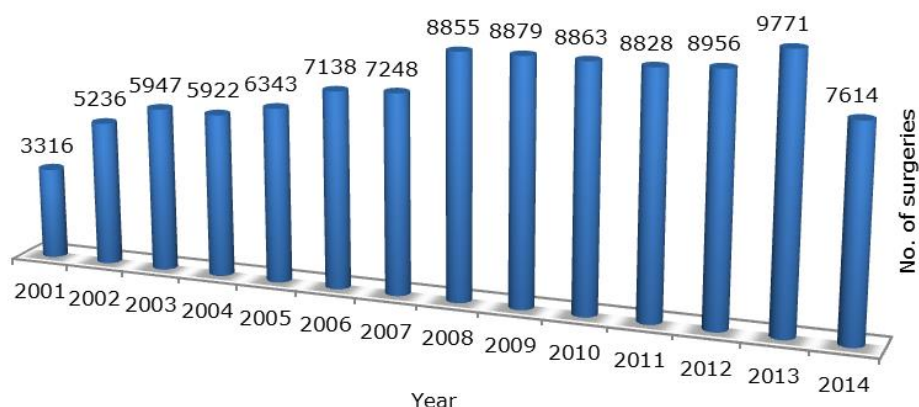


Figure 1. Romanian hip arthroplasty annual statistics 2001-2014

Secure fixation of THP components can be achieved either by using a cemented or acementless (uncemented) design.

Cemented total hip components imply the use polymethylmethacrylate (PMMA) commonly known as bone cement in order to fix the prosthesis to the underlying bone. Meanwhile, cementless designs accomplish fixation by means of mechanical interlock (press fit) and bone ingrowth, using a roughened, porous or coated contact bone surface.

In some cases, only one of the components is cemented and the other is cementless. This type of THP is called a hybrid total hip replacement.

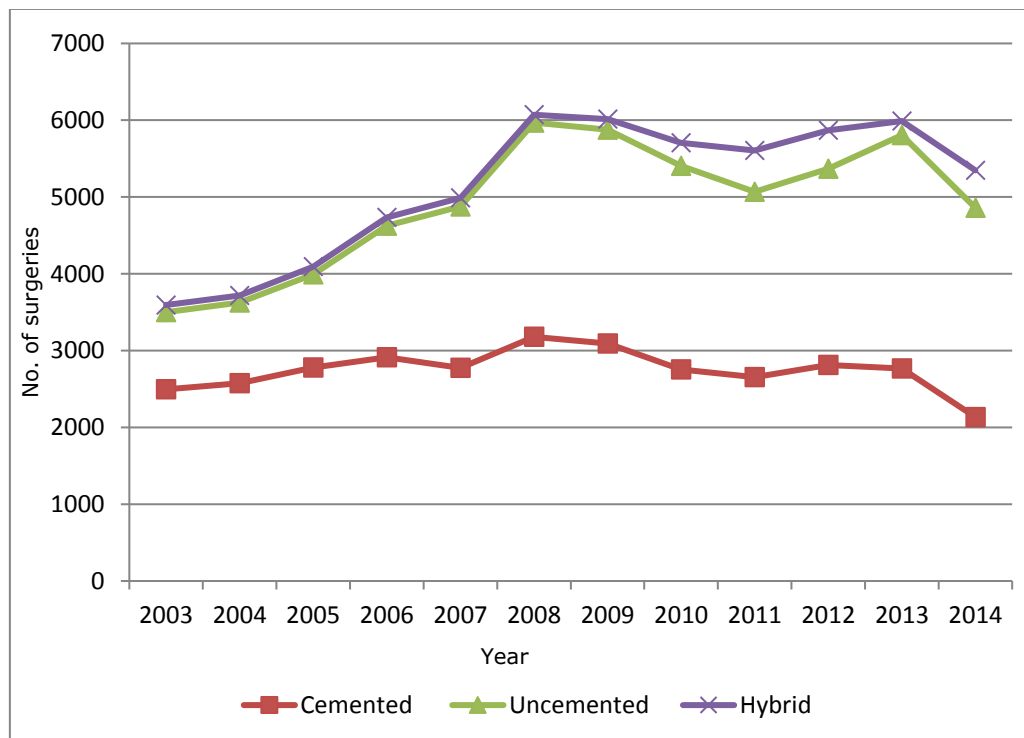


Figure 2. National hip joint surgery statistics by fixation type [1]

As there is no standard method for selecting the most appropriate implant for a particular patient, surgeons usually base their choice of implants on the age, bone quality and level of activity of the patient.

This thesis addresses many aspects concerning the stability of cementless acetabular reconstruction, as in 2013 approximately 47% of THR in Romania were cementless, as highlighted in Figure 2.

The effects of numerous surgical and implant-related factors were studied, which may ultimately affect implant performance and survival.

In order to assess the outcome of rehabilitation programs, clinical interventions or disease progression, reliable outcome measures are essential. In the case of kinematic gait analysis, reliability refers to the amount of change in angular displacements that is dependent to measurement error and not actual improvement or deterioration of the gait.

Clinical success of hip replacement depends upon achieving an adequate initial fixation and maintaining the fixation for a long term, secondary fixation. As the incidence of hip replacement in younger and more active patients is increasing, prolonging the life of hip replacements becomes even more important.

Although hip replacement is a very successful procedure, one of the main reasons of THR failure is represented by aseptic loosening of the acetabular component.

Failure of cementless THR can be caused by poor primary or secondary stability of an implant or by extensive bone resorption. Even though a good primary and secondary stability of cementless implant is assured, it may not be sufficient for long term implant survival.

After THA, due to the changes in load distribution, bone tissue will be stress-shielded and will adapt to the new mechanical conditions.

As a dynamic tissue, bone density is maintained by mechanical stimuli and, in accordance to Wolff's law, an adaptive remodeling process will start in the underlying bone, process caused by the reduction of stimuli leading to osteoclast resorption of bone to adapt to the new biomechanical environment. This implies external remodeling (geometry) and also internal remodeling (density adaptation) until the mechanical stimulus is normalized. This remodeling process is known as retroacetabular stress shielding and may impair the survival of prosthetic components [2], [3].

Another critical issue in the performance of THP is how well positioned the acetabular implant is within the acetabulum, since improper cup positioning may lead to reduced range of motion, impingement, increased polyethylene wear and a higher risk of dislocation [4], [5], [6].

Previous studies have addressed this issue by determining dislocation rates with respect to acetabular cup orientation. However, no attempts have been made to analyze the effects of cup orientation on stress distribution within the peri-acetabular underlying bone.

In order to reduce the incidence of stress shielding, more research is needed to better understand the factors which contribute to this effect. To address the lack of understanding, this thesis evaluates the possibility of acetabular cup orientation, design and amount of oversize as contributors to poor stress distribution to the bone tissue surrounding the acetabular component and stress shielding.

Experimental studies utilizing cadaveric specimens or bone substitutes and finite element analysis studies are recognized as substantial adjuvant for the clinical investigation of cup fixation. In the present thesis, research using a finite element model suitable for patient-specific analysis was developed from clinical imaging investigation methods. The use of a finite element model helps to quantify the effect of various factors including the considered geometrical parameters.

In summary, this thesis shows a broad spectrum of THR geometrical parameters related to the loosening of uncemented acetabular components. Studies presented in this thesis focus on designing finite element models and mechanical test methods to assess influence of these factors as a tool for pre-clinical prediction of implant survival.

Research goals

The thesis represents a sequel of the research initiated during undergraduate and dissertation work due to the high incidence of hip replacement and also its importance in restoring joint mobility and reduces pain.

Analysis of this problem has led to the study of aspects relating to the design, theoretical and experimental analysis of the acetabular component.

The specific objectives of this research are to realize a comprehensive study regarding the current state of research on:

- Anatomy and pathology of the hip joint;
- The main types of hip prosthesis;
- Hip joint biomechanics, gait analysis;
- Evaluation of the geometrical parameters of the components of hip prostheses and analyze their importance in the prosthesis performance through the use of 3D joint reconstruction, CT / MRI, CAD modeling techniques, and design of experiments.

To assess implant performance, the following factors were considered:

- effect of implant spatial orientation and acetabular liner design on periprosthetic stress distribution, as the alteration of the natural stress pattern leads to bone remodeling and thus, implant loosening;
- bone strain related to impaction of the cup, as excessive bone strain can result in bone fracture;
- primary stability, as it is related with cup geometry, impaction force and bone quality.

The effect of variability of the aforementioned factors is difficult to predict. Thus, in the present thesis, computational methods are employed to assess the effect of multiple variables on the performance of the cementless acetabular replacement.

The computational studies used finite element analysis (FEA) and probabilistic methods to assess the implant performance. Afterwards, experimental studies were carried out on selected implants in order to add consistency to the computational results.

Research activities are focused on theoretical and applied studies in the hip joint prosthesis, the main research objective being to provide a detailed background of the effect and geometrical parameter dependence of acetabular component performance and survivorship for the development of a new model of the acetabular component of hip prostheses.

Static and dynamic biomechanical analysis of anatomic pelvis-femur system in order to determine the loads developed in hip joint during normal gait, assuming:

- An analysis of bipedal locomotion by identifying the kinematic and dynamic parameters;
- Determination of the importance of anatomic landmarks identification and hip joint center estimation methods on the gait parameters during gait analysis.

Design and analysis of acetabular components:

- Determine and analyze parameters influencing the performance characteristics of acetabular components (spatial orientation, shape, material, implantation required force, fixation capability) that can cause the failure of the prosthesis;
- Design of experiments, statistical description and optimization of design parameters for the design of new models of acetabular components.

Layout of the thesis

The thesis treats the significant aspects of the hip joint biomechanics such as the influence of geometrical parameters, failure causes and performance of the acetabular components of the hip prostheses with the aim to improve their survivorship rate. Being able to predict the optimum combination of the studied geometrical factors is potentially useful for surgeons, as it could aid in preoperative planning, namely choice of implant size, design and spatial orientation.

The thesis is organized as follows:

Chapter 1: Aspects of hip joint structure, pathology and function presents a review on anatomical and biomechanical aspects of the hip joint. This chapter is divided into three main sections:

- The first section represents a literature review of the hip joint structure and function;
- The next section focuses on the main pathological and traumatic disorders causing the necessity of replacing the hip;
- The third section reviews the hip joint biomechanics, focusing on joint mobility and human gait cycle.

Chapter 2: Total hip replacement overview represents a study of the evolution of hip replacement surgery. It describes the most common types of prosthesis classified based on the materials used for bearing surface and fixation mode. Proposed research addresses the clinically relevant issue of implant failure following total hip replacement, the main post-operative failure reasons are listed in this section along and a review of the literature related to their incidence.

Chapter 3: Reliability of gait parameters in gait analysis investigates the effect of anatomic landmarks estimation methods on the angular parameters during gait analysis.

The study describes the methods used for determination of hip joint center, the apparatus and methodology employed in the three-dimensional kinematical analysis.

Further data analysis consisted of descriptive statistics was used to characterize the gait cycle and estimate of reliability of hip joint center estimation methods. From the resulted data, a straightforward statistical method was developed to correct the initial gait data in order to allow for a better estimation using non-invasive methods.

Chapter 4: Computational studies on the effect of geometrical parameters on implant performance describes the materials used and the methodology employed for the computational studies.

Optimizing the acetabular component of total hip prostheses represents a highly complex task where many of the individual design factors have massive impact on the system. The combined effect of variability of the geometrical factors is difficult to predict, thus separate computational models were needed to assess prospective behavior.

The first part of the study describes the steps taken to achieve the assembly models: 3D reconstruction of the hip joint model using programs such as Mimics and SolidWorks.

Secondly, the study explains the steps used to generate a specific finite element models when the implant is positioned in different orientations defined by inclination and anteversion of the acetabular component. The prosthetic hip joint has been simulated for three separate cup orientations. Choice of materials and the applied total hip joint forces have been established from literature.

In addition to 3D reconstruction and FE simulation, the study employs experimental design (DOE) in order to identify the most significant factors for acetabular component behavior and predict the best configuration of acetabular spatial orientation angles within the constraints of the Lewinnek's safe zone in order to minimize peak contact pressures.

In the third part of the study, using finite element analysis, two designs of chamfered acetabular liners were compared with a full hemispherical design. Von Mises equivalent stress and contact pressures of at the bone-implant interface were analyzed assessing the effect three different loading scenarios to highlighting the changes caused by implanting in their pattern and magnitude.

Chapter 5: Mechanical testing of acetabular implants describes an experimental method to assess the effect of the degree of interference fit and bone quality to the amount of primary fixation.

With the intention to provide a consistent and uniform material with properties similar to those of human cancellous, the first section describes the basic material properties of polyurethane foams, the methodology and physical requirements needed to validate them as bone substitutes for mechanical testing. Two artificial bone models were chosen to simulate normal and high quality cancellous bone.

In the second part of the study, the material and methodology for the impaction of an oversized acetabular component are described. This consisted on the artificial bone blocks being reamed for different amounts of press fit of an Atlas uncemented acetabular component. The forces necessary for impaction of the cup to a complete seating were recorded and analyzed to define the effects of degree of underreaming and bone quality.

Subsequently, primary stability of the previously fitted implants was determined in a lever-out test setup to analyze the dependence of stability against loads that cause out of plane rotations.

Chapter 6: Conclusions and future research contains the discussion and conclusion of this thesis, presents the outlines the personal contribution and how this present research can be used in the future.

1. ASPECTS OF HIP JOINT STRUCTURE, PATHOLOGY AND FUNCTION

The hip joint (*articulatio coxae*) represents the primary connection between the lower limbs and the upper body, and is designed to be a stable, multi-axial, weight bearing joint.

It is formed by the articulation of the spherical head of the femur and the concave acetabulum of the pelvis being referred to as a spheroidal or ball and socket type joint. The head of the femur fits into the acetabulum where it is held firmly by a fibrous, flexible synovial capsule, allowing the leg a considerable range of motion but prohibiting the proximal femur from dislocating. The femur and acetabulum are covered with a thin layer of cartilage that provides load absorption and smooth articulation.

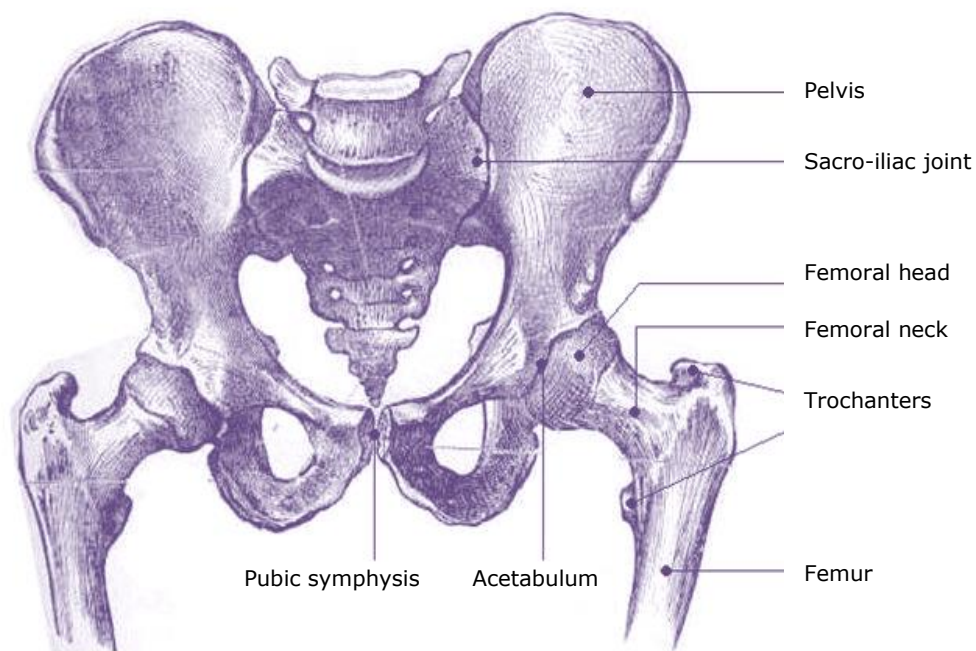


Figure 3. Anatomy of the hip joint

Muscles and cartilages provide stability and actuation forces for movements in all three planes: coronal (flexion-extension), sagittal (abduction-adduction), transverse (internal-external rotation) with respect to the pelvis.

1.1. Bony structure

1.1.1. Pelvic bone

The bony pelvis or pelvic skeleton is the part of the skeleton that connects the sacrum region of the spine to the femurs. The pelvis is composed of the sacrum and the coccyx, having two symmetrical hip bones, hemi-pelvis, one on the right and one on the left side of the body joined together at the pubic symphysis by a fibrous cartilage and at the sacroiliac joint, formed between the auricular surfaces of the sacrum and the two hip bones.

Its primary function is, together with a number of muscles and ligaments, to transfer the weight and energy of the upper body to the lower skeleton during standing and locomotion. In order to withstand the high loads, the pelvis has a sandwich structure with a cortical bone shell filled with cancellous bone.

The pelvis (coxal bone) is a large, flattened, irregularly shaped bone that forms a girdle which protects the digestive and female reproductive organs.

It is formed from three parts, referred to as the innominate bones, the ilium, ischium, and pubis, which are separate in children, but are fused into one bone by adulthood, the union of the three parts forming a large cup-shaped articular cavity, called the acetabulum.

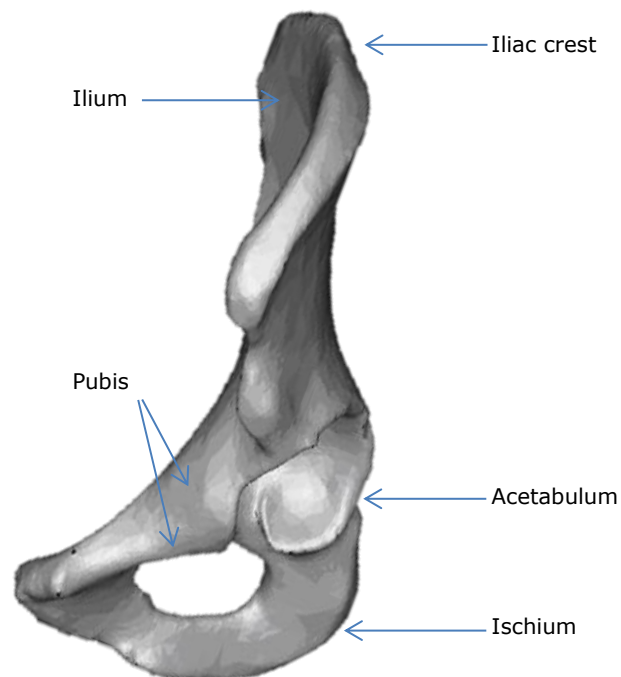


Figure 4. Bony structure of the pelvis

The **acetabulum** is the cup-shaped socket on the lateral aspect of the pelvis, which articulates with the head of the femur to form the hip joint. The bony structure of the acetabulum is formed from by fusion of the ilium, ischium, and pubis [7]. The ischium provides the lower and side boundary of the acetabulum, while the ilium forms the upper boundary. The rest of the acetabulum bony structure is formed by the pubis. The weight-bearing surface of the acetabulum is the dome or roof.

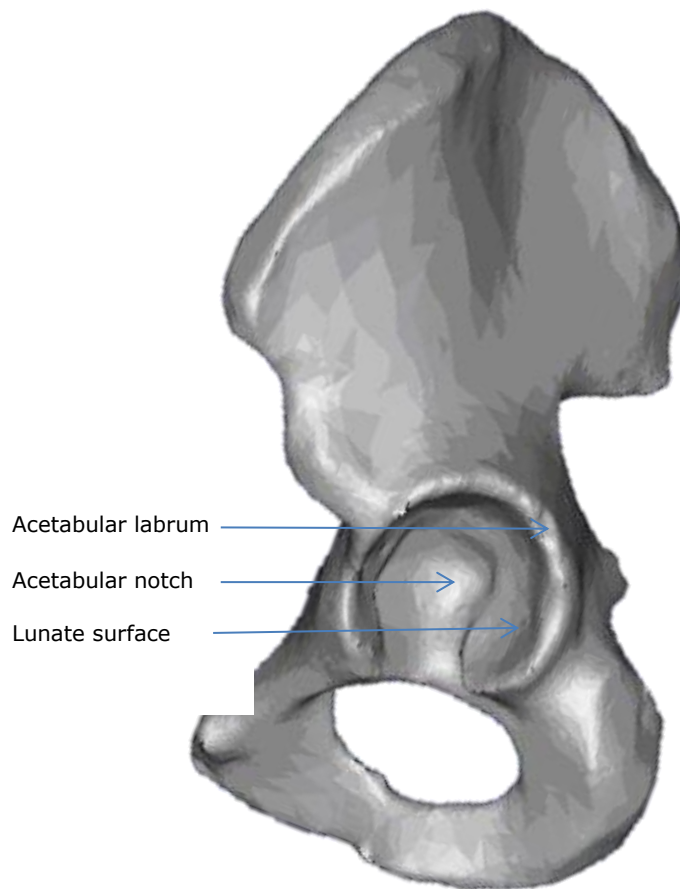


Figure 5. Acetabular bony anatomy

Anatomical orientation utilizes physical bony land-marks to define the geometry of the acetabulum. Acetabular orientation is generally defined by two angles: inclination and anteversion [8].

The anatomical inclination is defined as the angle between the acetabular axis and the longitudinal axis, whilst the anteversion angle as angle between the transverse and the acetabular axis projected on the transverse plane. With neutral pelvic alignment, anatomic acetabular inclination angle values range between 39 and 54 degrees and anatomic anteversion range from 15 to 22 degrees [9].

The anteversion is directly affected by the amount of pelvic tilt or rotation in the sagittal plane.

Its articular surface is represented by a curved, horseshoe shaped layer of articulating hyaline cartilage with a thickness ranging from 1.2 to 2.3 mm in normal adults, known as the lunate surface [10]. The non-articular floor is referred as the acetabular fossa, a rough circular depression at the bottom of the cavity, continuous with the acetabular notch.

The acetabulum is bounded by a prominent uneven rim, which is thick and strong on the superior part, but deficient on the inferior part at the acetabular notch. The rim serves as an attachment for a fibrocartilaginous margin called the acetabular labrum, which deepens the surface to create a deeper socket for the junction with the femoral head. The transverse acetabular ligament is located along the inferior aspect of the acetabulum preventing the femoral head from moving inferiorly by deepening the acetabulum inferiorly.

As stated above, the **ilium** forms the superior part of the acetabulum and it is the largest part of the hip bone, providing a little less than two-fifths of the structure of the acetabulum. It is a large, flattened bone, having a large arched crest along its superior border, terminating at both ends as the anterior superior and posterior superior spines. These form the prominence of the hip acting as important anatomical landmark and provide attachment sites for many muscles.

Posteriorly, the ilium has a rough surface providing attachment for the sacrum at the sacroiliac joint while anteriorly it connects to the ischium.

The **ischium** represents the inferior aspect of the pelvis. The ischium is divided into the body, superior ramus of the ischium, and inferior ramus of the ischium. The superior part of the ischium takes part in forming the lateral and inferior aspects of the acetabulum, whilst its inferior parts forms, along with the pubis, the obturator foramen. The **obturator foramen** is a large opening formed by both the ischium and the pubis to allow the passage of major blood vessels and nerves to the legs and feet.

The **pubis** forms the medial part of the hip bone and contributes to the anterior part of the acetabulum. The pubis bone can be devised into a flat body, a superior and an inferior ramus.

From the acetabulum, the pubis extends medial and downward and articulates in the middle line with the pubis bone of the opposite side at the pubic symphysis, forming the front of the pelvis and supporting the external organs of reproduction. The anterosuperior border of the joined pubic bones forms the pubic crest. The pubic crest has small projections at the lateral ends called pubic tubercles, where the inguinal ligaments attach medially, which are extremely important landmarks of the inguinal regions.

1.1.2. Femur

The femoral bone (thigh bone) is the longest and strongest bone in the human skeleton [11]. Like other long bones, it is divisible into a cortical body (shaft) and two extremities (epiphyses), filled with cancellous bone. Proximally, it consists of a head and a neck, two condyles (medial and lateral) distally and the body is comprised of a diaphysis.

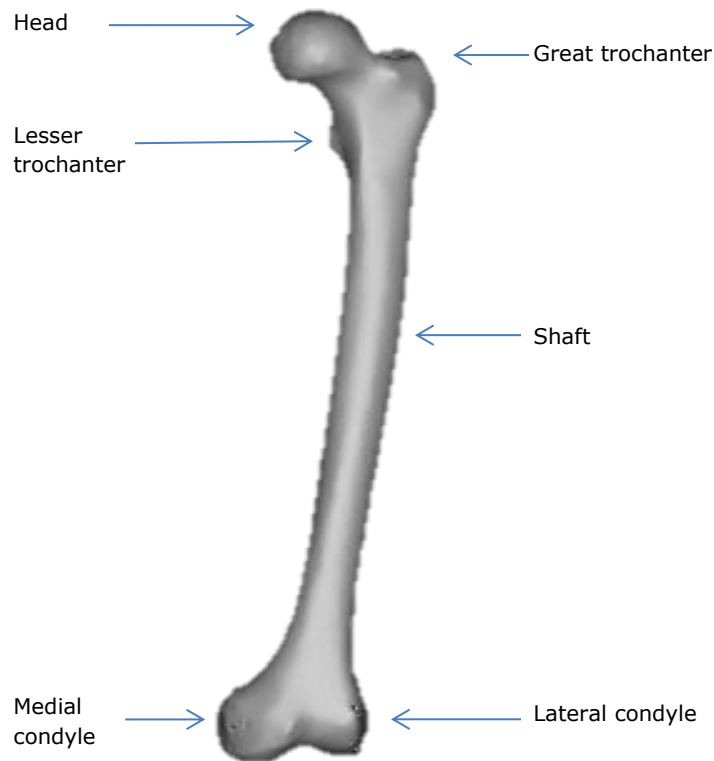


Figure 6. Anatomy of the femur, anterior view

The **shaft** of femur is almost cylindrical in form, while the proximal femur that contributes in forming the hip joint is irregular in shape, consisting of a spherical head, neck and two bony protrusions, the greater and lesser trochanters.

The **head of the femur** is approximately spherical in shape and serves as the ball of the ball and socket joint. It has a smooth surface, being coated with articular hyaline cartilage, except for a small depression on the medial surface referred to as the femoral head fovea (fovea capitis femoris), that gives attachment for the ligamentum teres. The normal thickness of femoral cartilage for an adult ranges from 1.0 to 2.5 mm [10].

The femoral head and greater trochanter are filled with cancellous bone down to the level of the lesser trochanter.

The head of the femur connects to the femoral shaft at an angle called angle of inclination. The angle of inclination is the angle of the femoral neck in the frontal plane. This angle normally varies between 90 degrees and 160 degrees, with an average of approximately 127-135 degrees, greater during childhood and adolescence, but gradually recedes to that seen in adults.

If, in adulthood, the femoral angle of inclination is less than 120° the resulting deformity is called coxa vara (varus), whilst when the angle is above 140° the condition is termed coxa valga (valgus) [12], [13].

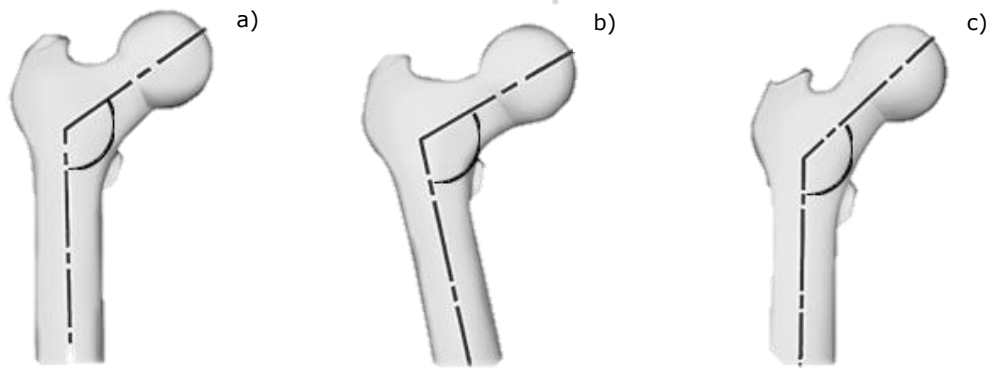


Figure 7. Angle of femoral neck inclination: (a) Normal ($\sim 135^\circ$), (b) Coxa vara ($< 120^\circ$) and (c) Coxa valga ($> 140^\circ$)

Another important factor for hip stability and normal walking is the anteversion angle, defined as the angle between the axis of the femoral neck and the femoral shaft axis in the coronal plane, a value of 15 to 20° being considered normal.

The **neck** meets the shaft of the femur forming the **greater trochanter** on the lateral aspect and the **lesser trochanter** on the posteromedial side, which are connected anteriorly by the intertrochanteric line and posteriorly by the intertrochanteric crest. The trochanters are bony prominences on the proximal shaft of the femur that serve as attachment for the muscles involved in hip motion. An imaginary line can be drawn between the greater and lesser trochanter called the **intertrochanteric line**.

The distal femur, with its two large condyles, makes up the top part of the knee joint, where it meets the upper part of the tibia (shinbone) and the patella (kneecap).

1.2. Capsule, ligaments and muscles

In addition to the solid bony structure, the hip joint has additional structures that contribute to the joint's stability and range of motion.

The **labrum**, a ring of fibrocartilagenous tissue that surrounds the rim of the acetabulum, that helps protect, deepens and stabilizes the joint.

A strong, fibrous articular capsule surrounds the entire hip joint. The capsule is attached to the periphery of the acetabulum, near the acetabular labrum, and attaches to the femoral head along the intratrochanteric line. To support the capsule, the iliofemoral and pubofemoral ligaments add reinforcement to its anterior portion, while the ischiofemoral ligament provides reinforcement to the posterior capsule.

The **iliofemoral ligament** extends from the ilium to the femur. It has an inverted Y shape and is considered to be the strongest ligament in the human body and serves to strengthen the joint by resisting excessive extension and provide posture support [7].

This ligament is usually referred to as the Y-shaped ligament of Bigelow, and

its upper band is frequently named the **iliotrochanteric ligament**.

The **pubofemoral ligament** is attached to the obturator crest of the pubic ramus and merges with the fibres of the iliofemoral joint at the intratrochanteric line, resisting excessive abduction of the hip and limits extension.

The **ischifemoral ligament (ischiocapsular ligament)** helps stabilize the joint during extension. It consists of a triangular band of fibers that go from the ischial part of the acetabulum to the posterior aspect of the capsule.

The **ligamentum teres** is an intra-articular ligament originating from the acetabular notch inserting into the fovea of the femoral head. Within this ligament, there is a foveal artery originating from the obturator artery that serves as an important conduit to supply blood to the head of the femur in childhood.

Furthermore, the stability of the hip joint is enhanced by muscular reinforcement. The hip joint has 3 degrees of freedom and can perform flexion, extension, abduction, adduction, and rotation using several muscles attached between the pelvis and femur. Most of the hip muscles are responsible for more than one type of movement in the hip as different areas of the muscle act on tendons in different ways. Twenty-two muscles cross the hip and provide the forces required for its functional range of motion, balance, and gait.

The primary hip flexor muscles are the iliopsoas major, rectus femoris and Sartorius. The pectineus, iliacus, adductores longus and brevis, and the anterior fibers of the glutei medius and minimus also contribute to the hip flexion.

Extension is performed by the gluteus maximus, assisted by the hamstring muscles and the ischial head of the adductor magnus.

The adductors include the adductores magnus, longus, and brevis, the pectineus, the gracilis, lower part of the gluteus maximus, the glutei medius and minimus, and the upper part of the gluteus maximus.

The muscles producing internal rotation of the thigh do this as a secondary function. These muscles are the gluteus minimus, anterior fibers of the gluteus medius, tensor fasciae latae and the iliacus and psoas major.

Finally, outward rotation is performed with the help of the posterior fibers of the gluteus medius, the piriformis, obturatores externus and internus, gemelli superior and inferior, quadratus femoris, gluteus maximus, the adductores longus, brevis, and magnus, the pectineus, and the Sartorius [14].

Table 1. Primary muscle groups and their action [15]

Muscle	Action
Adductor group	
A. brevis	Adduction
A. longus	Adduction, flexion, internal rotation
A. magnus	Adduction, flexion, extension
Pectineus	Flexion, adduction
Gracilis	Adduction
Gluteal group	
G. maximus	Extension, external rotation
G. medius	Abduction, internal rotation
G. minimus	Abduction, internal rotation
Tensor fasciae latae	Abduction, flexion, internal rotation
Lateral rotator group	
Obturator	External rotation
Piriformis	External rotation
Gemelli	External rotation
Quadratus femoris	External rotation
Iliopsoas group	
Iliacus	Flexion
Psoas major	Flexion

With respect to the position relative to the joint the muscles are: anteriorly, the psoas major and iliacus; superior, the gluteus minimus and rectus femoris; medially, the obturator externus and pectineus and posteriorly the piriformis, gemellus superior, obturator internus, gemellus inferior, obturator externus, and quadratus femoris.

1.3. Hip joint disorders

The hip is subject to diseases mainly due to improper development, acute trauma or mechanical wear. The most common disorders include arthritis (rheumatoid arthritis, traumatic arthritis, osteoarthritis), avascular necrosis (osteochondritis dissecans, Perthes disease), slipped epiphysis, bursitis, developmental dysplasia of the hip and femoro-acetabular impingement.

In order to relieve the pain and restore normal hip function, the majority of patients undergo a total hip replacement surgery.

1.3.1. Joint pathology

The repetitive loading of the hip joint leads to degeneration of the surrounding articular cartilage and cortical bone and can result in acetabulum bone defect and osteoarthritis.

A degenerated hip joint can be treated in early stages by weight control, physical therapy, intra-articular injections and, as a last resort, by replacing the joint.

The most common cause of intra-articular disorders is cartilage degeneration. This section briefly discusses the ways in which the function of the hip joint can be impaired.

Usually, hip degeneration is known to be caused by three main causes that include mechanical dysfunctions, circulatory disorders and inflammatory disorders.

The hip is particularly prone to osteoarthritic degeneration being such a heavily weight bearing joint.

Osteoarthrosis (OA) describes the degeneration and progressive loss of normal structure and function of articular cartilage. Osteoarthritis is the most common type of arthritis in the hip (coxarthrosis) and is associated with other disorders such as avascular necrosis, slipped epiphysis, impingement and dysplasia. Osteoarthritis may be primary or secondary. **Primary OA**, when it develops with no underlying cause or joint deformity can be found and **secondary OA**, when it is the result of a congenital or acquired joint deformity (joint fractures, infection, severe ligament injuries or vascular lesions following an accident).

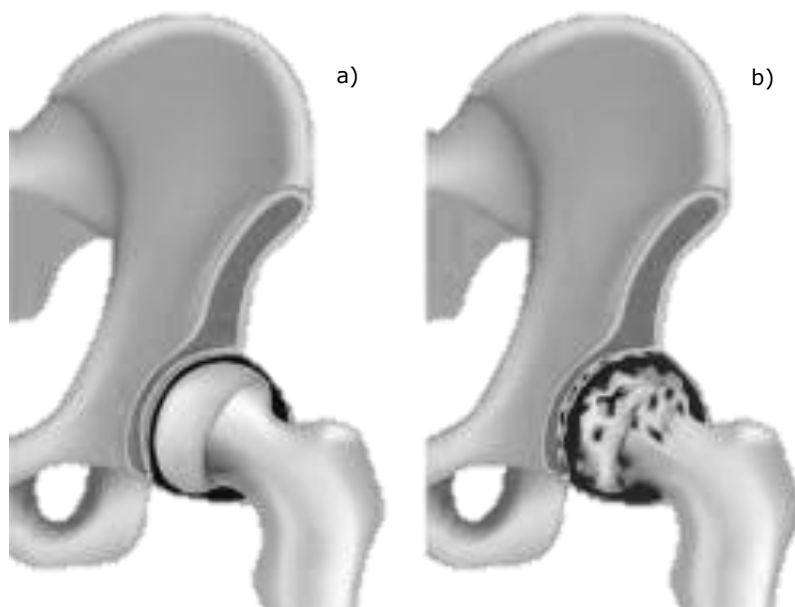


Figure 8. Comparison of normal hip joint (a) and a joint with osteoarthritis (b) [16]

Radiographically, OA can be defined as the narrowing of the joint space between hip and femur as a sign of cartilage loss and osteophyte (bony spurs) formation.

The treatment of osteoarthritis of hip joint varies from conservative rehabilitative exercises to surgical treatments such as osteotomies or total hip arthroplasties.

Bellow, there is a short review of the most common disruptions that may lead to coxarthrosis.

Acetabular labrum tears

The labrum, because of its function in distributing weight-bearing forces, is susceptible to traumatic injury from repetitive forces associated with twisting, pivoting, and falling.

Labral tear is a common intra-articular soft tissue injury that can lead to disruption of joint stability, causing abnormal motion between the femur and acetabulum, accelerating the process of osteoarthritis.

Femoracetabular impingement (FAI) occurs when the head of the femur has an abnormally large radius (bony prominence) or the socket is too deep

(overcoverage), the neck touching against the rim of the acetabular socket causing pain and deterioration to the labrum or hip joint itself [17]. It usually occurs because the hip bones do not develop normally during the childhood. Impingement is not usually caused by dysplasia. It can also be caused by a socket that is too deep. The mechanisms of impingement have been defined as caused by cam bone spur, pincer bone spur or sometimes both, causing joint damage.

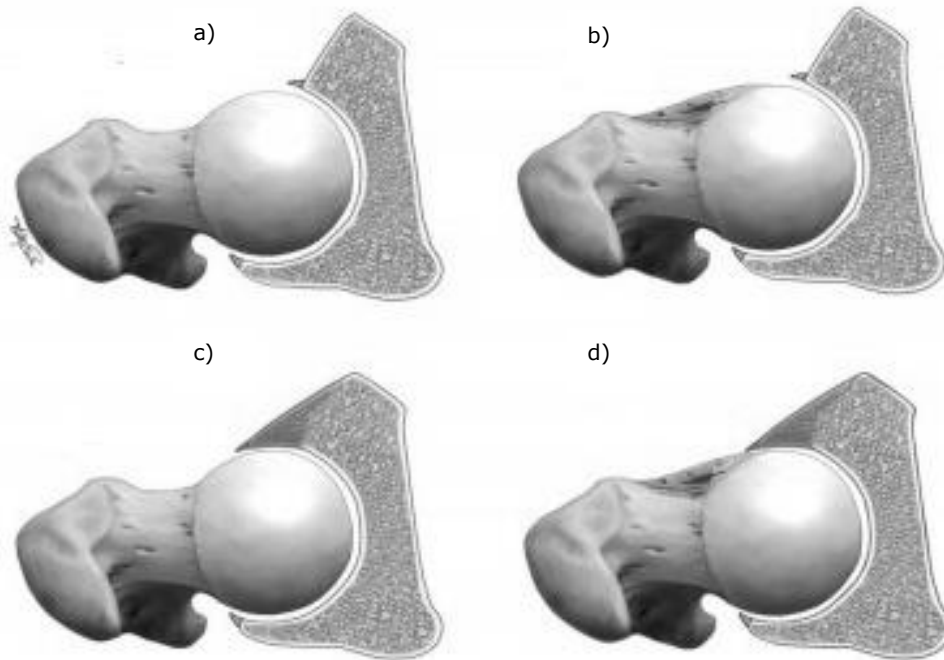


Figure 9. Geometry of the normal hip (a), cam (b), pincer (c) and mixed impingement (d) [18]

Cam impingement is characterized by an abnormal bony prominence on the femoral neck, just below the head, which impinges on the acetabulum during flexion and internal rotation.

Pincer impingement is caused by a pincer bone spur extending out over the normal rim of the acetabulum leading to acetabular over-coverage of the femoral head. This may cause jamming of the acetabular labrum during flexion and internal rotation between the rim and the femoral neck.

Combined impingement refers to a condition where both the pincer and cam types are present.

The term **developmental dysplasia of the hip** refers to a continuum of abnormalities in the immature hip. Hip dysplasia describes an abnormality in the size, shape, orientation, or organization of the femoral head, acetabulum, or both. This causes increased force, and abnormal wear on the cartilage and labrum.

Retroverted acetabulum is a specific variant of dysplasia in which the alignment of the acetabular opening and its proximal roof are not oriented in the normal anterolateral direction, but lie at an angle of retroversion with respect to the sagittal plane, decreasing the posterior coverage of the femoral head.

Acetabular dysplasia is characterized by an immature, shallow or malpositioned acetabulum that doesn't completely cover and support the femoral head, causing subluxation or dislocation of the femoral head.

In a **subluxed hip**, the head of the femur is displaced from its normal, centered position but still makes contact with a portion of the acetabulum.

With a **dislocated hip**, the head of the femur slides out of the acetabular socket completely, leaving no contact between the articular surface of the femoral head and the acetabulum. Hip dislocation is often associated with trauma but can also be caused by a congenital abnormality, i.e. dysplasia.

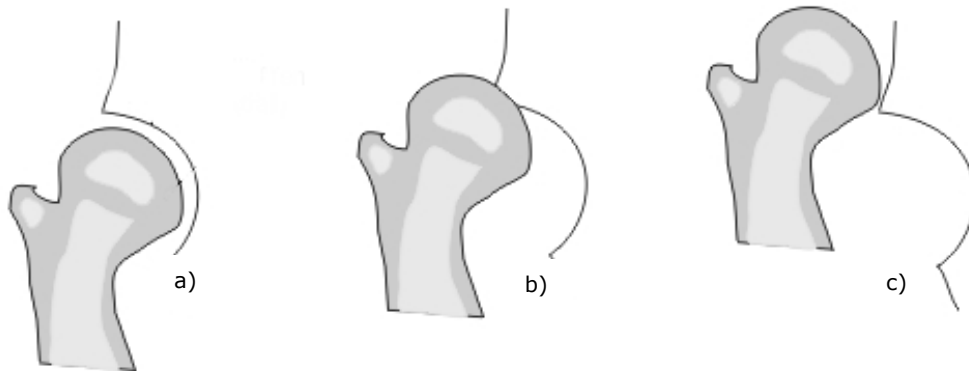


Figure 10. Types of misalignments of femur head into the socket in hip dysplasia:

(a) Normal; (b) Subluxation and (c) Dislocation.

A hip can become dislocated during many kinds of accidents, including falls and motorcycle or car accidents. A traumatic hip dislocation must be treated immediately because the injury stops blood from irrigating the top of the femur, causing avascular necrosis of the femoral head.

Avascular necrosis (AVN) or osteonecrosis is a progressive, severe condition resulting from temporary or permanent disruption of blood supply to the head of the femur, depriving the bone of its vital oxygen supply, causing the death of trabecular bone tissue and as a result, bone collapse.

Although it can occur in any bone, osteonecrosis most often affects the hip. AVN may be caused by traumatic injuries such as dislocation and femoral fractures, by extended corticosteroid medications or other medical conditions.

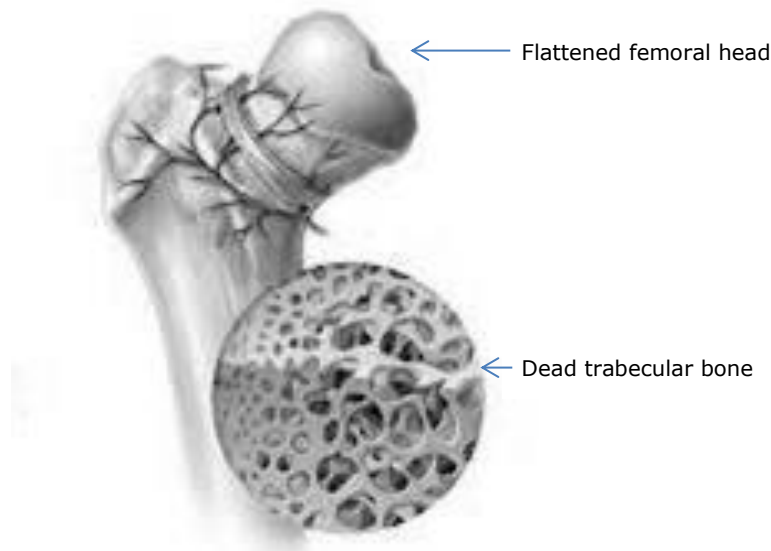


Figure 11. Avascular necrosis of the femoral head

Unlike osteoarthritis, **rheumatoid arthritis** of the hip joint is a chronic inflammatory disorder caused by the body's autoimmune system attacking the cartilage of the joint. The disease process leads to severe, and at times rapid, deterioration of multiple joints, resulting in severe pain and loss of function. Rheumatoid arthritis occurs most frequently in middle age and is more common among women.

Osteoarthritis can also be secondary to the damage to cartilage caused by rheumatoid arthritis.

1.3.2. Hip fractures

Older people are more prone to sustain hip fractures, osteoporosis, a disease characterized by the excessive loss of bone, tissue increasing the risk of hip fractures [19]. This condition is referred as pathologic fracture.

Over 90% of hip fractures are caused by falling, but any trauma can potentially cause a hip fracture [20]. Depending upon the mechanism of the injury, the fracture could occur at the femur or a portion of the pelvis may be fractured.

1.3.2.1. Femoral fractures

Femoral fractures are generally separated into three broad categories depending on the position of the fracture: proximal femur fractures, femoral shaft fractures and supracondylar (distal) femur fractures. A hip fracture is generally a fracture of the proximal third of the femur bone.

Proximal femur fractures are more common in the elderly and involve the upper-most portion of the thigh bone and include fractures of the head, neck, intertrochanteric, and subtrochanteric regions.

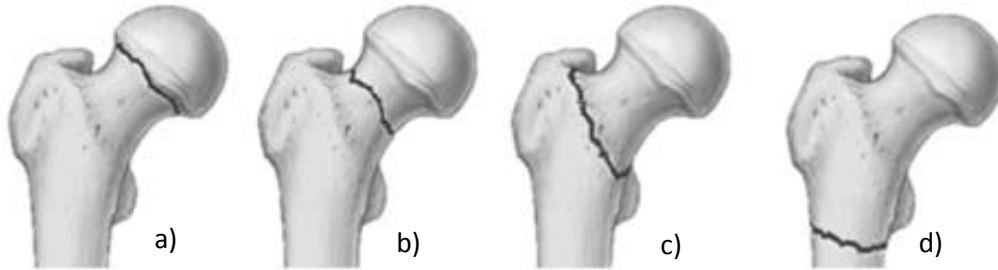


Figure 12. Most common proximal femur fracture types based on

AO classification of long bone fractures [21]: (a) subcapital neck fractures; (b) transcervical neck fracture; (c) intertrochanteric fracture and (d) subtrochanteric fracture

Intertrochanteric and femoral neck fractures are the most common and account for 90% of the proximal femoral fractures occurring in elderly patients [22].

1.3.2.2. Acetabular fractures

Acetabular fractures either occur with high-energy trauma (e.g. falls, car accidents, etc.) or as an insufficiency fracture. Fractures of the acetabulum occur as a result of the force exerted through the head of the femur to the acetabulum. In case of young patients when an acetabular fracture occurs, there is always significant trauma and commonly associated injuries. In elderly patients, acetabular fractures can occur due to bone weakened from osteoporosis, the degree of underlying bone osteoporosis determining the resultant fracture characteristics [23].

Acetabular fractures in the elderly population are marked by a high degree of variability in terms of patient and fracture characteristics.

The accepted standard classification used for acetabular fractures is the Judet and Letournel classification system. The Judet and Letournel is a simple morphologic classification system based on the fracture morphology and patterns [24].

For the purpose of classification of fracture patterns, Judet & Letournel considered the acetabulum to be located in the cavity of an arch formed by two columns of bone, anterior and posterior. The anterior column consists of the anterior border of the iliac wing, the anterior wall, and the superior pubic ramus. The posterior column comprises the greater and lesser sciatic notches, the ischial tuberosity, the posterior wall, and the entire retroacetabular surface.

Judet and Letournel divided acetabular fractures into elementary and associated fracture types. The elementary fractures consist of a single fracture (posterior wall, posterior column, anterior wall, anterior column and transverse), whereas associated fractures involve combinations of elementary fractures (T-shaped, posterior column and wall, anterior wall or column with posterior hemi-transverse, and both column).

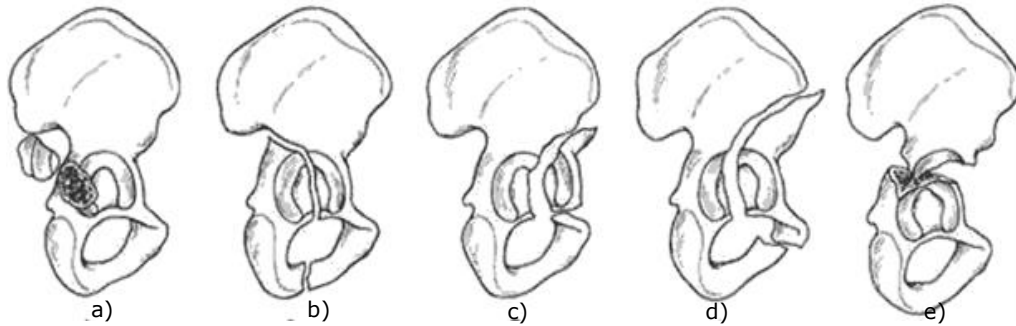


Figure 13. Elementary fracture Letournel classification: (a) posterior wall; (b) posterior column; (c) anterior wall; (d) anterior column and (e) transverse fractures

Furthermore, the AO-classification gives a solid basis for scientific evaluation with its clear structure with types and groups, ascending according to the severity of the damage.

Table 2. AO classification of acetabular fractures [25]

Type A	Partial articular, involving only one of the two columns
	<ol style="list-style-type: none"> 1. Posterior wall fracture 2. Posterior column fracture 3. Anterior wall or column fracture
Type B	Partial articular, involving a transverse component
	<ol style="list-style-type: none"> 1. Pure transverse fractures 2. T-Shaped fractures 3. Anterior column and posterior hemi-transverse
	Complete articular fractures, both columns
Type C	<ol style="list-style-type: none"> 1. High variety, extending to the iliac crest 2. Low variety, extending to the anterior border of the ilium 3. Extension into the sacroiliac joint

1.4. Hip joint biomechanics

Biomechanics is a dynamic science evaluating the effect of forces and loads across an anatomic structure. Understanding the biomechanics of the hip is vital to advancing the diagnosis and treatment of many pathologic conditions. Biomechanical principles also provide a valuable perspective to our understanding of the mechanism of injury.

1.4.1. Hip joint mobility

Kinematic measurements in the hip joint are typically described in terms of femoral rotation. The translational component of this joint is relatively small and difficult to quantify. Joint mobility refers to the range of motion (ROM) in the planes in which the joint is designed to move.

As a ball and socket joint, the hip has three degrees of freedom allowing movement in all three principal axes of motion passing through the center of the femoral head.

The main motions of the hip, excluding circumduction, are flexion-extension (transverse axis), abduction-adduction (sagittal axis), and internal-external rotation (longitudinal axis).

Both soft and hard tissues limit the range of motion in a normal hip joint. Goniometry is the most widely used method for measuring ROM. Table 3. Hip motions average amplitudes .lists the average ranges of motion for normal adults.

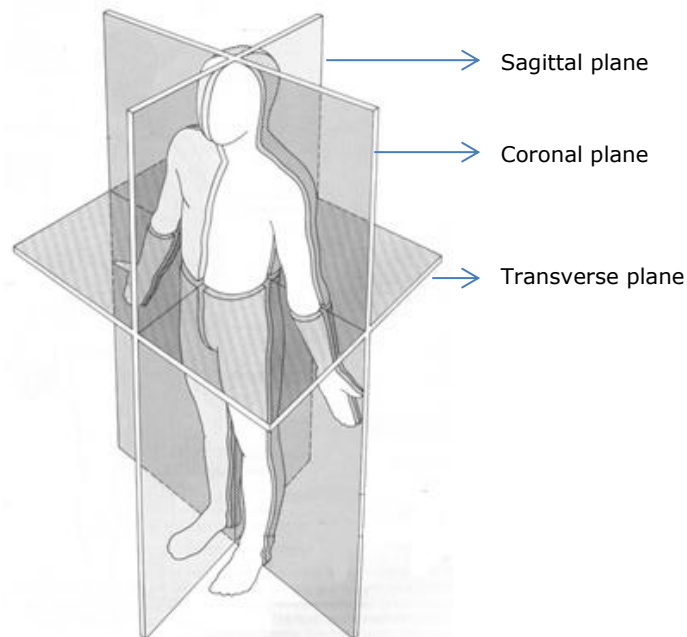


Figure 14. Anatomical planes definition

Hip flexion and extension range of motion are dependent on the position of the knee, full flexion of the hip being achieved only with the knee flexed. Clinically, normal range of motion for flexion is about 135° , while normal extension about 40° . However, if the pelvis is fixed into a neutral position and not allowed to rotate, true hip flexion and extension angles are slightly lower.

Internal and external rotation occurs along a longitudinal axis extending from the femoral head to the inter-condylar region of the distal femur. Rotation of the pelvis produces lateral rotation of the hip and medial rotation of the contralateral hip.

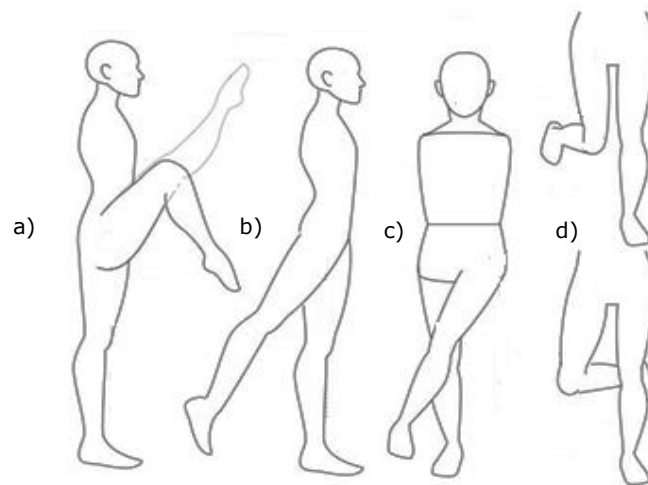


Figure 15. Lower limb hip movements: (a) flexion, (b) extension, (c) abduction, (d) internal-external rotation

Circumduction in the hip joint is the result of a combination of movements that includes flexion, abduction, extension and adduction. The basic motion of hip circumduction involves moving the distal end of the limb in a circle around. More accurately, circumduction is described as the conical movement due to the cone formed by the rotating leg [26].

Table 3. Hip motions average amplitudes [27].

Motion	Average ROM
Flexion	120°
Extension	12°
Abduction	41°
Adduction	27°
Internal rotation	44°
External rotation	44°

Normally, these ranges vary depending on anatomic variants of femoral and acetabular version, or pathology within or about the hip joint. The motion is limited by bony anatomy, ligamentous and capsular restraints, and active motor tension [13].

The **functional mobility** of a joint represents the range of motion healthy individuals require to fulfill everyday life tasks. Most daily activities do not require the full amplitude of hip movements, a functional ROM of at least 120° flexion, 20° abduction and 20° of external rotation being required.

In order to extend the functional motion ability of the hip joint, hip movements are accompanied by lumbar-pelvic motions [28].

1.4.2. Gait cycle

The human **gait cycle** is used to describe the complex activity of bipedal walking, or gait pattern. Gait is a sequence of consecutive, uniformly locomotion events in space and time, a movement repeated in defined time intervals.

The cycle describes time interval or the motion sequence from initial placement of the supporting heel on the ground to when the same heel contacts the ground for a second time. This periodic leg movement is the essence of the cyclic nature of human gait.

The gait cycle is divided into a stance phase usually lasting 65% of the cycle and a swing phase of the same leg about 35% of the cycle [29].

Stance is the term used to describe the period during which the foot is on the ground and can be subdivided in double limb and single limb stance. It starts when the heel touches the ground, lasts as long as foot contacts the floor and ends at the moment when the toes leave the ground.

There are two periods of double support or double limb stance, where both limbs are in contact with the ground, and both of these last for about 10% of the gait cycle. The first double support begins at initial contact and ends when the opposite foot leaves the ground at preswing, while the second starts as the opposite limb contacts the ground and ends when it leaves the ground at toe off.

The duration of double period support varies with the speed of walking, its complete disappearance marking the transition from walking to running.

The period of time when the leg is not weight-bearing and in the air for limb advancement is called **swing**. It starts when the toes leave the ground, lasts as long as the leg swings and ends when the heel touches the ground again.

Every gait phase is subdivided in consecutive periods based on the movement of the foot and quantified by their temporal aspect within the cycle. Stance comprises of five periods: initial contact/heel-strike, loading response/foot-flat (0-10%), midstance (10-30%), terminal stance/heel-off (30-50%) and preswing/toe-off (50-60%).

The swing phase includes two periods: initial swing/acceleration (60-70%), midswing (70-85%) followed by terminal swing/deceleration (85-100%).

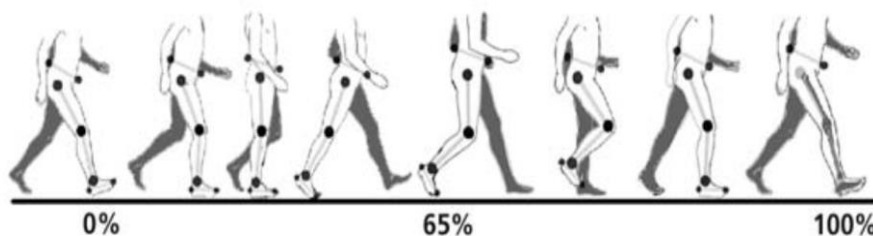


Figure 16. Human normal gait and phase duration

1.4.2.1. Gait parameters

Stride length represents the distance travelled by a person between two successive placements of the same foot (stride). It consists of two step lengths, left plus right, averaging 70-82 cm for normal men.

Stride width is the transverse distance between the axes of the two feet, usually measured at the midpoint of the back of the heel during floor contact, with an average of 8 cm [30].

The **toe out** or **toe in** is the angle between the direction of progression and the reference axis of the foot.

The **cadence** is the number of steps taken in a given period of time. As there are two steps in a single gait cycle, the cadence is a measure of half-cycles usually quantified as number of steps per minute.

The importance of the normal hip in any daily activity is emphasized by its role in movement and weight-bearing. A complete understanding of the biomechanics of the hip joint is important for evaluating joint function, diagnosis of pathologic conditions and design of hip prostheses.

During normal walking, the human hip joint undergoes cyclic loading that develop forces three to five times those of body weight on prosthetic components.

The typical range of motion curves over one cycle of normal walking for an average person are shown in Figure 17. The positive angles are for flexion, abduction and lateral rotation.

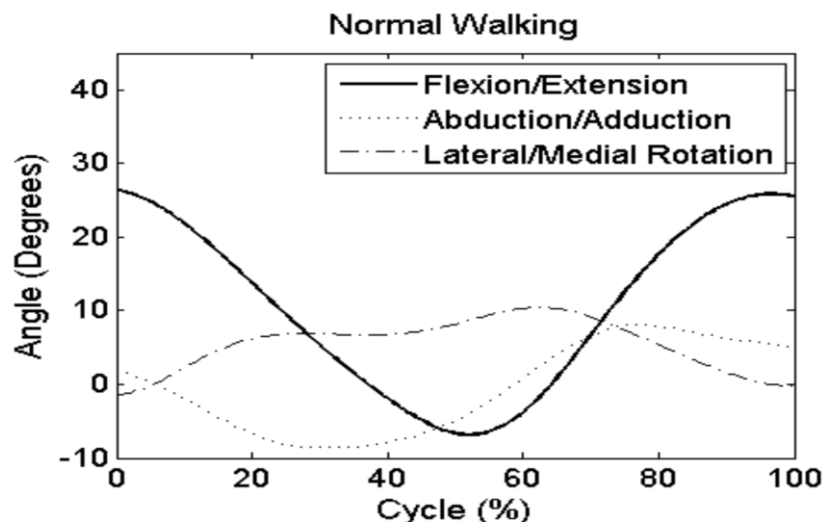


Figure 17. Range of motion during one cycle of normal walking [31]

During different phases of the gait cycle, different forces act on the joint. Approximately two thirds of the hip force is developed by the abductors. The estimated load on the hip in the stance phase of gait is equal to the sum of the force created by the abductors and the body weight.

2. TOTAL HIP REPLACEMENT OVERVIEW

Hip replacement is an operative technique that involves replacing of the weight-bearing components of the hip joint with a prosthetic implant, with the aim to solve the effects of degenerative pathologies of the human hip joint, reducing pain and offering renewed stability and function of the joint.

Hip replacement surgery is one of the most successful orthopaedic procedures, alleviating pain and improving patient's quality of life. In Romania, orthopedic surgeons perform approximately 8000 hip replacement surgeries each year and the rate is increasing [1].

Hip replacement surgery can be performed as a total replacement (THR) or a partial replacement (hemiarthroplasty). THR or total hip arthroplasty (THA) consists of replacing both the acetabulum and the femoral head while hemiarthroplasty generally only replaces the femoral head.

As described in the anatomy section, the hip joint is a true ball-and-socket joint due to the spherical head of the thighbone (femur) moving inside the cup-shaped socket (acetabulum) of the pelvis.

Depending on the type of pathological condition or injury, a number of components are required to build a suitable prosthesis that restores the normal joint function. In order to duplicate the joint's movement and action, in the case of THR, both the femoral head and the acetabular socket are replaced by an artificial joint that consists of two parts: the femoral component and the acetabular component. Each component comes in various sizes to accommodate various body sizes and types. Together, these components used for total hip replacement are referred to as total hip prostheses (THP). In modern designs, the femoral stem, neck and ball are separate pieces, resulting in modular designs. This modularity allows for greater flexibility in customizing prosthesis sizing and fit.

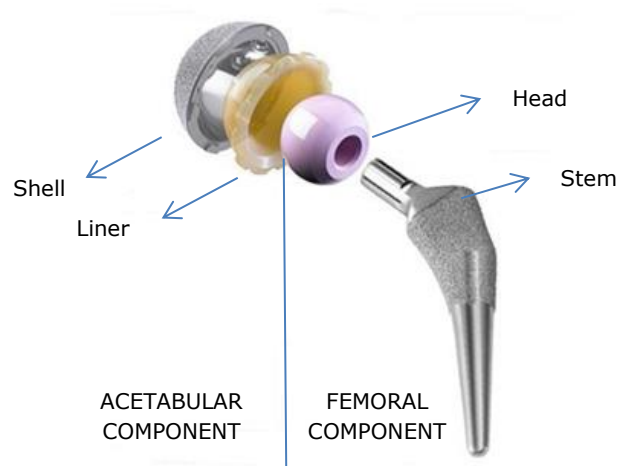


Figure 18. Components of THP [32]

The **acetabular component** is a cup that replaces the damaged acetabular socket. Acetabular components can be constructed of a single piece (monoblock) or with two components (modular), which feature a shell and a liner that acts as a bearing to reduce friction and allow a smooth articulation against the femoral head.

The **femoral component**, also known as the stem, is the prosthetic component that fits into the femur bone, providing attachment to the prosthetic head. The femoral stem fits into the intramedullary canal of the femur's proximal diaphysis and metaphysis. Also, the femoral component can be of a single piece monoblock or modular construction, stem modularity offering the possibility of adapting the geometry of the prosthesis to the joint morphology of each patient.

Modular components consist of a variety of separate stem and neck components that can be combined to allow for variability in femoral neck offset and also in leg length in order to achieve a better biomechanical restoration of the joint with respect to the morphology of the patient. This solution provides useful flexibility during primary surgery and assures simplified revisions [33], [34].

With the stem fitted, the ball of the ball-and-socket hip joint can be inserted on top of the stem. The damaged femoral head is replaced by a prosthetic ball.

2.1. Bearing surface

Biomaterials are used to assist, repair or replace tissue or organs that function under an acceptable level. Therefore, the materials used for each component of the prosthesis must have the properties necessary to replace the natural tissue and restore joint function.

Biomaterials include a wide range of materials such as ceramics, polymers and metals. Combinations of these types of materials are used in most joint replacement prostheses, thus leading to minimize wear.

The primary mechanical requirement for the acetabular cup is the ability to support the joint loads, while friction coefficient and wear rate are the most important properties regarding the bearing material of the acetabular liner.

Because a number of factors can influence the friction and fatigue resistance between components, a number of different combinations of materials are currently on the market. Contemporary hip bearings include four bearing combinations may be generally classified as either hard-on-hard or hard-on-soft.

The materials used in the implant depend on several factors, including the age of the patient, the activity level of the patient, and the surgeon's preference. Each component can be made of one of several materials.

Hard-on-hard hip bearings incorporating metal-on-metal (MOM) or ceramic-on-ceramic (COC) articulations were widely adopted in orthopedics due to their very low wear rates. Stainless steel, cobalt-chrome and titanium alloys represent the common used metals while contemporary ceramic femoral heads may be produced from alumina or zirconium composites. In hard-on-hard bearing couples transition forces between prosthesis and bone may be increased, as there is no soft material to provide a dampening effect. There are also concerns about metal ions generated from the use of metal-on-metal implants.

Hard-on-soft couples are the most commonly used in hip replacement. Hard-on-soft couples usually include cobalt-chrome or titanium on polyethylene, but also ceramic or ceramic like materials on polyethylene.

Crosslinking has shown to dramatically decrease wear in polyethylene prostheses components, but wear continues to produce small particles.

40 Total hip replacement overview

There is no one ideal material or combination for all patients and medical conditions. As shown in Table 4, each material has distinct benefits and limitations.

Table 4. Main advantages and disadvantages of common hip prosthesis bearing materials

Material	Advantages	Disadvantages
Metal	-Low wear rates -Allows the use of larger femoral heads, lower risk of dislocation	- Risk of adverse reaction to metal debris - Unknown effect of metal ions
Ceramic	-Very low wear rates -Inert wear particles	- Most expensive - Can cause squeaking - Low modularity, brittle
Cross-linked polyethylene	-Most commonly used, successful clinical history -Non-toxic debris	- Susceptible to wear - More prone for revision

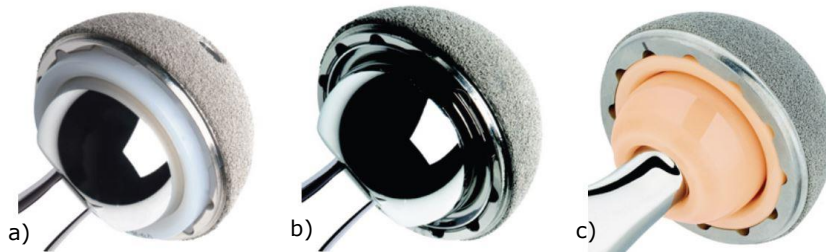


Figure 19. Most common THR bearing combinations: (a) metal on polyethylene, (b) metal on metal and (c) ceramic on ceramic

The requirements of low friction bearing to minimize surface wear to reduce inflammation in surrounding tissues and risk of loosening lead to the development of new bearing materials.

Oxidized zirconium, or Oxinium (Smith & Nephew) is a metal-ceramic alloy where metal Zirconium is treated with high pressure and heat in the presence of oxygen, leading to the transformation of its surface into a smooth, black ceramic surface. This results in an implant that has remarkable surface properties of ceramic, while retaining the solid metal strength characteristics. This is documented to reduce wear by 98% compared to standard cobalt chrome [35].

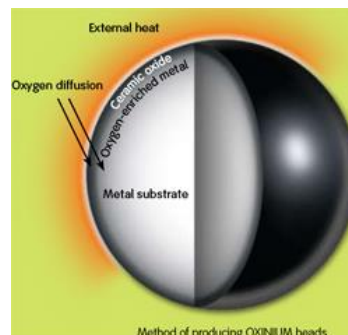


Figure 20. Method of thermal processing of Oxinium femoral components [36]

2.2. Fixation

Since the beginning of hip replacement, there has been constant development in the technology associated with it, leading to better functional performances and longer life span.

Depending on the type of fixation used to hold the implant in place, there are three major types of THP: cemented, uncemented or cementless prostheses and hybrid prostheses. Hybrid prostheses usually consist of cemented stems and cementless cups.

There are certain general guidelines for the choice of appropriate type of THP based upon age, bone quality, weight, lifestyle, but also the surgeon's past experience is an important decision factor.

In fact, many surgeons justify the choice of cemented or cementless implant based on the patient's age and therefore quality of bone and activity level.

Cementless implants are recommended when good mechanical interlock and osseointegration are expected, which is more likely to happen with young patients with good quality bone; whereas cemented implants are most often used to treat older patients.

2.2.1. Cemented THP

In 1962, Sir John Charnley inserted a small stainless steel ball on a stem into the femoral bone and a high density polyethylene cup to replace the acetabular (socket) part of the joint. Both of these components were fixed to the bone with the use of an acrylic polymer commonly referred to as bone cement [37].

After the breakthrough of Sir John Charnley which resulted in decreased loosening, the traditional method of bonding the prostheses to bone involved the use of cement.



Figure 21. Charnley cemented THP

There have been many improvements in both the materials and the methods used to anchor the prosthetic components to the bone, the most commonly used bone cement being a self-curing acrylic polymer called poly methyl methacrylate (PMMA).

Cemented fixation provides immediate postoperative advantages in terms of rapid implant to bone bonding, which ensures early pain relief and weight-bearing.

In cemented prostheses, space is intentionally left between the stem and the prepared femoral canal and between the reamed acetabulum and the cup in order to be filled with cement.

Bone cement acts as a non-adhesive supportive material that forms assures mechanical bonding between the cement and the bone and the cement and the prosthesis, filling the voids between the surface of the implant and the surrounding cancellous bone.

Bone preparation is an important requirement for ensuring a long survivorship cemented arthroplasty as poor cement coverage and inadequate intrusion into trabecular bone are associated with implant loosening. The aim of bone preparation is to provide a clean, non-bleeding, stable bony interface for cement penetration into the remaining cancellous bone.

While shaping of the bone in order to receive the prosthesis is achieved by reaming, proper bone penetration of the cement is obtained through cleaning strong cancellous bone by brushing and pulsatile lavage and afterwards pressurizing the cement onto the prepared bony surface [38], [39]. However, cement pressurization is considered the most decisive factor in assuring a proper locking interface.



Figure 22. Section view representing a cemented stem and cement penetration

For adequate cement pressurization for acetabular cup insertion, commercially available pressurizers are used that create a stable congruent cement mantle.

2.2.1.1. Cemented acetabular prostheses

In order to improve the stability of the cement mantle in the acetabular region, flanged cups were developed. The use of flanged cups was intended to improve cement pressurization during cup insertion by increasing the intra-acetabular pressure, whilst improving cement penetration [40].



Figure 23. Cemented cup designs. (a) Unflanged Baumer Muller auto retaining cup [41] and (b) Symetrical flanged DePuy Synthes Elite Plus cup [42]

However, the efficacy of flanged designs shown in in-vitro studies [43], [44] has been repeatedly questioned, suggesting that the effect of flanged cups on the cement penetration isn't significant with respect to unflanged designs [45], [46].

2.2.1.2. Cemented stem

In cemented arthroplasty, prosthetic stems are classified into two basic designs [47], [48], namely "force-closed" or load tapered and "shape-closed" or composite beam. These designs use different methods to transmit the axial loads from the stem to the cement without generating damaging peak stresses and increased micro-movement.

The force-closed method uses a taper to transfer the loads to the cement and maintain a tight fit. The principle of tapered fixation relies on shortening and subsidence to create frictional forces at the stem-cement interface to balance the external forces. A polished surface finish is important in the success of these taper stems.



Figure 24. Examples of taper stems: Stryker Exeter polished stem [49] and Zimmer Collarless polished tapered stem [50]

The shape-closed design uses collars, ridges, or profiles in order to transfer a large portion of the axial load directly to the cement mantle, contributing to the mechanical stability of the implant. In the case of shape-closed stems there must

be perfect bonding at the stem-cement interface resulting in identical strain in the stem and the cement at the interface.



Figure 25. Charnley Elite Plus stem with centralizer (DePuy) [42]

Along these basic design methods, several shape features may influence the outcome of cemented stem fixation. These include the surface finish, overall shape (straight or anatomical), the cross-sectional shape, the presence of a collar, use of a centralizer, etc.

Anatomically shaped femoral stems are designed to fit in the intra-medullary canal, allowing a homogenous cement mantle thickness, thus becoming more stable [51]. Anatomic design is also considered a shape-closed design feature.



Figure 26. Biomet Olympia anatomical stem [52]

As stems designs that have a circular cross-sectional shape have decreased rotational stability, oval, rectangular or irregular cross-sectional shaped stems are used in order to improve the rotational stability [53].

With regard of surface finish, loaded-taper stems are recommended to be polished to promote subsidence, whereas the composite-beam stems use polished or a rough adherent surface finish to increase the stability of the stem [54].

Advanced cemented fixation of the stem requires plugging the femoral canal with cement restrictors or distal plugs. Plugging the intramedullary canal increases penetration of cement into the cancellous bone proximal to the intramedullary plug by improving the ability to pressurize the cement and limiting the extent of the cement column to the desired length.

Distal plugs come in different shapes and sizes, and are usually made of polyethylene, titanium, cement, resorbable materials or even bone.



Figure 27. Biomet femoral pressurizer and OptiPlug distal plug [52]

The primary advantage of cemented THA is the immediate primary stability ensured by a stable interface between the implant and the cement and a solid mechanical bond between the cement and the bone. While bonding the implant and bone together, the cement mantle also solves superficial irregularities of the intramedullary canal by filling the voids.

However, the main problem with cemented hip implants is the mechanical deterioration of the cement layer. Cement particles generated from micro cracks along with polyethylene debris from component friction may lead to aseptic loosening. The occurrence of implant loosening and loss of bone stock was seen with greater frequency in younger and more active patients [55], [56], [57].

As a result, cemented THR is more commonly recommended for older patients or for younger patients with poor bone quality.

2.2.2. Cementless THP

To prevent aseptic loosening and the complications of cemented THA revision, uncemented prostheses were developed using different principles of fixation such as press-fit, screw rings or screw fixation. The idea was to implant prostheses without cement that will eventually become part of the living body. Uncemented THA is commonly used in younger, more active patients with good bone stock.

Cementless fixation is based on the press-fit concept to guarantee that both the femoral and the acetabular component are firmly anchored to the bone in the immediate post-operative period achieving primary or initial stability. Primary mechanical fixation is obtained by press-fitting an oversized component into the preformed bone cavity.

The reaming procedure is mandatory to prepare the acetabulum for prosthesis in order to obtain good apposition of the implant. As the acetabulum must be converted into a hemispheric cavity to match the shape of the prosthetic component, the acetabular reamer is designed to remove arthritic bone and cartilage from the hip socket in order to obtain a rim fit of the acetabular cup. In order to facilitate this growth, it is necessary that the preparation of the bone be done with care and accuracy, ensuring a close, tight fit. This means that, in case of an effective prosthesis, the stability will be maintained and improved with the passage of time [58].

Secondary stability of cementless THP is achieved by means of bone osseointegration, where the prosthesis is placed in close apposition with living bone tissue, generating bone grow on to or into the surface of the prosthesis stabilizing the implant and ensuring a long term bonding [59]. The type of bond depends on the surface characteristics of the implants. Ingrowth occurs when bone grows inside the porosity of the surface of the metallic cup, while ongrowth occurs when bone grows onto a roughened surface. This process has been demonstrated being highly dependent on the interface between prosthesis and bone. Ingrowth surfaces include sintered beads, fiber mesh, and porous metals, while ongrowth surfaces are created by grit blasting or plasma spraying.



Figure 28. Microscopic view of several osseointegration surface treatments:

(a) Ti fiber mesh; (b) Co-Cr beads and (c) Ti plasm spray

Additional coating of the implant surface with bioactive and bio inductive materials, such as hydroxyapatite (HA) and tri-calcium phosphate may improve biological fixation, both of which resemble natural bone mineral. HA is osteoconductive and encourages growth of mineralized bone, it can be applied to both porous and nonporous surfaces by plasma-spraying.

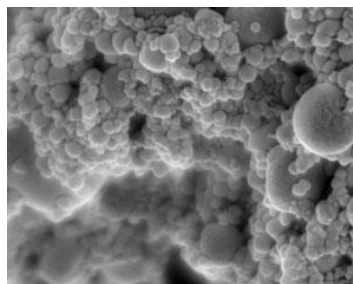


Figure 29. Hydroxyapatite nanoparticles

Both initial and secondary prosthesis stability are affected by its ability to engage with the host bone. Early studies concluded that bony ingrowth will only occur with relative micromotions of less than 150 μm between the implant and bone, while micromotions of $>150 \mu\text{m}$ lead to fibrous tissue formation [60], [61].

2.2.2.1. Cementless stem

The objective of cementless total hip stems is long-term stability by strong mechanical stability. Successful cementless stem replacement is dependent on both primary and secondary fixation of the implant to the bone and should resist subsidence, tilting and torsional forces.

Cementless femoral component fixation can be accomplished by either distal fixation in the diaphysis or proximal loading in the metaphysis, porous surfaces being located where fixation is desired. Thus, stem designs are often classified as proximally porous-coated tapered or fully-coated cylindrical [62].

Fixation of tapered stems is based on a self-locking principle, proximal femoral diaphysis and metaphyseal fixation and loading is enhanced by its proximal geometry. Most tapered stems achieve fixation in the high diaphyseal cortical bone just below the lesser trochanter, while reaming of the femoral canal isn't required before implantation.



Figure 30. Tapered stems: (a) Biomet Taperlock [52] and (b) Zimmer M/L [50]

Unlike the tapered stems, which provide mostly proximal fixation, the cylindrical stem relies on fixation along the entire prosthesis, engaging cortical bone in the femoral diaphysis [63].

Cylindrical prosthetic stems achieve distal fixation by means of a "scratch fit" between the rough porous surface of the implant and the underreamed femoral canal [64]. A proximal collar enhances axial stability by resisting distal migration and transmits forces to the calcar [65].



Figure 31. DePuy anatomic medullary locking (AML) distal fixation stem [42]

Bone conservation is an important aspect of total hip arthroplasty. Thus, the use of shorter femoral stem designs helps conserve the bone stock. By removing as little bone as possible during a primary operation and preserving diaphyseal tissue, more options are available for any potential later revision. Preservation of femoral neck provides greater torsional stability and reduces distal migration of the femoral stem.

Short stems are more easily utilized when performing minimally invasive surgery through an anterior approach, this type of components depending mostly on metaphyseal fixation.

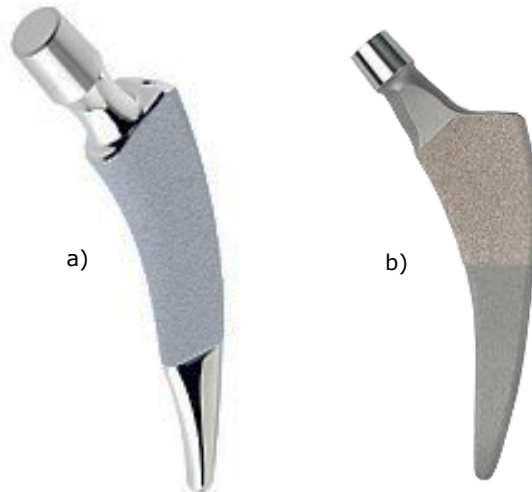


Figure 32. Most commonly used metaphyseal fixation stems:
(a) Smith&Nephew Nanos [36] and (b) Zimmer Fitmore [50]

2.2.2.2. Press-fit acetabular component

High initial stability of the cup in the acetabulum is needed for success of the implant. One of the major failure modes of cementless acetabular components is the loosening of the acetabular cup, which is mostly attributable to insufficient initial stability.

The acetabular component of a cementless total hip replacement also has a coated or textured surface to encourage bone growth into the surface. Earlier cementless cup designs were used with a line to line reaming, the size of the component equal to that of the prepared acetabulum. In order to achieve sufficient stability, these designs used supplementary fixation devices like cancellous bone screws, spikes, anti-rotational pegs or fins around the rim.

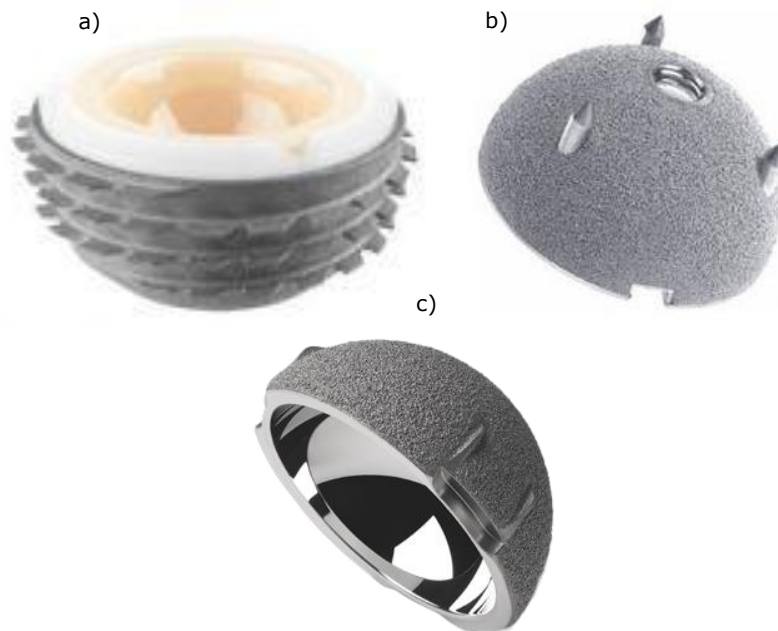


Figure 33. Cementless acetabular shells with supplementary fixation: (a) *Smith and Nephew Bicon-Plus threaded cup*, (b) *Reflection spiked cups* [36] and (c) *Zimmer paired fins MMC Cup* [50]

Modern modular components use press-fitting technique by having a larger outside diameter than the reamed acetabular cavity. These consist of an intra-osseous metallic shell and a liner, which receives the femoral ball and acts as a bearing surface, the main advantage over threaded designs being the ease of insertion. They are designed to accommodate multiple bearing options to provide flexibility to the surgeon. The liner is usually made of polyethylene or alternatively ceramic.



Figure 34. Modular acetabular component: Smith & Nephew R3 multi-bearing acetabular system [36]

The amount of initial contact between the outside porous surface of the cup and live bone, especially at the equatorial rim, is an important factor in obtaining an optimal implant-bone interface, respectively the initial stability of the shell. For improvement of the press-fit fixation and to deal with any extra bone removed during hemispherical reaming, the diameter of the cup is usually 1 to 2 mm larger than the diameter of the last used reamer [66].

A hemispherical or modified hemispherical shaped cup with a porous coating which is inserted with press-fit fixation and secured with several screws is one of the most commonly used methods.

The use of additional screw fixation may increase the initial stability and osseointegration ensuring a strong fixation that could help prevent rotation and micromovements [67].

Screw fixation was thought to encourage problems such as aseptic loosening and osteolysis by means of metal wear debris produced between the screw and cup and dispersion of wear debris through the screw hole [68].

To avoid the potential problems associated with screw fixation oversizing of the component has been recommended [69]. Component fixation by press-fit without screw fixation decreases the possibility for loosening to occur, eliminating the path for wear debris to enter the acetabular roof, as screw holes are not present.

Studies recommend the use of an implant from 1 to 3 mm larger than the last reamer used to prepare the acetabulum in order to obtain sufficient implant stability [69], [70], the compressive forces transmitted to the periphery potentially eliminating the need for adjunctive screw fixation.

An increase of the oversizing the cup in relation to the reamed acetabulum may prevent full seating of the components, resulting in gaps at the dome of the cup and, respectively, the recommended bone contact [71].

Although most press-fit cups have a hemispheric design, non-hemispherical cups were developed to increase the compressive forces on the periphery. These include less than hemispherical, elliptical and multi radius cup design. Non-hemispherical cups have a wider profile at the periphery and a flattened pole and have the ability to fully seat into the bony acetabulum with less force required at impaction [72]. In addition, the flattened pole and oversized equator should promote more physiologic load transmission in the equatorial region of the shell.



Figure 35. Zimmer elliptical Trabecular Metal Modular Acetabular System [72]

The optimal method of fixation for primary THR, particularly fixation with or without the use of cement is still controversial because of the influences of confounding variables, such as patient age, sex, body weight, and diagnosis.

The good long-term survivorship of cemented femoral stems along with unsatisfactory acetabular performance has resulted in the use of hybrid prostheses, a procedure with the acetabulum uncemented and the femoral component cemented [73].

2.2.3. Alternatives and variations of hip replacement

There is an alternative type of surgery to hip replacement, known as hip resurfacing. This involves removing the damaged surfaces of the bones inside the hip joint and replacing them with a metal surface.

An advantage to this approach is that it is less invasive and leaves you with a greater range of movement after surgery. However, it is usually only effective in younger adults who have relatively strong bones.

Hip resurfacing is a variation of hip replacement that has the potential to conserve the femoral neck as well as a portion of the femoral head itself. It differs from traditional total hip replacement because the worn out or arthritic surfaces of the hip joint are the only parts that are replaced.



Figure 36. Components of hip resurfacing prosthesis, Smith & Nephew BHR [36]

Resurfacing hip replacement may be considered for younger, active patients requiring hip replacement for osteoarthritis or inflammatory arthritis. If failure occurs with a resurfacing hip arthroplasty, revision to a conventional arthroplasty remains an option and may be better than a standard revision because of the amount of bone that is available to work with.

Resurfacing prostheses have a large articulating head, similar to the natural geometry of the hip, which helps maintain stability and improve range of movement with a reduced risk of dislocation and impingement [74].

However, hip resurfacing is not suitable for everyone. It may usually be recommended for younger patients, typically below the age of 65 with a relatively active lifestyle.

Hemiarthroplasty is a surgical procedure which replaces one half of the joint with an artificial surface and leaves the other part in its natural state. Hemiarthroplasty is a procedure commonly used to treat low demand patients suffering of a femoral neck fracture. The procedure is performed by removing the head of the femur and replacing it with a metal or composite prosthesis. The most commonly used prosthesis designs are unipolar prostheses as the Austin Moore prosthesis and the Thompson Prosthesis [75].

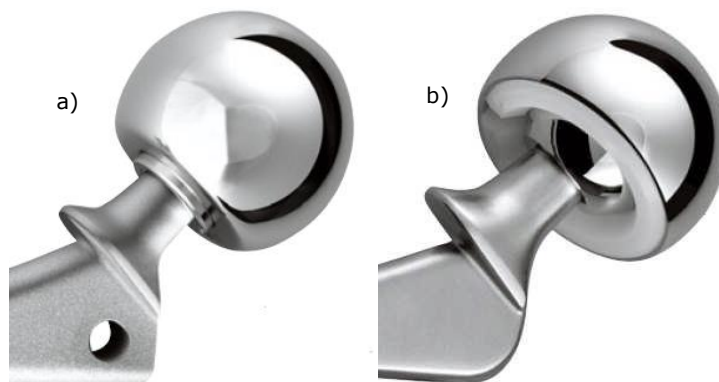


Figure 37. Unipolar (a) and bipolar (b) hemiarthroplasty implants

The **bipolar prosthesis** comes in a two-piece version that is designed to allow movement of both parts in multiple planes within the hip socket. One part serves as the femoral head, while the other is sized-matched to the patient's socket for best fit and stability. Once snapped together, the bi-polar moves freely upon itself, in multiple planes, for free mobility within the patient's own socket. It is believed that this type of hip head implant shows less wear on the patient's host socket, and is frequently used in a younger patient in an effort to delay an additional revision surgery.

2.3. THR failure

Revision of hip replacement is a procedure to replace a worn out or failed implant. A revision of a hip replacement is generally more challenging than the initial operation and the results of surgery and the durability of the revised hip replacement are less predictable than those of the primary operation.

Hip replacement loosening occurs over time, and can cause problems with the normal function of the hip replacement prosthesis. Failure of THR requiring revision surgery is shown to occur at a rate of approximately 1% per year for the first 15 years. Thus, approximately 15% of patients with THA must undergo a hip replacement revision surgery due to eventual failure of the initial replacement [76].

The causes for THR failure leading to revisions can be classified into three groups [64], [77]:

- Patient-related factors that predispose the event of infection and recurrent dislocation;
- Implant-related factors such as osteolysis and aseptic loosening, resulted from the mechanical failure or periprosthetic fractures;
- Failures related to inadequate surgical technique such as malpositioning of the components.

In uncemented total hip replacement osteolysis and aseptic loosening, resulting from the wear of bearing surfaces, are considered to be the most predominant problem of both cemented and uncemented acetabular components leading to revision surgery, accounting for approximately 75% of failed total hip replacements [78].

Aseptic loosening is generally accepted as being loosening in the absence of infection and can be the result of inadequate initial fixation or mechanical loss of fixation over time. Bone mass is maintained by a balance between the activity of osteoblasts which are the cells responsible for bone formation and mineralization, and osteoclasts which are the cells that degrade bone to initiate bone remodeling and mediate bone loss in pathologic conditions. Several studies concluded that bony ingrowth will only occur with relative micromotions of less than 150 μm between the implant and bone, while high values of micromotion limit bone growth and lead to instability over time due to an unstable primary fixation between the acetabular cup and the surrounding bone as well as lack of adequate bone fixation thereafter [60], [61].

Stress shielding of the bone near the interface of the acetabular components can also lead to aseptic loosening over time, resulting in component failure. As the density of the bone is determined by the long-term distribution of stress in joints, the increased stiffness of the implant's metal backing in comparison to that of the surrounding cortical and trabecular bone tends to alter stress distribution on the underlying bone while bearing a large portion of the weight bearing load [86]. It was found that metal backing of the cup tends to reduce stresses in the underlying bone at the dome of the cup and generate higher stress peaks at the cup edges [2], [80], [81].

In accordance with Wolf's law, which states that bone will adapt to the loads that are placed upon it, after a part of bone is replaced by an implant, a bone remodeling process occurs, changing its shape and internal structure to adapt to the new stress distribution. As bone density is maintained by mechanical stimuli, the adverse bone remodeling in THR leads to resorption of peri-prosthetic bone, which reduces cup stability and may finally result in implant loosening.

3. RELIABILITY OF GAIT PARAMETERS IN GAIT ANALYSIS

With life expectancy increasing, there is now an emphasis on sustaining an active lifestyle. Gait analysis is more often used to assist in identifying diagnostic measures in gait disorders or monitoring of the rehabilitation process by determining changes in gait patterns [82].

Complex clinical gait analysis usually includes kinematics, kinetics and electromyography that are fundamental for the purpose of characterizing gait patterns.

A kinematic gait analysis evaluates the movement of the lower extremities, the angles of their segments and the way in which they alter during walking [83]. Joint angle analysis is important because it enables to quantify the functional range of motion of the joint, describing the orientation of a given segment in relation to another.

There are several methods available to evaluate the human gait from a kinematical point of view [84]:

- electrogoniometry;
- ultrasound and electromagnetic tracking systems;
- optical (video based) systems;
- inertial systems.

Three-dimensional kinematical analysis enables the evaluation of gait from three viewing positions in order to better describe all the motions of the lower limbs:

- **sagittal view** to measure the flexion and extension of hip, knee, and ankle joints;
- **frontal view** to measure abduction and adduction of the hip joints and extremities, respectively, as well as the pelvic obliquity;
- **transversal view** to measure the rotations of the limbs.

It is well documented that, in the case of measuring systems using body markers, skin movement artifacts cause measurement errors that may affect accuracy [85], [86].

As three-dimensional human movement analysis requires the reconstruction of joint reference systems, another variable that is important in the determination of accurate angular parameters and consequently joint loads is the hip joint center (HJC) estimation.

The hip joint center is a fundamental landmark in the identification of lower limb mechanical axis, being the point with respect to which hip joint moments are calculated.

One of the main goals of the hip replacement is to preserve the integrity of the hip kinematics, therefore it is especially important to preserve the anatomical

center of the hip as errors in its location may lead to substantial inaccuracies in both joint reconstruction and in gait analysis.

A degeneration of the hip joint can lead to a reduction in the range of motion (ROM) of the joint. Therefore, in order to assess the outcome of rehabilitation programs, clinical interventions or degeneration progression, reliable outcome measures are essential. In the case of kinematic gait analysis, reliability refers to the amount of change in angular displacements that is dependent to measurement error and not actual improvement or deterioration of the gait.

Gait abnormalities are abnormal, uncontrollable walking patterns. They may be inherited or caused by other factors, such as diseases or injuries. Walking abnormalities may affect the muscles, bones, or nerves of the legs.

Table 5. Hip gait abnormalities and their underlying cause [87]

Hip motion abnormality	Cause
Excessive flexion	Hip flexion contracture, excessive knee flexion
Limited flexion	Weakness of hip flexors
Internal Rotation	Weak external rotators, femoral anteversion
External Rotation	Retroversion, limited dorsiflexion
Abduction	Reference limb longer
Adduction	Secondary to contralateral pelvic drop

This analysis represents a preliminary study on a healthy female, performing normal walking. The goal of the study was to develop a reliable and valid tool for evaluation of the hip joint mobility based on a 3D kinematic analysis in practical investigation routine in order to quantify how misestimating of anatomic landmarks, namely articular hip joint center, influence the results of hip joint angle trajectories during ultrasound-based gait analysis.

3.1. Methods

In gait analysis hip joint center location is usually estimated noninvasively based on the distance between external markers placed over bony landmarks at the pelvis, or by radiographic methods [88], [89], [90].

The goal of this research was to test if the default setting of the measuring system, estimating the HJC at 20% offset from the external marker placed on the greater trochanter, can represent a reliable option for estimation of HJC coordinates in gait analysis.

To accomplish this, the default apparatus method was compared with two other estimation methods: the greater trochanter (GT) method [91] that places the HJC at one-quarter of the distance from the ipsilateral to the contralateral greater trochanter and the radiographic method.

The measurements were realized in the Motion Analysis Laboratory of Politehnica University of Timișoara using Zebris measuring system CMS-HS that allows an objective three dimensional kinematic analysis of the human gait by means of analyzing the tracks of body surface markers.

The measuring method is based on the determination of spatial coordinates of miniature ultrasound transmitters, the spatial position of the markers being determined by triangulation [92].



Figure 38. Zebris CMS-HS Gait analysis system

After the anatomic landmarks are marked with the pointer, the dedicated software creates the geometrical model, as seen in Figure 39. The marker spatial positions (determined by trilateration) and geometrical model of the investigated subject are calculated and displayed during the subject motion, using the provided WinGait Software.

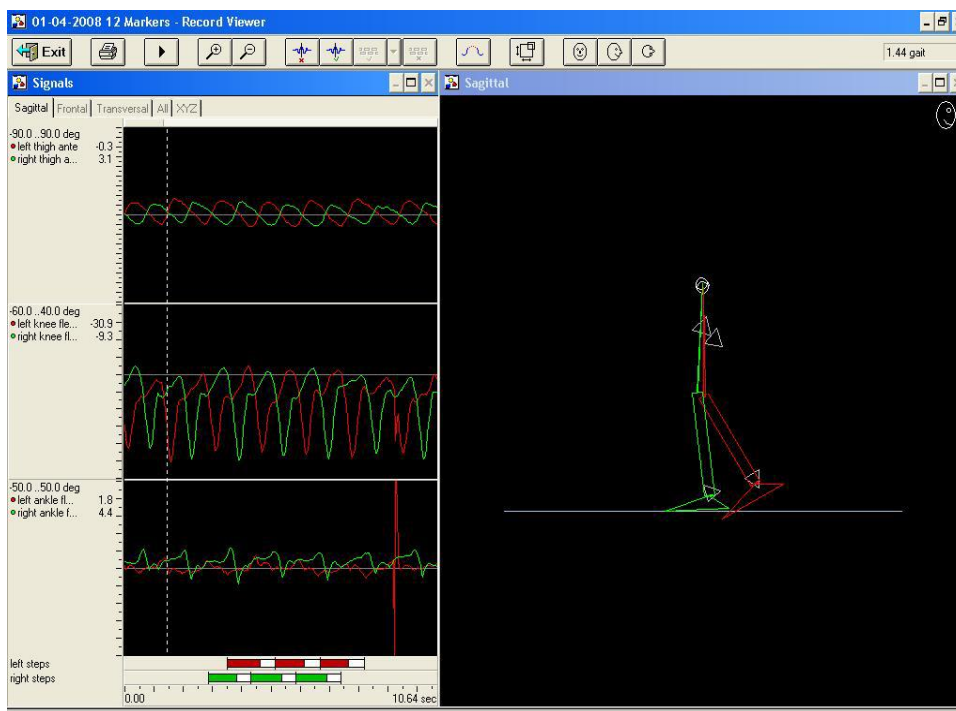


Figure 39. Geometrical model and movement graphs in Zebris WinGait software

The preliminary study was based on a healthy 30 year old female subject, with no previous history of musculoskeletal disease.

After the attachment of the ultrasound marker triplets and the definition of anatomic landmarks, the subject was advised to walk at a comfortable self-selected velocity and was allowed 5 minutes training time to get used to the marker attachments and walking range.

Under the mentioned condition, angular variation for each individual joint in all the possible movements (flexion-extension, adduction-abduction and rotation) were assessed in order to identify those influenced by the HJC location.

The study consists in three different scenarios: a default value of the hip distance of 60%, the value of 50% defined with the GT method and a value obtained using radiographic measurements (45%).



Figure 40. Detail of the radiographic method.

Caption from RadiAnt Dicom Viewer [93]

The radiographic measurements were made on an antero-posterior topogram of the subject that recently underwent a CT scan. The radiographical HJC location was estimated as the center of the optimal fit circle drawn over the femoral head. The distance between the two defined points yielded a ratio of 45% in relationship to the measurement of the distance between the skin points that are usually defined as the great trochanter position during gait analysis.

Three sessions of walking were recorded for each scenario in order to check the inter-trial reliability of kinematic gait parameters, with a sampling rate of 25Hz. Anatomical landmarks, marker position and calibration were kept unaltered during the analysis. From observing the data plots, the best cycle for each scenario was considered, resulting in 9 sets of data, paired for each scenario. This number of records was kept for all the movements in order to calculate the average. The lack in overlapping of the cycles indicates the variability of amplitudes and velocity during gait.

3.2. Data analysis

Subsequent data analysis was done for the motions of interest, hip movements, using SPSS 20 (SPSS Inc, Chicago, IL).

The reliability of the angular pattern was assessed using Pearson's r for each pair, as an inter-class correlation coefficient. As product-moment correlations only reflects reliability in the sense of parallelism of scores between data sets and did not offer quantitative measures, furthermore, the degree of agreement between the measurements of each pair was evaluated using a hypothesis test for equivalence, the intraclass correlation coefficient (ICC) [94], and Bland-Altman statistics [95].

ICC(2,1) measures the extent of absolute agreement or interchangeability of the methods(or scenarios in this given case), which is based on the two-way random-effects ANOVA.

$$ICC(2,1) = \frac{MS_S - MS_E}{MS_S + (k-1)MS_E + \frac{k(MS_T - MS_E)}{n}} \quad (1)$$

where MS_S indicates subjects mean square, MS_E indicates error mean square, MS_T indicates the trial mean square, n is the size of the sample and k is the number of methods [94], [96].

Thus, the intraclass correlation coefficient then provides a scalar measure of agreement or concordance between all the methods.

Bland-Altman analysis, also known as the method of differences, has been used for measuring the degree of agreement. With this method, the differences between the two settings (60% and 50%) and the radiological reference measurement are emphasized.

3.3. Results and discussions

As segmenting walking data into gait cycles resulted in different lengths data (1.2-1.4 seconds), it was necessary to use time-normalization technique. Thus, the experimentally recorded kinematic data's time axes were converted to an axis representing percentage of gait cycle.

After cycle selection and time normalization we were left with 9 sets of measurements, 3 for each investigated motion of the hip, namely flexion/extension, adduction and rotation.

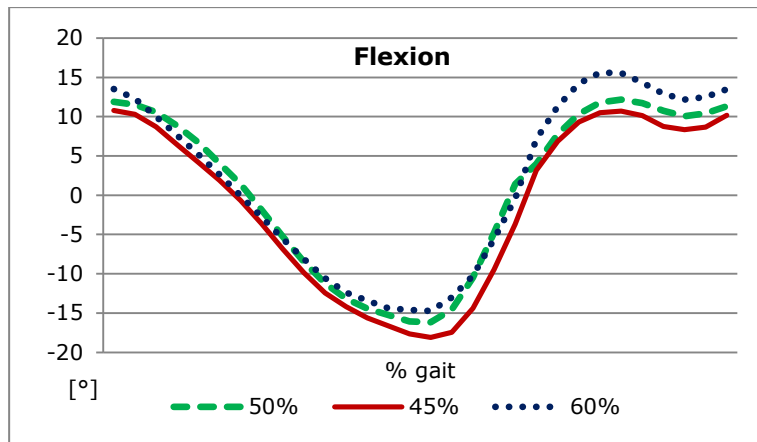


Figure 41. Initial angular variation profiles for hip flexion-extension

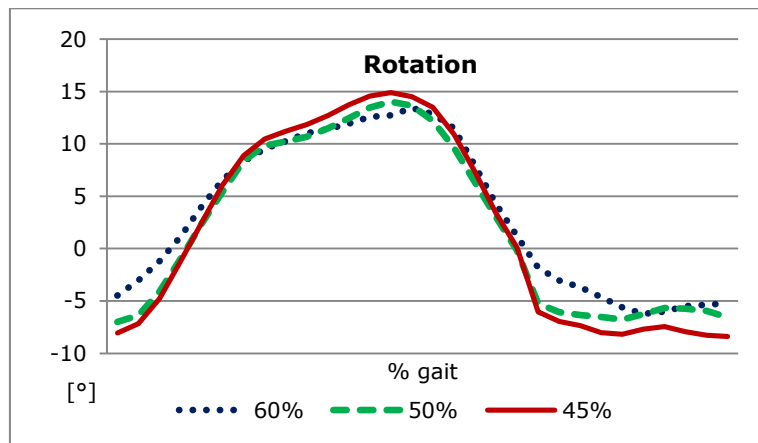


Figure 42. Initial angular variation profiles for hip rotation

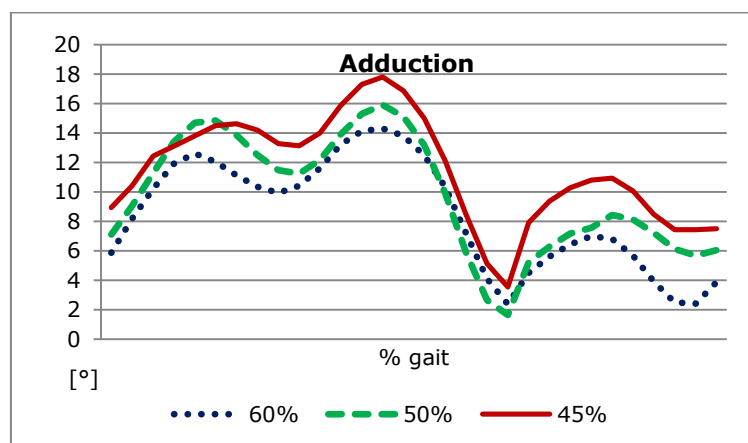


Figure 43. Initial angular variation profiles for hip adduction-abduction

Table 6. Analysis results: Pearson's correlation, ICC and Bland-Altman statistics

Movement	Group	<i>r</i>	ICC	Mean diff	SD_{diff}
Flexion	45%-60%	0.992	0.956	2.911	1.370
	45%-50%	0.993	0.976	1.969	1.225
Adduction	45%-60%	0.958	0.749	-2.935	1.136
	45%-50%	0.976	0.892	-1.727	0.948
Rotation	45%-60%	0.993	0.956	1.332	2.082
	45%-50%	0.998	0.991	0.178	1.167

As stated before, Pearson's correlation coefficients give information about the degree of association between two sets of data, and not reliability.

As we can see in Table 3, the measurement pairs are highly correlated ($p < 0.001$) despite a systematic difference of up to approx. 3° between scenarios. In this case, correlation reflects the extent to which measurements co-vary in identical testing situations. This is a measure that indicates a good agreement in time-dependent phases of gait between scenarios. This may be accounted for by the training previously undertaken by the subject.

ICC scores indicate strong (0.7-0.8) and excellent agreement (>0.8) between the tested pairs of measurements at 95% confidence interval.

Even though we notice that the overall results show a strong correlation, we could not conclude that the magnitude of the difference is acceptable in clinical use.

Thus, knowing that the data are linearly correlated, regression models were used to model the relationship between data pairs in order to predict the value of a variable from the value of another variable, using the formula:

$$Y = a + bX \quad (2)$$

, where Y is the predicted score, b is the slope of the line and a is the Y intercept.

These models were used as corrections for the data sets that are observed to have low agreement and, from these data sets predict new sets that closely resemble those of the radiological defined HJC.

After calculating the regression coefficients and new data sets were generated from the 50% and 60% scenario data on all considered movements. These sets represent predictions of the radiological results based on the results of the 50% and 60% after the correction, in this case noted 50%' and 60%'.

The predicted data sets were plotted against the 45% measurement set to illustrate the precision of the predictions, and consequently, the improvement in the amplitude disagreement of the measurements.

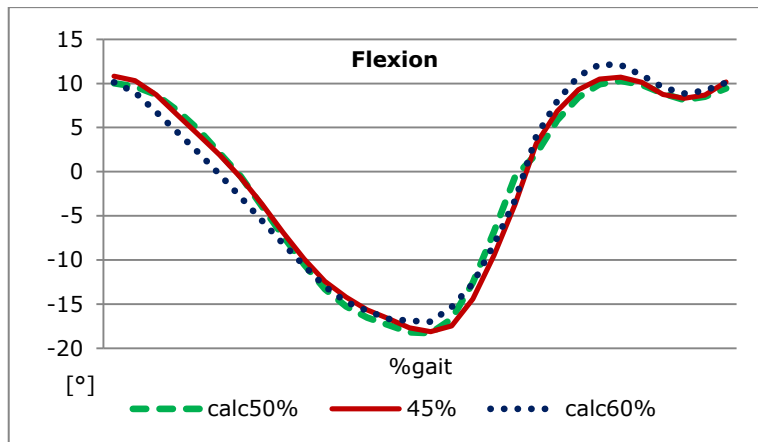


Figure 44. Angular flexion-extension variation profiles for processed data series

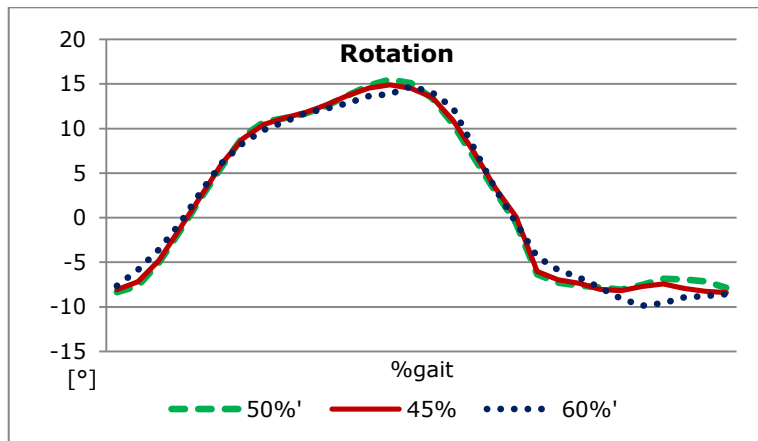


Figure 45. Angular rotation variation profiles for processed data series

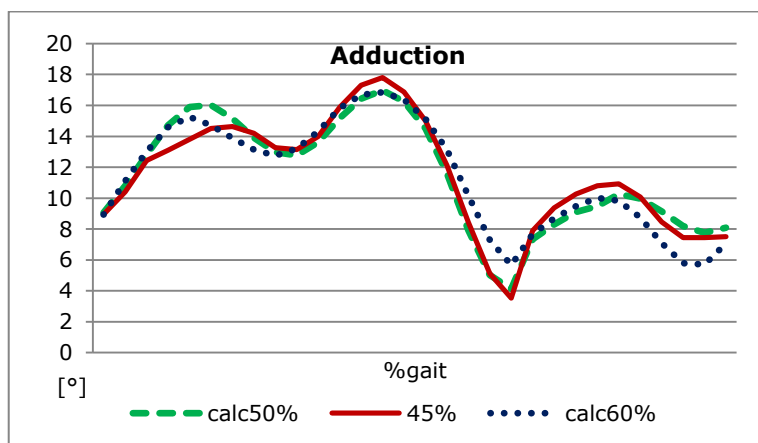


Figure 46. Angular adduction-abduction variation profiles for processed data series

The statistical calculations were redone for the new sets of predicted data in order to quantify the degree of agreement.

Table 7. Analysis results: Pearson's correlation, ICC and Bland-Altman statistics for the predicted data sets

Movement	Group	<i>r</i>	ICC	Mean diff	SD_{diff}
Flexion	45%-60%'	0.992	0.993	0	0.920
	45%-50%'	0.993	0.993	0	0.864
Adduction	45%-60%'	0.958	0.959	0	0.784
	45%-50%'	0.976	0.976	0	0.601
Rotation	45%-60%'	0.993	0.994	0	0.735
	45%-50%'	0.998	0.999	0	0.337

We notice that the mean difference of the newly generated data sets equal 0, suggesting that the prediction errors were equally distributed above and below the values of the reference data.

Also, an approximately 8% increase of the ICC (0.8-28%) was achieved using this simple method of prediction.

As expected, most of the improvement was in the case of adduction movement, which, for the initial data, had the lowest correlation indexes.

3.4. Concluding remarks

Our results demonstrate that different methods used to estimate the location of the HJC can produce rather different results in gait cycle kinematic analysis.

The intraclass correlation coefficient was used as an index of interchangeability between measures of the same patient, same methodology, in order to emphasize the influence of the estimation of HJC. In addition, the ICC and Bland and Altman results can be important for their clinical application, deciding whether the errors gave by misestimating the position of the HJC can be mistaken as changes occurred in the patient.

Based on the preliminary results, is clear that hip adduction-abduction has the greatest variability of all the outcome measures considered. Given the variations illustrated in this study, it must be concluded that the default hip distance setting of the apparatus may not be reliable.

When analyzing the processed data, we noticed that some of the systematic differences caused by the mislocation of HJC position were removed, the trajectory shape pattern dissimilarities being minimal after correction was applied.

The results of this method of correction suggest that even though the differences between the three scenarios were not statistically high, there is still room for improvement using simple statistical regression. This is reflected by the high correlation coefficients and low mean differences.

The main limitation of this study is the use of a single patient, and the validity of the considered method could only be demonstrated by increasing the size of subjects. In order to validate this method for clinical use, it would be necessary to combine the findings with data from test-retest reliability studies.

Knowing that the magnitude of difference is not a statistical decision, we would need to get a conclusive feedback regarding the clinical importance of the found differences gait analysis, and also research of the influence of this anatomical landmark calibration and propagation in joints situated lower on the limb, i.e. knee and ankle.

If the differences within mean \pm 1.96 SD are not clinically decisive, the methods of HJC position estimation may be used interchangeably.

Despite the study limitation of small sample size, the data provides preliminary evidence suggesting that as the estimation error of HJC increases, the agreement between the outcome measures decreases.

Future work will consist in growing a data base that would include patients of both genders and all ages, and, using noninvasive methods, generate a mathematical formula that would help the examiner to better estimate the position of the joint center.

4. COMPUTATIONAL STUDIES ON THE EFFECT OF GEOMETRICAL PARAMETERS ON IMPLANT PERFORMANCE

Clinical success of hip replacement depends upon achieving an adequate initial fixation and maintaining the fixation for a long term. As the incidence of hip replacement in younger and more active patients is increasing, prolonging the life of hip replacements becomes even more important.

Although hip replacement is a very successful procedure, one of the main reasons of THR failure is represented by aseptic loosening of the acetabular component. The data from the Dutch Arthroplasty Register (LROI) confirms this in the 2007-2011 and 2012 reports, stating that about 40% of revision surgeries were caused by loosening of the acetabular component, while femoral component loosening accounts for just 30% percent of failures [97].

Total hip prostheses aim to restore the natural biomechanics and loading of the natural joint, however, the insertion of metallic hemispherical acetabular components have been shown to disrupt the natural load distributions.

It is generally accepted that the development of aseptic loosening is caused by either focal bone loss (osteolysis) or regional bone loss. This adaptive bone remodeling phenomenon is known as stress shielding and relates to bone being shielded from load by stiffer metal implants.

The incidence of pelvic osteolysis when using cementless cups is mainly related to the quality and thickness of the polyethylene (PE) liner or the screw insertion site.

The use of advanced materials, such as highly cross-linked polyethylene or ceramic bearings seems to minimize the risk of osteolysis occurrence due to wear debris. The design factor is also of importance on the extent and distribution of peri-implant osteolysis, as the effective joint space and liner fixation mechanism can favor or inhibit wear debris flow to the bone.

While osteolysis is not likely to occur in short-term follow-up, bone mineral decrease immediately proximal to the press-fit acetabular implants has been attributed to an alteration in regional bone stress caused by the presence of the press-fit implants [98], [99].

This occurs when the elastic modulus of the implant material is significantly greater than that of bone resulting in the implant supporting most of the internal loads rather than the bone. The elasticity mismatch between the bone and the metal acetabular backing causes a change in the magnitude and distribution of stresses at the implant-bone interface. The main drawback represents the attenuation of bone stresses at the dome region of the acetabulum and generation of high stress peaks at the cup periphery relative to the normal joint.

As a dynamic tissue, bone density is maintained by mechanical stimuli and, in accordance to Wolff's law, an adaptive remodeling process will start in the underlying bone, process caused by the reduction of stimuli leading to osteoclast

resorption of bone to adapt to the new biomechanical environment. This implies external remodeling (geometry) and also internal remodeling (density adaptation) until the mechanical stimulus is normalized.

This remodeling process is known as retroacetabular stress shielding and may impair the survival of prosthetic components [80], [100]. As the location and amount of periprosthetic bone stock are critical factors determining the success of acetabular reconstruction, the changes in bone mineral density (BMD) adjacent to the implant are usually observed and quantified using dual energy X-ray absorptiometry (DEXA) or quantitative computed tomography (qCT) osteodensitometry.

Bone remodeling research studies attribute short-term post-op bone loss to retroacetabular stress-shielding. Using qCT analysis, Wright et al. [98] reported a 20% to 33% decrease of cancellous bone density at 1 year follow-up in a group of twenty-six patients who underwent primary hybrid THA. Subsequently, Pitto et al. [3] reported that periacetabular cancellous bone density loss (up to 34%) is higher than cortical BD loss in two patient cohorts undergoing THA with press-fit cups and soft and hard linings. Both studies cited demonstrate that the magnitude of stress-shielding is greatest immediately adjacent to the implant, most specifically the dome of the cup.

Moreover, periprosthetic fractures are an increasing problem as continuous bone loss proves to be disadvantageous for the long term success of THR.

A loose acetabular component will compromise proximal acetabular bone stock. Revision acetabular cups are therefore a bigger size and designed to replace the damaged zone in order to achieve initial stability from press-fit, making it harder to maintain the normal biomechanical behavior of the joint. Revision surgery is frequently complicated by periacetabular osteolysis as radiological images do not reveal sufficient information about the amount of osteolysis.

Thus, we hypothesize that periprosthetic acetabular bone remodeling after Total Hip Arthroplasty is a complex phenomenon that depends on several parameters: mechanical properties of the bone, fixation mode, implant geometry and stiffness [98] and modifications in the design of implant components would have beneficial effects on adaptive bone remodeling, aiming for a better long-term fixation and survivorship.

Geometrical parameters influence the performance of a hip implant significantly. These geometrical parameters are design as well as non-design related parameters. The long term success of an implant may be achieved by optimizing design related parameters. Improper selection of geometrical design parameters of acetabular components significantly increases the rate of implant failure. Consequently, the emphasis is put on those biomechanical aspects related to design and implantation procedure, which directly or indirectly influence the occurrence of loosening.

To help reduce the incidence of stress shielding, more research is needed to better understand the main contributing factors. To address the lack of understanding, this study evaluates the possibility of acetabular cup orientation and cup design as influential variables contributing to poor stress distribution to periprosthetic bone tissue.

The current study tests the hypothesis that malalignment of hemispherical acetabular components results in the alteration of the stress distribution pattern and optimize component orientation, and the second part analyses the design parameters of acetabular liner that may improve the pressure distribution.

This chapter is based on two own studies, Study I [101] that focused on the effect of acetabular component spatial orientation and Study II that focused on the effect of liner design on the periprosthetic pressures [102].

Based on the continuous progress of computers technology, graphical and mathematical models have been used more and more in clinical applications. Computer simulations allow in-vitro analyses, constructing 2D and 3D joint models and prosthesis, assigning material properties and physiological loads at points of interest. Thus, it is useful to evaluate the potential effects of various geometrical parameters without requiring a large patient population or numerous experimental tests.

4.1. Development of the hip joint model

4.1.1. Three-dimensional model reconstruction

Under the action of external loads a certain state of stress, strain, and deformation occur in both hard and soft tissues. In case of hard tissue such as bones deformation is small which allows using a linear deformation analysis. Deformations and strains appearing in the human body during daily activities can be determined or estimated using experimental or theoretical methods.

Numerical analysis based on Finite Element Method (FEM) is one of the most used methods to predict the biomechanical behavior of anatomical segments of human body. In order to get realistic results, due to the complex biomechanics of the hip joint, it is desired that the finite element analysis be accomplished with a three-dimensional model similar to the shape and architecture of the pelvic bone.

Thus, the purpose of this study was to develop a realistic three-dimensional finite element model of the pelvis and observe the stress variations of the periprosthetic bone under realistic loads.

In order to accomplish these objectives, a 3D model of the hip joint was reconstructed from Computer Tomography (CT) scans of a patient. The Digital Imaging and Communications Medicine (DICOM) images have been obtained in sequential mode with 1 mm resolution. The DICOM images are composed of pixels with varying shades of gray intensity, which correspond to different structures, including tendons, soft tissue, cortical and trabecular bone, and cartilage. The 3D reconstruction was accomplished using Mimics Innovation Suite 10.01 software and Solid Edge V 19 environment.

Using Mimics image-processing software, cortical and cancellous bone mask surfaces were automatically generated using density segmentation. Furthermore, thresholding was used to effectively separate the components of the CT scan based on their local bone mineral densities in order to construct the masks needed for the 3D reconstruction of the hemi-pelvis. Thresholding is based on Hounsfield units (HU) that evaluate a quantitative measure of radiodensity through linear transformation of X-ray attenuation.

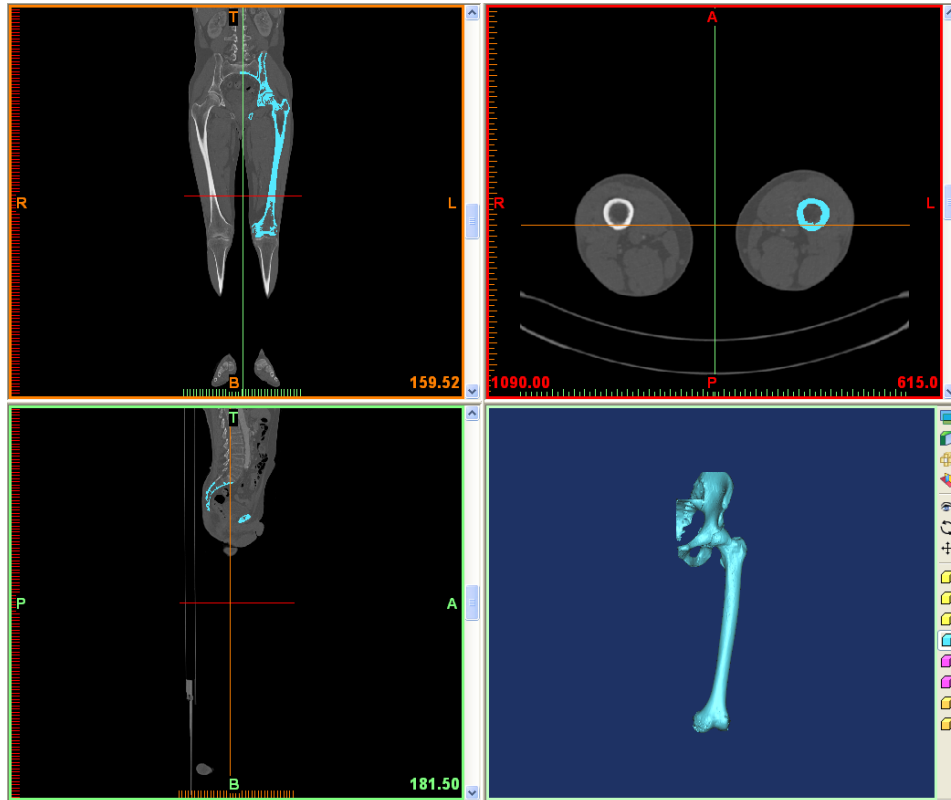


Figure 47. Selection of areas of interest in Mimics Software

To effectively separate both the bone tissue from any surrounding tissue further manual thresholding was done to reduce residual noise within the tissue interfaces and create separate masks for hemipelvis and femur. Afterwards, cavity fill tool was used to eliminate voids between pixels within the mask space.

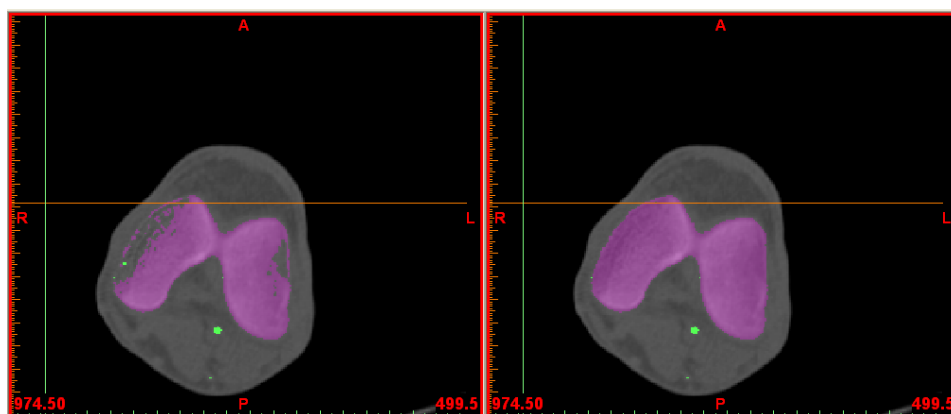


Figure 48. Manual contour and cavity fill

The region growing process allows splitting the segmentation into separate parts, each part corresponding to one mask that can be distinguished by the different applied color. In order to achieve geometrical separation, the adjacent masks must not be connected with any residual pixels.

Each mask was then used to generate a separate 3D reconstruction for both the considered bones, as seen below in Figure 49 and Figure 50

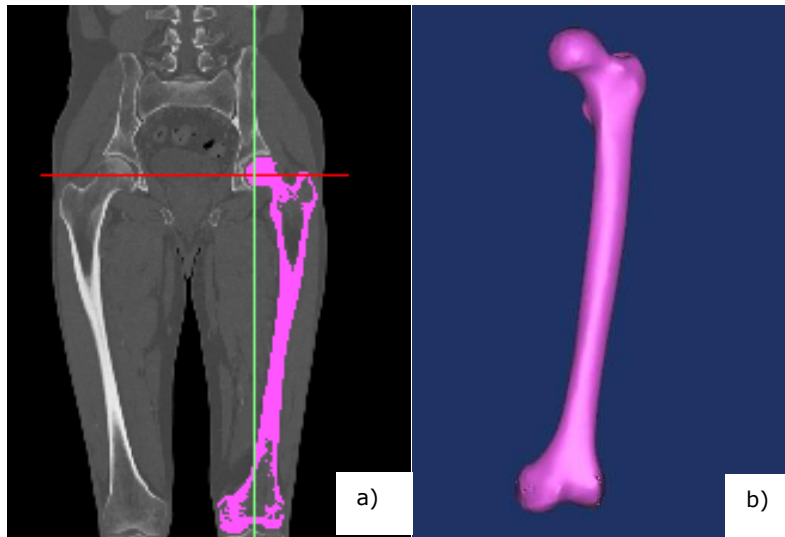


Figure 49. Segmentation of the femur: (a) fuschia mask of femoral bone tissue and (b) 3D model of the femur

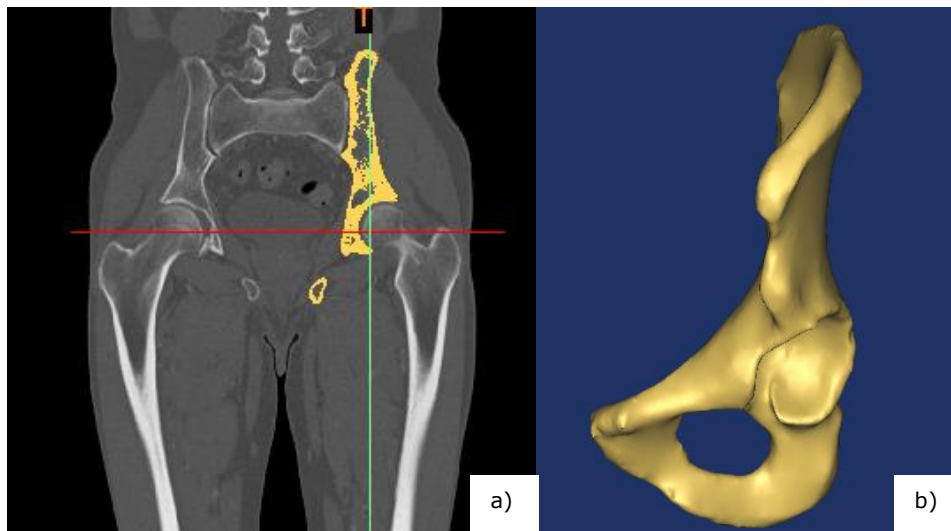


Figure 50. Segmentation of the hemipelvis: (a) yellow mask of the hemipelvic bone tissue and (b) 3D model of the hemipelvis

After obtaining the hip and femur masks, their 3D model interpretations were imported into Mimics Remesher module. As the Mimics 3D model based on the mask information contained a large number of triangles of various shape and size, the remesh module was used to significantly improve the quality of STL models (Stereolithography), allowing rapid transformation of irregular triangles in more or less equilateral triangles.

After this step, the triangles mesh presented more even in size and shape, while the number of triangle was significantly reduced.

Following triangle reduction, which was used to reduce the number of the mesh elements, the Auto Remesh tool was used to remesh the model using a maximal geometrical error of 0.15. The smoothing function was also used to decrease the number of nodes and elements required for the discretization of the finite element model.

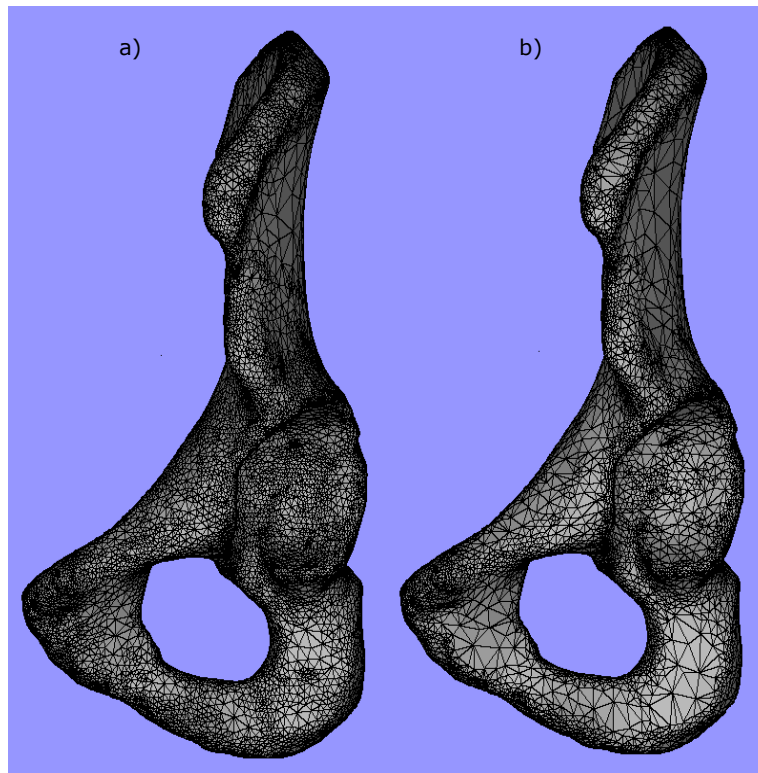


Figure 51. Hemipelvic 3D model before (a) and after smoothing and triangle reduction (b)

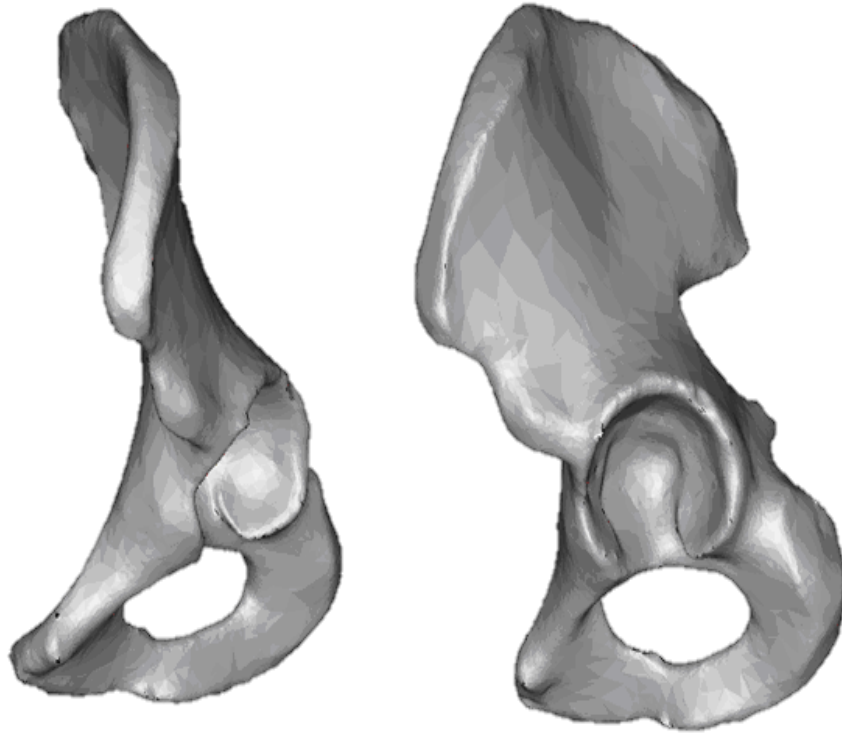


Figure 52. Completed 3D reconstruction model of the hemipelvis

Finally, the wrapped and smoothed hemipelvic bone reconstruction was exported to FEA software for further refinement and the creation of a tetrahedral volume mesh.

4.1.2. Finite element model

Usually, in order to quantify the difference in stresses between the natural hip and hip replacements in-vivo and finite element method tests are used. Considering the complex anatomical structure of the human pelvis, it is difficult to study its mechanical features in vivo. Furthermore, in vivo clinical measurements are invasive and change the natural joint structure.

Finite element (FE) analysis is a widely used, non-invasive method, relying on anatomical geometry and gait data to predict mechanical behavior of the implants and its influence on adjacent bone tissue.

The generated three-dimensional hemipelvic primary model was exported to a FEA package, Ansys Workbench v.11. The model was then prepared for the analysis by definitions of loads, boundary conditions, material constitutive models, kinematic constraints and mesh discretization processes.

This section enlists the parameters used to design the finite element model on which the studies are based.

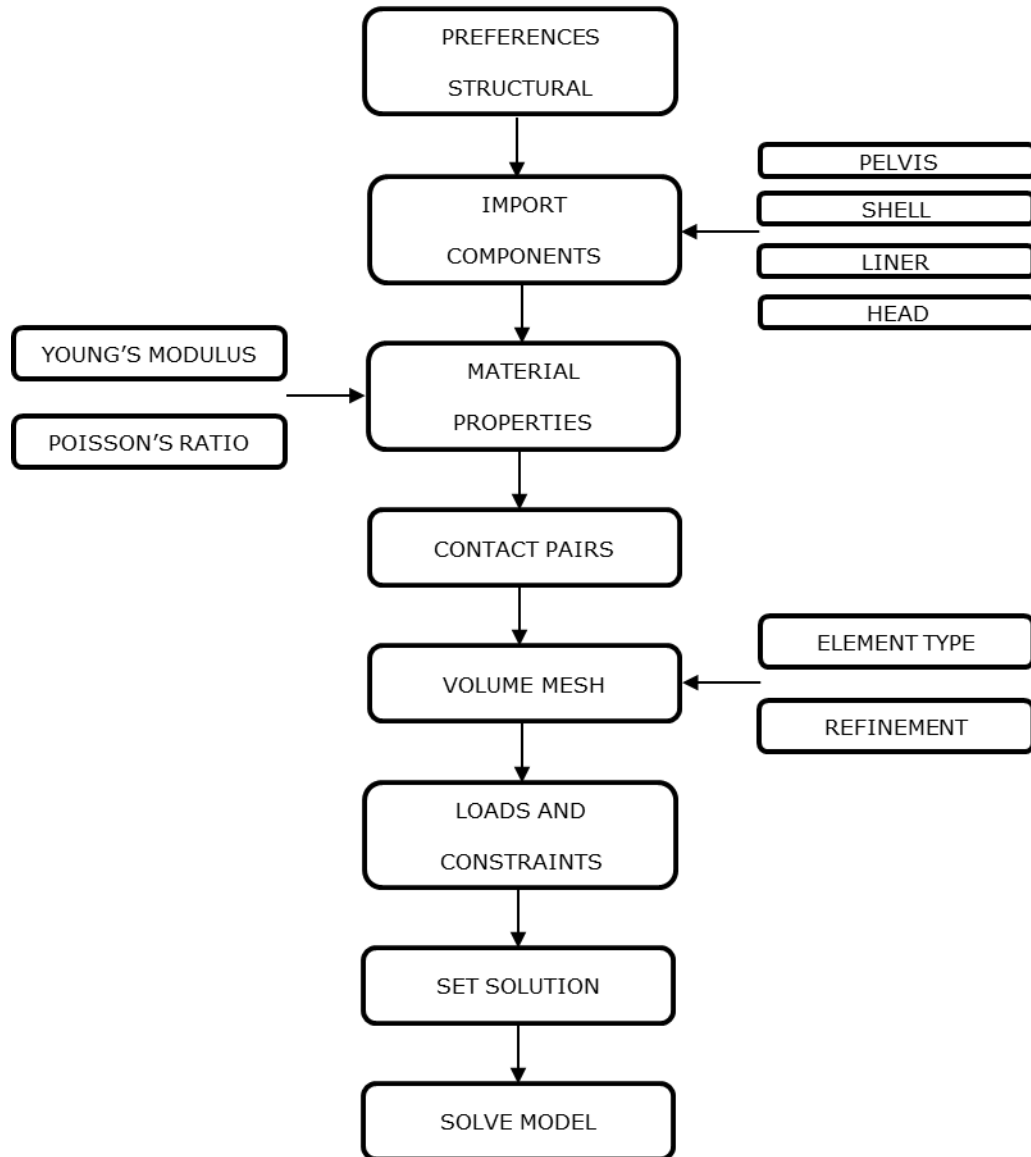


Figure 53. Necessary steps for FEA

4.2. Optimization of acetabular component orientation

One of the primary problems of long-term survival for total hip arthroplasty has been the behavior of acetabular component. Improper cup positioning may lead to reduced range of motion, impingement, increased polyethylene wear and a higher risk of dislocation [4], [5], [6], [103].

The acetabulum is generally spherical in shape and its orientation may be described by its abduction and anteversion angles. Abduction and anteversion angles can be observed in the coronal and mid-sagittal plane, respectively. Orientation can be assessed anatomically, radiographically, and by direct observation at operation [8].

Improper positioning of the acetabular component was defined as either a position more than 10 mm too cranial to the anatomical acetabulum, or an inclination of the component of more than 55° or less than 40° [104].

A malpositioned acetabular cup has is known to increase the risk of high wear rates and dislocations in total hip replacements. The differences in contact mechanics due to varying orientation of the acetabular cup may also significantly alter stress distribution in the acetabulum.

The study of Lewinnek et al. [105] presented recommendations for a spatial orientation safe zone of the acetabular cup (30-50° of abduction and 5° to 25° of anteversion) where the risk of dislocation may be reduced from 5% to 1%.

During hip arthroplasty, the acetabular abduction is often constrained by the available bone coverage resulting that the optimum range of acetabular anteversion must be found in order to establish an acceptable orientation. Additionally, the prosthesis must allow for an adequate range of motion at the joint.

Design of experiments (DOE) is an efficient approach useful in statistical experiment planning which identifies the most important experimental variables and establishes a relation between the independent and dependent variables to extract maximum information [106].

The aim of the study was to compare, using three-dimensional Finite Element Analysis (FEA), the state of stress in pelvic structures during walking for different acetabular orientations in order to find the influence of each positioning angle and combination and thus generate a mathematical optimization equation. The three-dimensional patient-specific reconstruction developed from CT scans was used to further explain the results of biomechanical testing and to create a full reconstruction of the intact hemi-pelvis, a reconstruction of the reaming process, as well as the effect of the prosthetic cup position.

This study examined these effects of acetabular orientation changes and their contribution to stress shielding using finite element analysis with the objective to create a mathematical formula that is able to calculate the peak contact stresses in the cup-bone interface.

4.2.1. Methods

Using SolidWorks 3D design software, a set of 9 different 3D models representing the prosthetic hips was created using the assumption that the contact surface between the pelvis and femur is spherical. The implant consists of a titanium alloy hemispherical shell with an outer diameter (OD) of 58 mm and a thickness of 4 mm, a polyethylene liner having 50 mm OD and 8 mm thickness and a titanium alloy ball of 34 mm in diameter.

For meshing of the structure tetrahedral type elements were used as this reduced the number of elements and nodes. Reduction in model complexity enables significant reduction in the computational time.

Meshing nodes were assigned at a certain density throughout the material depending on the anticipated stress levels of a particular area. To improve the analysis accuracy, a higher node density was demanded in the contact region. Therefore, a finer mesh was used at the interface surface near the acetabular cup, while a less refined mesh was utilized in distant areas of bone.

Model convergence was confirmed by comparing the von Mises stresses in one hip model with various mesh resolutions. The size of the elements on the two contact surfaces (acetabulum- implant) was progressively decreased until no important changes occur.

From the convergence study, it was seen that the model with a maximum mesh size of 2mm in the region of interest, i.e. periprosthetic tissue, provided satisfactory results. Therefore, the hemipelvic model was used for computational study having a mesh that consisted of approximately 87,000 tetrahedral elements and a volume of approximately 335.000 mm³.

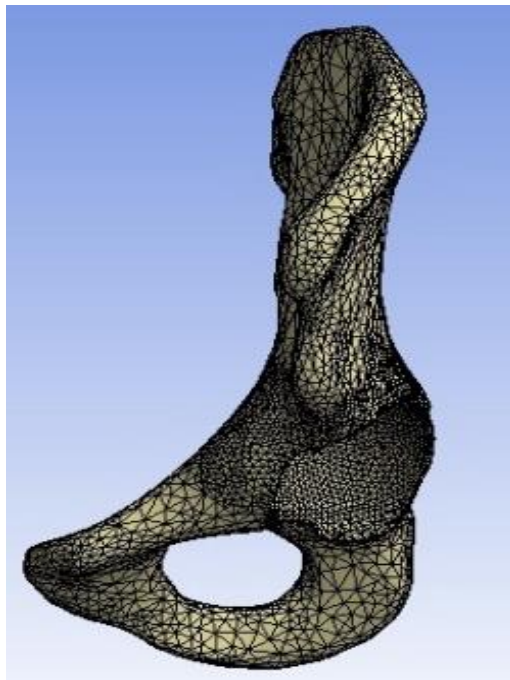


Figure 54. Meshing detail: tetrahedral elements (86874), contact sizing of 2 mm in the area of interest, edge proximity refinement in the pelvic part

Boundary conditions were chosen close to those anatomically existing. To simplify the constraining procedure flat surfaces were generated in the CAD software in the areas where the pelvic bone comes in contact with other structures in the normal anatomy.

To simulate the normal hip movement the nodes located in the sacro-iliac joint area were restrained for two degrees of freedom, translation along Y and Z axis and the nodes in the pubic symphysis area were restricted to move along X axis (Table 8). The displacement values were chosen by testing multiple options and keeping the ones that had the least influence on the results in the zone of interest.

Table 8. Anatomic position and characteristic of restraining areas

Boundary conditions	Position	X axis (mm)	Y axis (mm)	Z axis (mm)
Displacement	Pubic symphysis	0	-	-
Displacement 2	Sacro-iliac joint	10	0	0

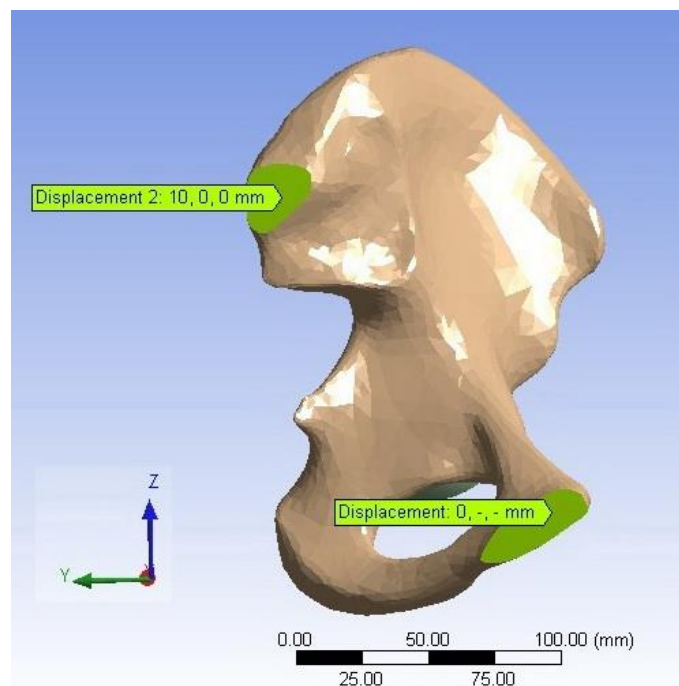


Figure 55. Definition of boundary conditions of the hemi-pelvis

The model representing the normal hip anatomy was created using the assumption that the contact surface between the pelvis and femur is spherical and articulation between the femoral head and the acetabular socket is concentric.

In order to realize this concentricity, a boolean subtraction was performed to simulate acetabulum was reaming. The relative sliding between the prostheses and bone were not taken into account, thus these interfaces of acetabular prostheses were considered to be fully bonded.

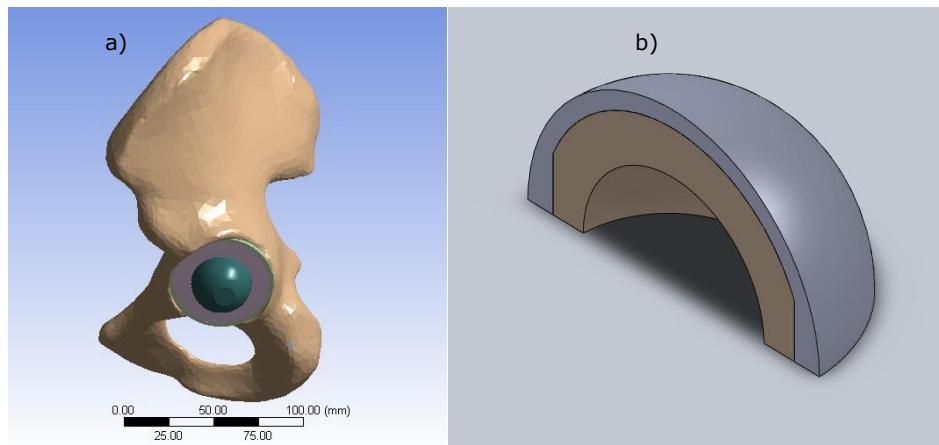


Figure 56. Lateral view of the prosthetic hip model geometry and section view of the cup/liner assembly: Shell (58mm OD, 4mm thickness), liner and a 34mm diameter Prosthetic head

The magnitude and direction of the resultant force were taken from previously published in-vivo hip telemetry measurements (maximum load during walking for a subject with a body weight of 1000 N, resulting in a hip force of 3761 N in the superior direction, 873 N in the medial direction, and 541 N in the posterior direction) [107]. As the center of gravity passes directly through the hip joint and into the center of the femoral head of the femur, the considered forces were applied through the center of the prosthetic ball.

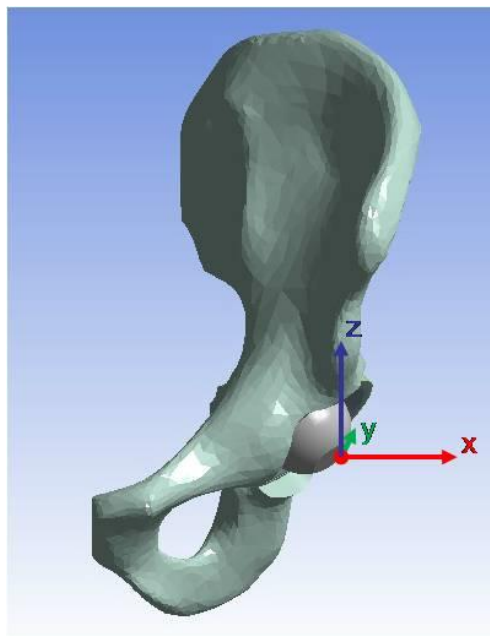


Figure 57. Force application position and its component coordinates

Regarding the material properties of each considered component, all materials (Subchondral bone, Polyethylene, Titanium alloy) were assumed to be isotropic, linearly elastic and homogenous. The values of the mechanical properties of the bone tissue and were taken from literature [108].

Table 9. Material properties of the assembly bone-implant

Material	Elastic modulus [MPa]	Poisson's ratio
Polyethylene	1100	0.42
Titanium alloy	96000	0.36
Subchondral bone	2000	0.30

In order to achieve a reliable comparison of the different scenarios, the boundary and loading conditions were constant throughout the computational study.

4.2.2. Experimental design

Based on the safe zone defined by Lewinnek et al. [105], a multifactorial experiment design was created using StatGraphics Centurion statistical analysis software to evaluate the effects and possible interaction factors.

The main purpose of the experiments is planning to establish a causal link between the independent, dependent variables and experimental research objective determining optimal experimental model with the minimum number of experiments. An optimal factorial experiment aimed at determining the data required for calculation defined a polynomial model which contains information on the effects of factors influence the objective function and the intensity of interactions between influencing factors [106]. Mathematical relationship of the experimental model contains all the information obtained from the factorial experiment.

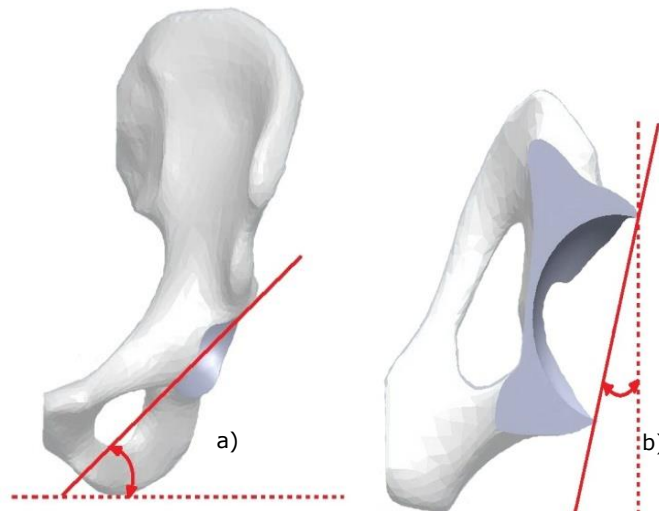


Figure 58. Anteroposterior pelvic view showing the inclination/abduction angle (a) and axial view revealing the anterior rotation/anteversion angle (b)

Normally, to highlight the influence of acetabular component orientation on the implant-bone contact pressures and assess the optimum orientation a great number of experiments should be performed.

The experiment was assigned a number of two experimental factors (abduction and anteversion angles) with three variation levels (inferior, superior and a centerpoint) and one 'to be measured' response variable (maximum contact pressure).

This resulted in a single block multifactorial design consisting of 9 experimental runs based on the combination of the variable variation levels.

	BLOCK	Abduction angle degrees	Anteversion angle degrees
1	1	30	5
2	1	30	15
3	1	30	25
4	1	40	5
5	1	40	15
6	1	40	25
7	1	50	5
8	1	50	15
9	1	50	25

Figure 59. Single block experimental matrix. Caption from StatGraphics software

A two-factor interaction model was used in order to assess the combined factor effect alongside each individual factor effect on the response variable.

To assess the effect of the implant positioning, a contact analysis was carried out for each implant position.

4.2.3. Results

Using the matrix obtained by experimental design (Figure 59), the contact pressures of bone-implant interface in all scenarios were determined.

The FEA suggests that peak contact stresses range between 5.6 and 16.0 MPa for the selected hemispheric cup and liner, depending on the abduction angle and the anteversion angle.

Two design variables were used, the angle of abduction of the acetabular component and angle of anteversion, respectively. The design objective was to minimize the peak contact pressures in the prosthesis-bone interface in order to delay or prevent cup loosening due to stress shielding.

Table 10. Simulation results for the specified scenarios

x₁- Abduction angle [°]	x₂- Anteversion angle [°]	y- Peak contact pressure [MPa]
40	5	5.623
40	15	9.738
30	25	15.545
50	25	16.029
50	5	7.365
30	15	11.642
30	5	9.118
40	25	14.805
50	15	15.586

Verification of the hypothesis that the distribution of von Mises stress between adjacent finite element nodes on each surface was not different from normality was performed using StatGraphics software. Of particular interest were the standardized skewness and standardized kurtosis, which can be used to determine whether the sample comes from a normal distribution. In this case, the standardized skewness and kurtosis values are within the range expected for data from a normal distribution.

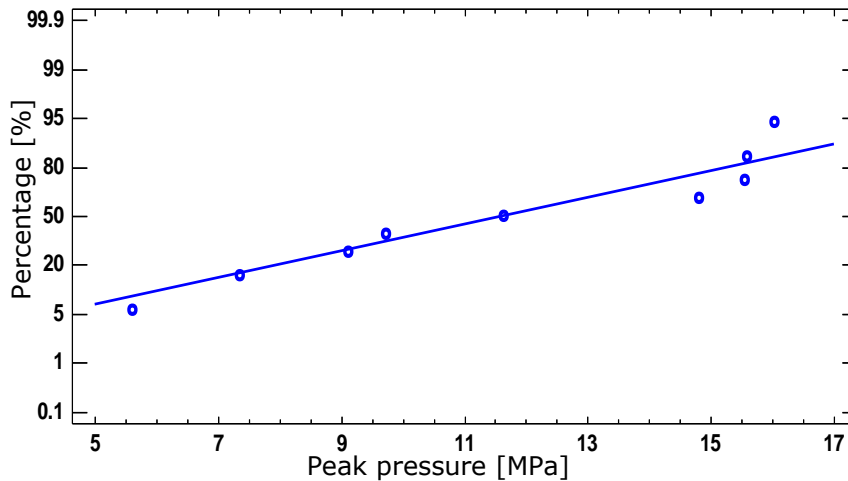


Figure 60. Normal probability plot

The results for abduction and anteversion indicate a strong relationship between orientation and contact stress. These apparent effects of orientation were further supported by analysis of variance (ANOVA). The Main Effects Plot shows the average outcome for every value of each variable, combining the effects of the other variables as if all variables were independent.

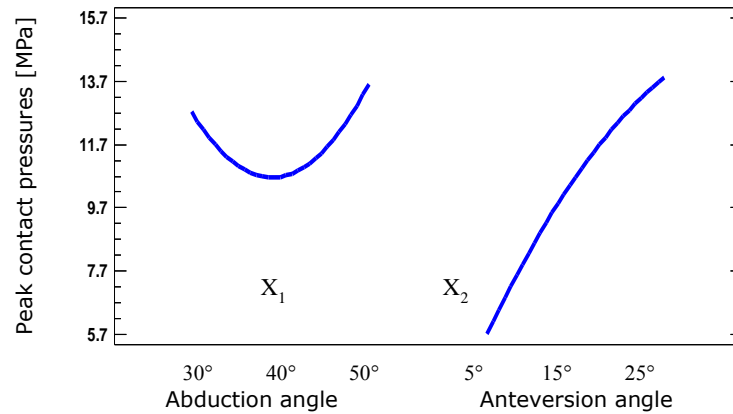


Figure 61. The main effect plot suggests that the anteversion angle effects are larger than the abduction angle effects on the contact pressures

Table 11. Correlation matrix for the selected variables showing Correlations, Sample Size and P-Value

	Abduction	Anteversion	Peak pressure [MPa]
Abduction		-0.3151	-0.0381
Anteversion	-0.3151		0.8942
Peak pressure	-0.0381	0.8942	
	0.9353	0.0066	

This table shows Pearson product moment correlations between each pair of variables. These correlation coefficients range between -1 and +1 and measure the strength of the linear relationship between the variables. The third number in each location of the table is a P-value which tests the statistical significance of the estimated correlations. P-values below 0.05 indicate statistically significant non-zero correlations at the 95.0% confidence level.

One of the methodologies that can help to reach the goal of optimum response is referred to as Response Surface Method. This method, introduced by Box and Wilson [109], is used to predict or optimize the response variables by examining the relationship between the response and the factors affecting the response. The main idea of this method is to use a set of designed experiments to obtain an optimal response.

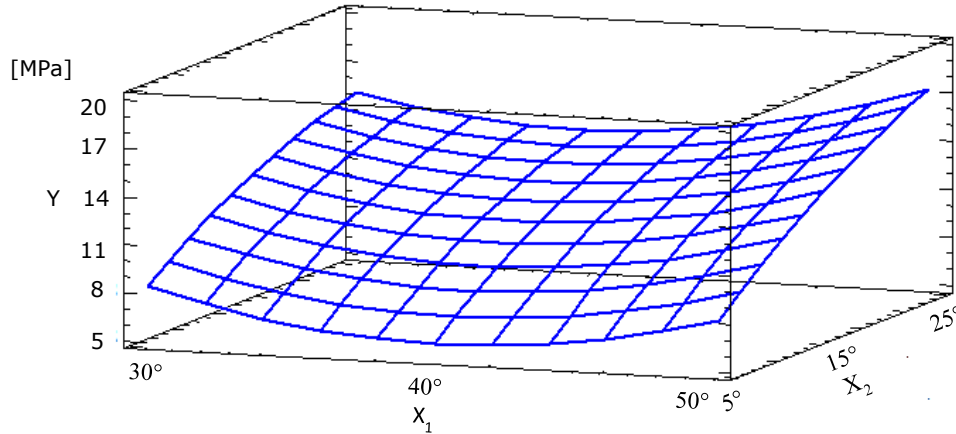


Figure 62. Graphical representation of the Response surface revealing the influence of independent factors x_1 (x axis) and x_2 (y axis) on the response y (z axis)

$$y = \beta_0 + \sum_{i=1}^k \beta_i x_i + \sum_{i=1}^k \beta_{ii} x_i^2 + \sum_{i < j} \beta_{ij} x_i x_j + \varepsilon \quad (3)$$

, where ε represents the level of noise (standard deviation) or error observed in the response y .

The regression equation including all the independent factors and their interaction which have been fitted to the data was subject to a backward elimination procedure. The backward method involves starting with all variables, deleting the least influential variable, and repeating this process until no further improvement is possible.

The equation of the fitted model is:

$$y = 40.568528 - 1.945433x_1 + 10.677167x_2 + 0.024873x_1^2 - 0.009077x_1x_2 \quad (4)$$

The R-Squared statistic indicates that the model as fitted explains 91.1% of the variability in the response y .

The adjusted R-squared statistic, which is more suitable to compare models with different numbers of independent variables, is 82.21%. The Durbin-Watson (DW) statistic tests the residuals to determine if there is any significant correlation based on the order in which they occur in the data file. Since the P-value is 0.02234, which is less than 5.0%, there is an indication of possible serial correlation at the 5.0% significance level.

4.2.4. Concluding remarks

The finite element analysis suggests that peak contact stresses range between 5.6 and 16.0 MPa for the selected hemispheric cup and liner, depending on the abduction and anteversion angles. This pressure interval is within the yield strengths reported in literature for human bone tissue [110]. However, these pressures were generated with the use of only one hip load representing the stance

phase of normal walking of a 1000 N individual.

Higher hip loads are generated during stair-climbing, stair-descending, and more strenuous daily activities [107].

The data of Hodge et al. also revealed up to 18 MPa cartilage pressures, non-uniform, with abrupt spatial and temporal gradients [111].

Results for the implanted acetabulum model showed that changes in component orientation caused substantial differences in contact stress. Analysis of the resulted values found that stress magnitude was mostly affected by the variation in cup anteversion, respectively increasing with increasing anteversion. With an orientation change of 5° of the anteversion angle resulting in an average peak stress difference of 29.2% (25.4-33%), contact stress demonstrated increased sensitivity to component orientation. From these results, it was concluded that acetabular cup orientation influences stress shielding which is determined by strain distribution. Therefore, greater emphasis is needed on obtaining the optimal acetabular cup orientation during surgery to prevent stress shielding effects and subsequent device failure.

Data analysis by response surface method revealed that the magnitude of periacetabular pressures was significantly reduced by the anteversion angle at its lowest value as well as the abduction angle located at the central point.

The results suggest that the higher pressures generated by higher abduction angles can be attenuated by appropriate anteversion. Overall, the results suggest that cup abduction angles at or around 40° and 5° anteversion provide the optimal combination of adequate pressure distribution and low peak contact pressures.

A fully developed analysis would require consideration of individual patient factors. That is why we must not conclude that placing the acetabular component into an average position is ideal for every patient.

The main limitation of the present study is that it is based on a single load scenario and for an individual bony geometry. Differences between previous studies and the present study may be explained by the differences in acetabular component shape, material properties and loading protocols used in the numerical analyses.

In order to be able to extrapolate the results, a greater number of patients must be scanned and tested under different loading conditions.

Nevertheless, we believe that the limitations did not greatly influenced the purpose of this study to develop a method that could help place the acetabular component in the optimal orientation to insure the best outcome for an individual patient.

4.3. Influence of acetabular liner design

The most common cause of implant dislocation following THR is represented by implant impingement, its incidence being as high as 6%. When the neck impinges on the socket at extremes of flexion, extension and abduction cause the head to lever out of the socket [112].

The reduced range of motion (ROM) following hip replacement leads to frequent prosthetic impingement, which may limit daily living activities and cause subluxation and dislocation.

To address this issue, elevated-rim acetabular liner designs are used as a potential means of improving stability after total hip arthroplasty as it has been shown that an optimally oriented component with elevated rim tends to improve joint stability. Several researches evaluated the effect of acetabular cup design, Cobb et al. demonstrating significant reduction in dislocation probability with the use of elevated-rim liners compared to standard ones [113], [114].

Although acetabular components with an elevated rim proved to improve the postoperative stability of a total hip prosthesis, the long-term effects of the elevated liner on wear and loosening are unknown.

The aim of this study was to understand the influence of the design parameters of the chamfered liners, which are primarily designed to increase the range of motion of the hip joint and reduce the risk of impingement, on the acetabular contact pressures.

Therefore, implant-bone interface contact pressures produced by different acetabular liner geometries were analyzed using Finite Element Method. The cup models consist of hemispherical metal shells fitted with normal and different chamfered polyethylene liner geometries, with the same degree of femoral head coverage.

Three-dimensional computational models of the bone-implant assembly were used to simulate periprosthetic bone loading and test polyethylene liner design parameters that would allow a more physiological load transfer to the surrounding bone, reducing the likelihood of component failure. We have investigated the effect of variations of the geometry of acetabular liner components on the pressure transfer patterns, specifically looking at the chamfer angle, while maintaining constant head coverage.

Furthermore, from another point of view, the study of the state of stress in the hip joint might prove to be helpful in a preoperative planning.

4.3.1. Methods

The disadvantages of less than hemispherical cups, regarding decreased bearing surface and ROM, were opposed by retaining the same head coverage for all designs, creating a chamfered rim elevation up to a full hemispherical outside shape.

This study proposes combinations of cup depths and chamfer angles of the bearing liner inspired from sub-hemispherical designs of metal-on-metal prostheses. Two design profiles of the liner models have been studied: 170° design and 165° design.

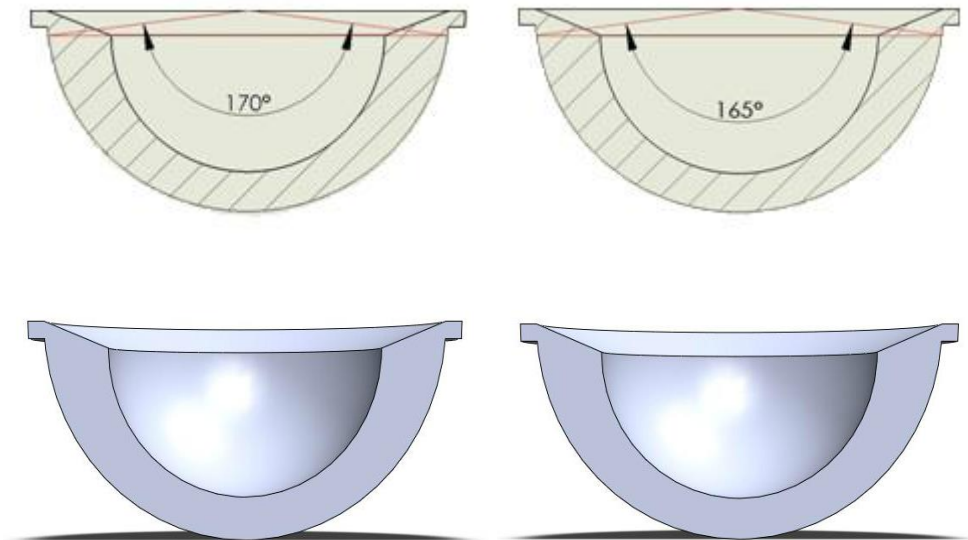


Figure 63. Geometric profile details of the proposed liner models: 170° design and 165° design

Since diminished functional bearing surface can lead to improper edge loading and diminished lubrication [115], the current design challenges these problems by building up from a sub-hemispherical liner, moving the center of rotation of the femoral head deeper in the acetabular component, in an attempt to encourage a more uniform loading.

Throughout the performed simulation, several basic design parameters were set as constants: the metallic shell design, the femoral head design and femoral head coverage, while the liner chamfer angles/design were altered so that the consequent changes in the simulated bone loading could be analyzed.

The reconstructed FE model human hemipelvis was adapted to include a non-cemented acetabular cup. The prosthetic model used consists of a pelvic part with an enlarged acetabulum simulating acetabular reaming, the prosthetic cup and a femoral ball.

The baseline model consisted of a 28 mm diameter femoral head, a hemispherical acetabular shell of 58 mm outer diameter (OD) and a 52 mm OD liner. All the cups were positioned at an orientation of 40° lateral abduction and 15° anteversion, well within the safe zone set by Lewinnek's studies. Also, our previous study reported that this cup orientation generates peak contact pressures situated in the mid zone of those tested in the Lewinnek's interval, considering a hip load generated during normal walking [101].

The region of interest for the analyzed model was the periprosthetic region between the acetabular shell and the acetabulum. The biomechanical performances of the proposed designs were evaluated in comparison with the normal hemispherical design. The titanium cups were assumed to be completely bonded to the peri-prosthetic bone, simulating full bone ingrowth.

Table 12. Meshing and mass details of the assembly components

Part Name	Material	Volume(mm ³)	Nodes	Elements
Head	Titanium alloy	20525	5245	3453
Shell	Titanium alloy	17644	5131	2307
Liner	Polyethylene	23020	1546	758
Pelvis	Subchondral bone	334645	74770	48207

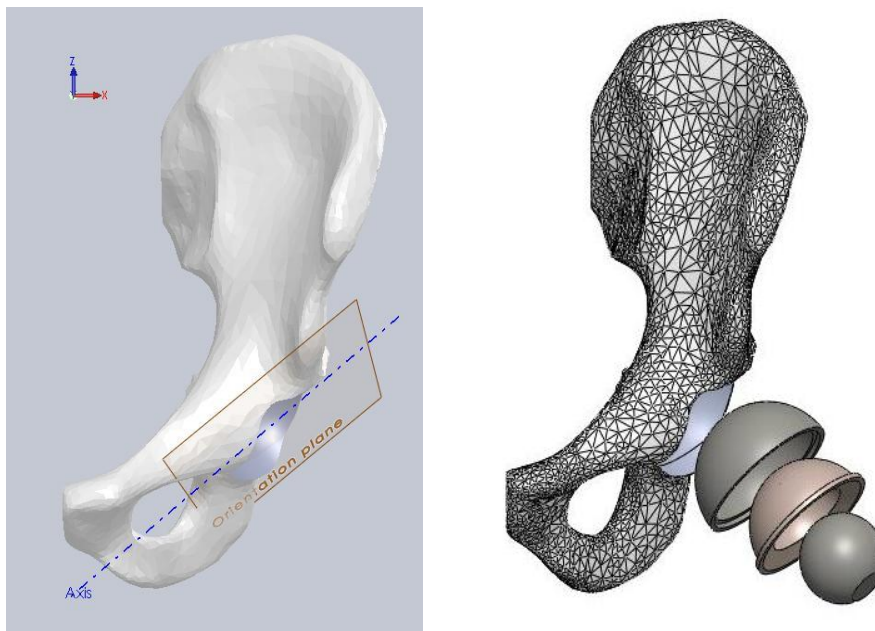


Figure 64. AP view of the orientation plane and exploded view of the hip-implant assembly

The materials of the analyzed artificial hip joint components were assumed to be homogenous, isotropic and linearly elastic. The femoral head and acetabular shell were assumed to be made of titanium alloy, while the acetabular liner was assigned polyethylene material properties. The values of elastic modulus and Poisson's ratio of the proposed materials were taken from literature and Ansys material library, being summarized in Table 9. Material properties of the assembly bone-implant

The loads used correspond to the most frequent activities of daily living. The used load values and directions represent the peak values from in-vivo contact measurements using telemeterized hip endoprotheses based on published data by Bergmann [107].

Apart from normal walking (peak 3900N), that was used in the first part of the study, the two most strenuous activities were analyzed, going upstairs and going downstairs (peak 4200N). These values represent loads for a subject with a body weight of 1000N.

Table 13. Details of the loading forces

Activity	Force (N)				Description
	X	Y	Z	Resultant	
Walking	-873	-540	3761	3898.57	Walking at normal speed on level ground, average speed:3.9km/h
Going upstairs	-985	-1025	3951	4198.96	Walking upstairs, stairs height 17cm, no support at hand rail
Going downstairs	-776	-613	4082	4200.08	Walking downstairs, stairs height 17cm, no support at hand rail

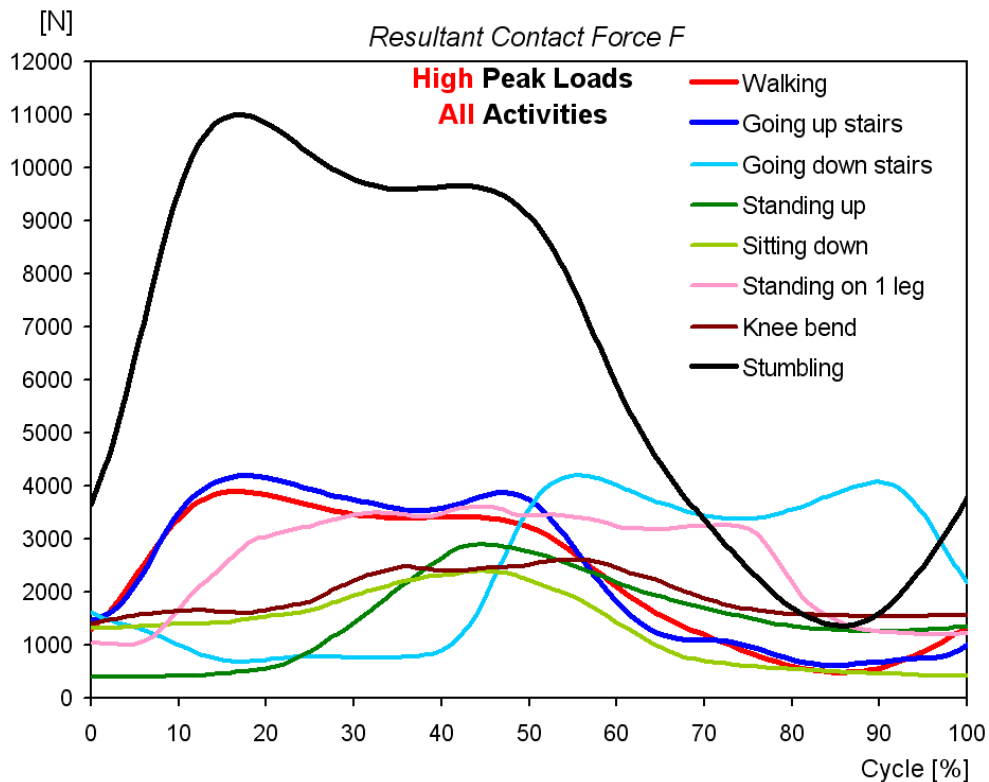


Figure 65. Bergmann's et al. graphical representation of hip joint peak loads during daily activities.
Caption from orthoload.com [107]

The loads were applied directly to the center of the ball representing the femoral head. To guarantee uniformity, the same kinematic position and loads were applied to each model.

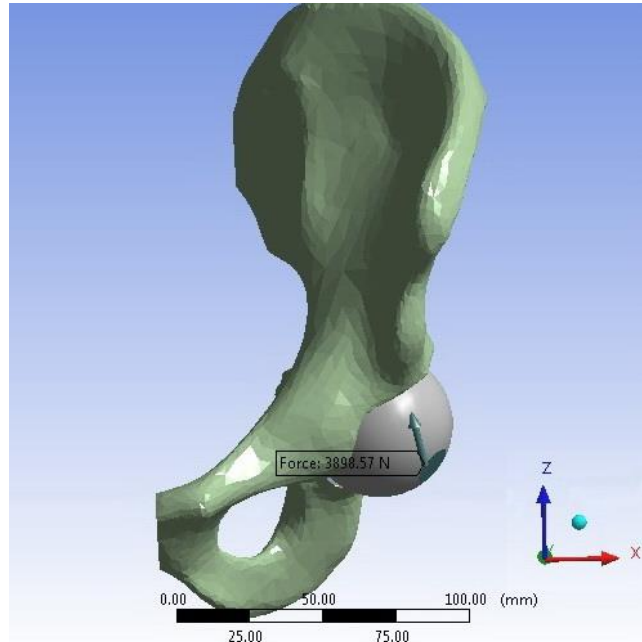


Figure 66. Force application on the finite element model

To simplify the boundary conditions, the hemipelvic model was fully constrained, being fixed at the pubic symphysis and at the sacroiliac joint.

The contact interface between the UHMWPE liner, metal backing shell, and pelvic bone was considered as completely bonded surfaces. Finite Element Analyses (FEA) of each individual implant design were then conducted.

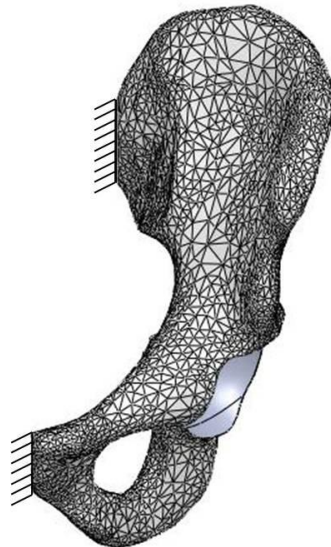


Figure 67. Boundary areas of the fully constrained hemipelvic model

4.3.2. Results

We evaluated the computed models based on the effects of the contact pressure on the periprosthetic acetabular surface, trying to reduce the maximum pressure values and therefore to get more physiological contact stress distribution. For all the tested models, namely full hemispherical or chamfered liner, the greatest pressure concentrations ranged between 14 and 23MPa.

Contact pressure and equivalent Von Misses in the prosthetic joint model were determined. The following figures illustrate the results from the Finite Element Analysis in the critical region inside the acetabulum for the three considered load cases (walking, going upstairs and downstairs). The von Misses stress consisting of all the individual stress components is non-directional and is a measure of the stress intensity.

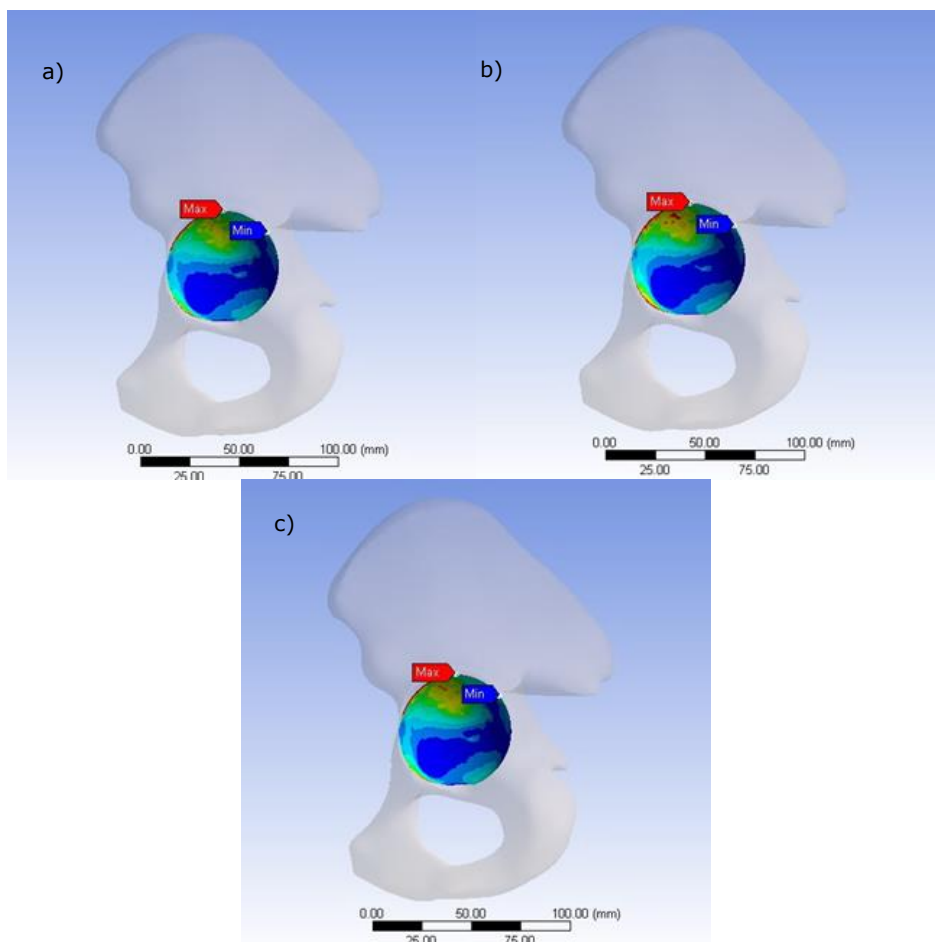


Figure 68. Contact pressure distributions in the acetabulum under loads corresponding to (a) normal walking, (b) walking upstairs and (c) stair descending

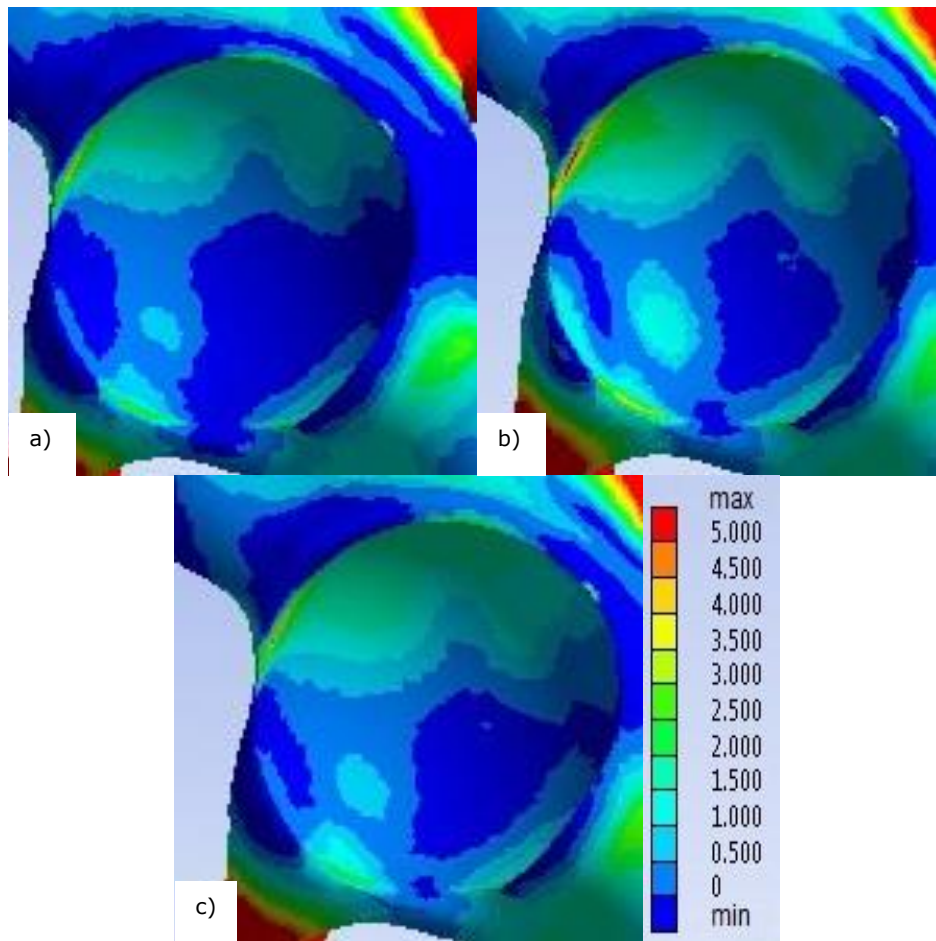


Figure 69. Equivalent von Mises stress distribution (lateral view) in the prosthetic joint: (a) normal walking, (b) walking upstairs and (c) stair descending

Contact pressures between the acetabular component and the bone model occurred more predominantly around the periphery of the acetabulum, as shown in the contour plots of the contact pressure distribution.

The values of stress during stair climbing and descending phases were obviously higher than that during walking, but there were no significant differences within the same group. A comparison of maximum values of contact pressure between the three prosthetic hip joint designs is presented graphically in Figure 70.

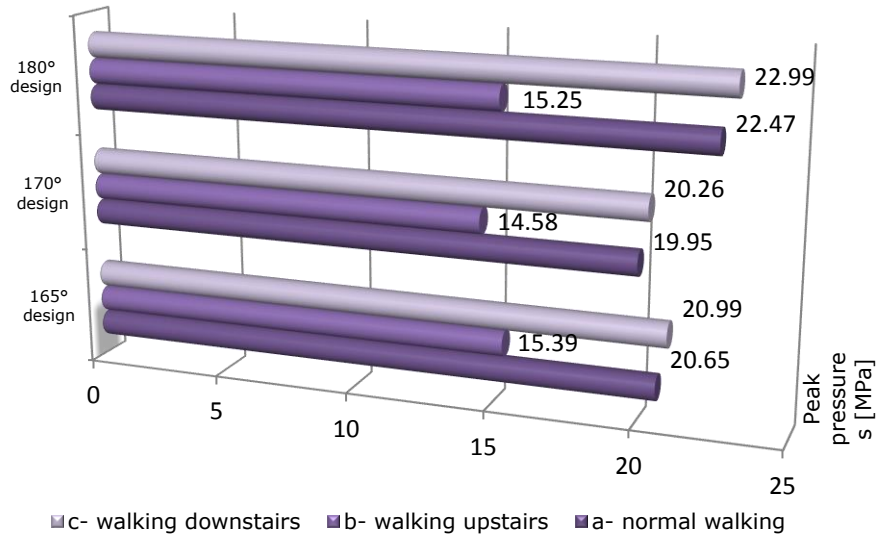


Figure 70. Graphical representation of the FE simulation results

For each configuration, higher stresses were present on the bone around the peripheral rim of the acetabular cup, with the highest stresses noted at the superior region of the acetabular wall.

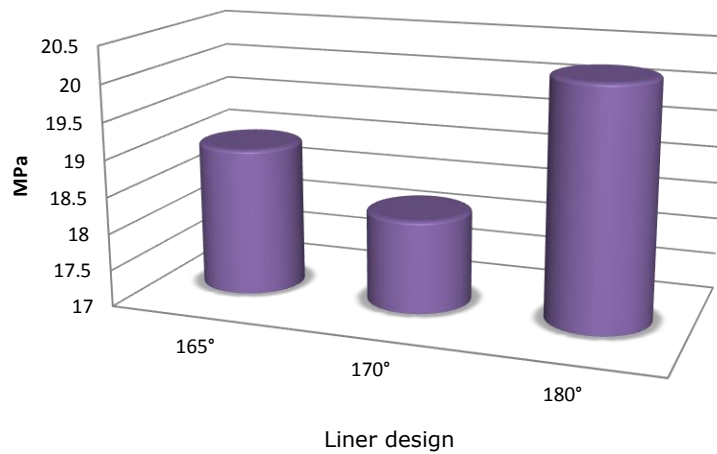


Figure 71. Average peak pressures for the investigated designs in all three load cases

The results show that the difference in the contact pressure between the normal and chamfer models was not substantial in the given orientation of the cup and shell design. Also, the increase of the chamfer angle has a small influence on the maximum contact pressures, although that could be also dependent on the reduction of the polyethylene thickness.

4.3.3. Concluding remarks

In the present study, static simulations of daily activities loads were applied to predict the influence of liner design parameters on contact pressures around acetabular cup implants. The results indicated that chamfered liner profiles have superior biomechanical compatibility with the bone compared to the full hemispherical design that was also tested. The pressure distribution on the acetabular cavity was improved when the chamfered liners were used, which provided lower periprosthetic peak pressures in each of the three considered loading scenarios.

Increasing the chamfer angle for the given design yielded a moderate reduction in the maximum contact pressure peaks between the cup and acetabulum. Accordingly, the maximum contact pressures for the 170° liner design were lower by 9.7% on average and by 6% when using the 165° design, compared with those of the normal hemispherical liner design. Also, with the use of chamfered acetabular liners, a general reduction in contact pressure magnitude was observed, evidenced in Figure 71.

The stress was higher when the hip force increased from 3900N and 4200N. In addition, a high stress area at the anterosuperior acetabular rim was also noted.

The results obtained by the simulations provide details for application in the design considerations that are expected to improve the implant's biomechanical performance, with the aim of achieving more stable fixations. Estimation of hip joint contact pressure during daily activities is useful for both preoperative planning and postoperative rehabilitation.

Because stress-shielding causing the bone adaptation is dependent upon the material and geometrical characteristics of the implant, the liner design can be optimized, in terms of selecting appropriate geometries to produce minimum bone loss, and therefore reduce the risk of implant failure.

Therefore, based on the results of the two computational studies, achieving correct prosthetic component orientation and allow ideal range of motion within the constrained prosthetic impingement limits is vital to operative success.

The optimal design should decrease the pressure at the cup edges and also maintain pressure in the bone at the central part of the acetabulum reducing the stress shielding effect and the likely incidence of bone resorption, and finally increasing the life of the implant.

Future work will involve use of the technique with different cup designs and spatial orientations, and comparison of these designs with conventional, full hemispherical designs, and also development of a dynamic simulation in order to achieve more realistic loading scenarios.

5. MECHANICAL TESTING OF ACETABULAR IMPLANTS

5.1. Introduction

Adequate initial stability of the acetabular cup is essential for stable osseointegration of the implant, as total joint prostheses that do not achieve adequate initial fixation will exhibit micromotion in response to load.

Interference fit or press fit fixation between two parts is achieved by friction after the parts are pushed together. For acetabular fixation, this involves inserting an acetabular component into an undersized prepared acetabulum (underreaming), the primary stability being achieved through the frictional compressive forces generated at the acetabular periphery [66], [71]. Reaming of the acetabulum is a very important factor in THR, as it must penetrate to the bleeding subchondral bone, to ensure the best possible vascularization and bone ingrowth.

Although recommended interference suggests a difference of the diameter between the last used reamer and the finally used cup range from 1 to 3 mm, most acetabular components are implanted with a diametral interference ranging between 1 mm and 2 mm [66], [69].

Given that the use of additional screws was documented to concentrate stresses and allow debris to penetrate the shell, underreaming the acetabular cavity in order to achieve sufficient primary stability is becoming widely preferred. In this case, the oversized implant is positioned in line with the hemispherical prepared acetabulum and impacted using an orthopedic hammer/mallet.

The term press fit describes the use of a prosthetic component larger than the prepared acetabulum, while underreaming and oversized refer to the extent of difference between the two.

The press-fit anchors the cup to the bone in the immediate post-operative period enhancing primary stability while osseointegration guarantees the long-term mechanical stability of the implant.

As biomechanical testing plays an important role in the research, development and validation of orthopaedic implants, our research plan included such mechanical tests in order to better understand the influence of different characteristics in the outcome of press-fit acetabular implants.

Although several studies have evaluated the initial stability of acetabular components, these studies had mainly focused on the size of the prepared acetabulum, surface finish and component design [116], [117], [118].

The aim of this study was to find a balance between the stabilizing effect of the impaction force and the risk of bone damage using mechanical testing and Design of experiments in order to obtain the forces necessary to fully seat the cup and to determine the resulting primary stability of the cups in-vitro, with the purpose of determining the effect of the amount of press fit and the quality of the bone substrate. Research of failure mechanisms and analysis of acetabular components is the best source for generating design improvements.

In order to evaluate new designs a list of requirements is needed, as an acetabular component must be able to restore the functions of the acetabulum.

Understanding this phenomenon may have several clinical implications and help the surgeon to optimize implant stability while preventing bone fractures.

5.2. Validation of polyurethane foams for implant testing

Since cadaveric models are hard to obtain and do not offer the needed uniformity because of the geometry and bone quality, with the goal of providing reproducible results, we decided to use a synthetic material as a substitute for human bone.

There are several studies that confirmed that bone surrogates possess mechanical properties adequate to evaluate the performance of implants and provide similar results to those of cadaveric bone [119], [120], [121].

Shim et. al. [122] concluded that although PU foams have a closed structure, whilst cancellous bone has an open porosity structure, the overall macroscopic structure shows close resemblance.

With the intention to provide a consistent and uniform material with properties similar to those of human cancellous bone to use as a test medium for acetabular components, the PU foams were tested in order to validate their use as synthetic bone surrogate.

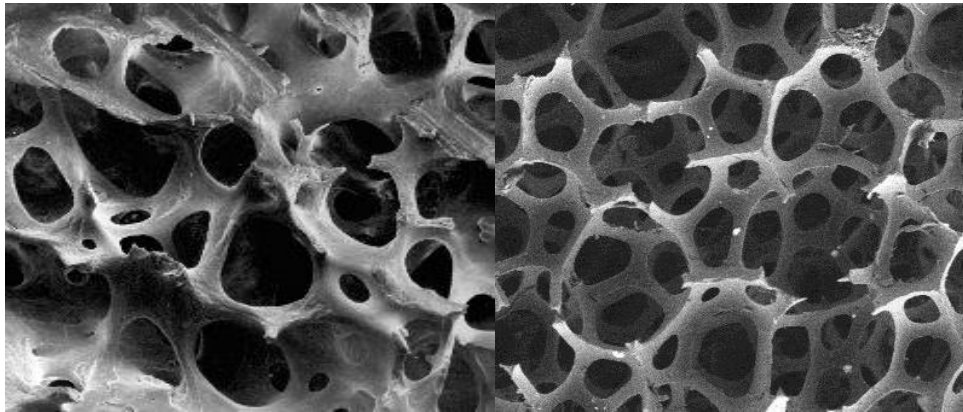


Figure 72. Microstructures of cancellous bone and polyurethane foam [122]

As American Society for Testing and Materials (ASTM) standards recommend the use of polyurethane (PU) foam blocks as bone surrogates for testing orthopedic devices and instruments, and as PU foams can be attained in different densities according to the desired mechanical properties, artificial bone surrogate in form of polyurethane foam blocks were selected [123].

The standard describes the test methodology, compositional, physical, mechanical requirements for rigid unicellular polyurethane foam for use in testing orthopedic devices or instruments.

Even though the main objective of this study is to characterize the influence of geometrical design of acetabular implants, we considered important to correlate it with the influence of various densities of cancellous bone surrogate. Therefore, specimens of PU foams were selected to be in the range of densities similar to those of pelvic cancellous bone.

5.2.1. Methods

Based on the number of experimental trials planned we opted for a commercially available PU foam, the choice was made based on price and shape.

In order to model different types of bone, the foam densities chosen were 0.24 and 0.35 g/cm³, similar to those of medium and normal pelvic cancellous bone [98], [120].

Table 14. Technical properties of the two selected PU foams [124], [125]

Density	ISO845	g/cm ³	0.24	0.35
Shore hardness	ISO868	-	D 25	D 38
Flexural strength	ISO178	MPa	5	9
E-Modulus	ISO178	MPa	150	310
Comp. strength	ISO844	MPa	4	8
Heat distortion temp.	ISO75B	°C	55-60	60

As the aim of the above stated ASTM standard is to provide a method for classifying foams as graded or ungraded based on the physical and mechanical behavior with a given density, the first thing was to check if the foams will pass the acceptance criteria for orthopedic device testing. The grade designation of the standard refers to the nominal density of the foam, in its solid final form, with mechanical requirements for each grade being specified.

Therefore, specimens of PU foams were prepared and their properties were mechanically tested using the methods described in ASTM F1839 standard: D 1622 Test Method for Apparent Density of Rigid Cellular Plastics, F 543 Specification and Test Methods for Metallic Medical Bone Screws.

Table 15. ASTM grade designation with nominal densities

Grade 10	160.2 kg/m ³
Grade 12	192.2 kg/m ³
Grade 15	240.3 kg/m ³
Grade 20	320.4 kg/m ³
Grade 40	640.7 kg/m ³

As the foams were supplied by a reputable producer and in solid final form, the requirements for voids, cracks and non-uniform areas were fulfilled after the preliminary examination.

5.2.2. Determination of foam density

The PU foam boards, now called Foam 1 and 2, were conditioned at $23 \pm 2^\circ$ for 24 hours before testing in accordance with ASTM Standard D1622-03, Standard Test Method for Apparent Density of Rigid Cellular Plastics.

From each PU foam board, three 25.4 by 25.4 by 25.4 mm (1 inch³) specimens were prepared, with a precision of $\pm 0.1\%$.

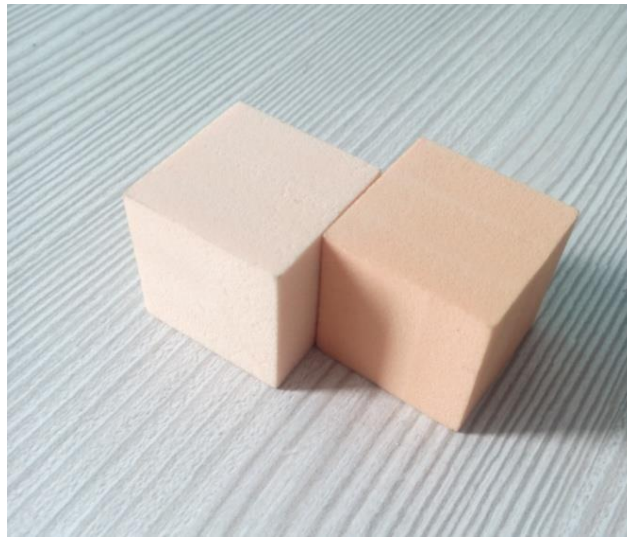


Figure 73. PU foam blocks prepared for density testing

The measurements were made using a Kern PRJ 620-3M precision scale, with an internal calibration and readability of 0.001g, available in the CIDUCOS Testing laboratory. All measurements were made a minimum of three times in order to eliminate user errors.



Figure 74. Kern PRJ620-3M Laboratory balance

The density calculations were made using the following formula:

$$D = \frac{W_s}{V} \quad (5)$$

where: D = density of specimen, kg/m³, W_s = weight of specimen, kg, and V = volume of specimen, m³.

Table 16. Results of the apparent density measurements

		Foam 1	Foam 2
Measurement 1	kg/m ³	252.394	334.166
Measurement 2	kg/m ³	250.258	333.312
Measurement 3	kg/m ³	253.371	334.471
Average	kg/m ³	252.008	333.983
Standard deviation	kg/m ³	1.592	0.601
Coef. of variation	%	0.006	0.002

From the results of the density measurements, we can now designate the tested foams to a specific grade. According to ASTM 1839 criteria, the tested foams are qualified as Grade 15 (224.3-256.3 kg/m³) and Grade 20 (304.4-336.4 kg/m³).

5.2.3. Determination of Compressive Strength

This test was meant to provide information regarding the behavior of cellular materials under compressive loads. The compressive strength was determined using the guideline from ASTM Test Method D 1621, Standard Test Method for Compressive Properties of Rigid Cellular Plastics.

Thus, five specimens, 50.8 by 50.8 by 25.4 mm were prepared from each grade of solid foam, with the thickness of the specimen parallel to the foam rise direction.

Many types of mechanical testing systems are currently in use for the purpose of mechanical and biomechanical testing of a wide variety of materials and systems. In this study, an INSTRON 8874 servo-hydraulic bi-axial testing machine was used for testing [126].



Figure 75. Foam block preparation using a milling machine

In order to apply the load to the specimen as uniformly distributed as possible over the entire loading surface of the specimen, a compression fixture was designed consisting of two flat plates, one acting as a base plate and one attached to the testing machine actuator.

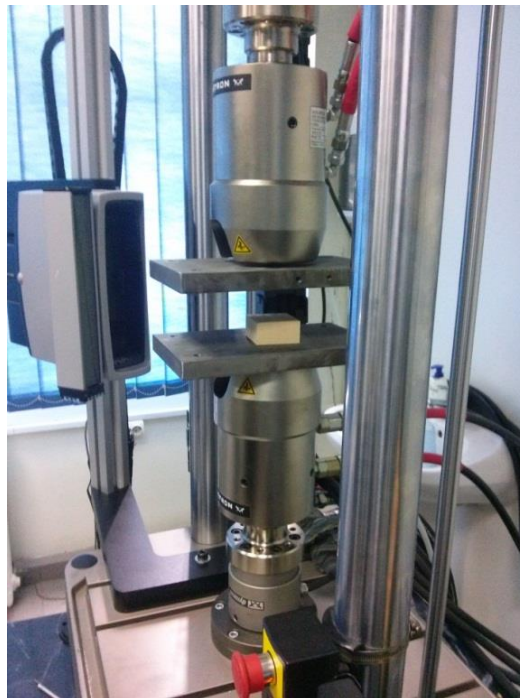


Figure 76. Experimental setup for compression testing

98 Mechanical testing of acetabular implants

The rate of uni-axial movement was defined at 0.25 mm/min for each 25.4 mm, and the total displacement was set at 3 mm. A number of 5 specimens were tested for each grade of PU foam available, Grade 15 (density 224.3-256.3 kg/m³) and Grade 20 (density 304.4-336.4 kg/m³).

The average compressive strength was calculated by dividing the load at yield by the initial horizontal cross-sectional area of the specimens.

The apparent compressive modulus was calculated in a convenient point on the load-deflection curve using the following formula:

$$E_c = WH/AD \quad (6)$$

where: E_c = modulus of elasticity in compression, Pa, W = load, N, H = initial specimen height, m, A = initial cross-sectional area, m², and D = deformation, m. The results are detailed in Table 17.

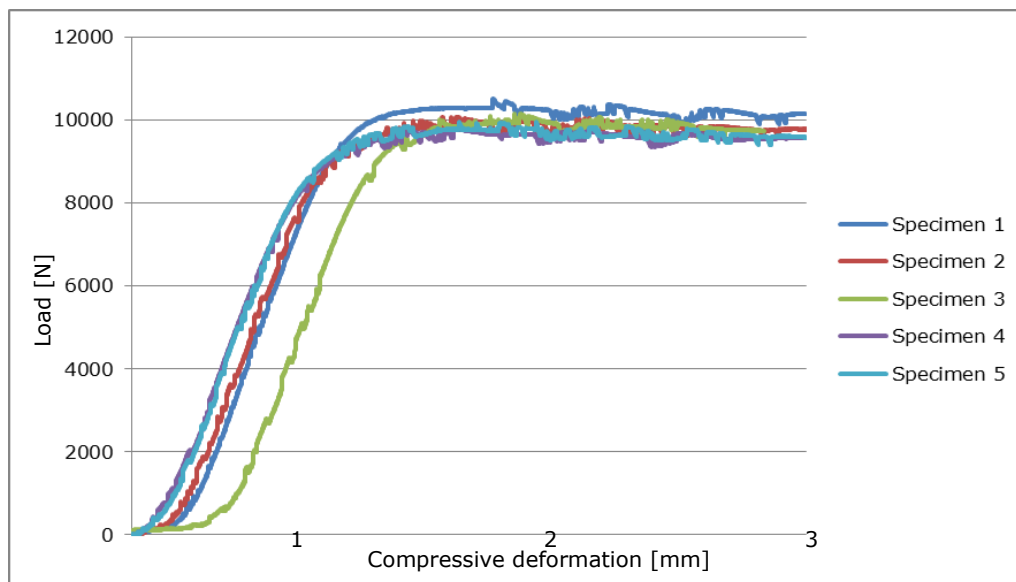


Figure 77. Load-deflection curve for Grade 15 PU foam

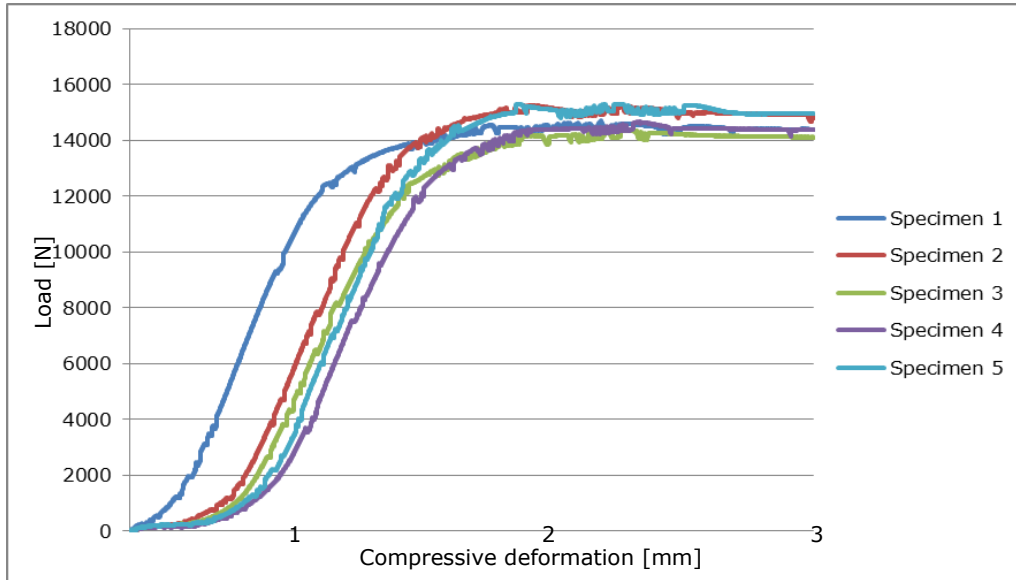


Figure 78. Load-deflection curve for Grade 20 PU foam

Table 17. Compressive strength and modulus results for the tested specimens

	Compressive strength [MPa]		Compressive Modulus [MPa]	
	Grade 15	Grade 20	Grade 15	Grade 20
1	4.07	5.65	148.2	197.2
2	3.90	5.90	146.3	201.3
3	3.93	5.56	168.5	172.6
4	3.79	5.60	141.7	190.2
5	3.85	5.92	145.7	241.5
Average	3.91	5.73	150.0	200.5
St. deviation	0.105	0.171	10.57	25.38
Coef. of variation [%]	0.03	0.03	0.07	0.13

5.2.4. Determination of Screw Pullout Strength

As surgical fracture stabilization often involves the use of bone screws, axial screw pullout is commonly used as a measure of screw fixation strength.

Thus, using to the *Test method for determining the axial pullout strength of medical bone screws* [127] as a guide, five PU foam blocks were prepared for each grade, 50.8 by 50.8 by 25.4 mm in size.

Cortical threaded 4.5mm diameter titanium alloy bone screws were used for grade 20 PU foam testing and 6.5 mm cancellous stainless steel bone screws for

100 Mechanical testing of acetabular implants

grade 15 PU. Pilot holes of 3.2mm were drilled in the center of each foam block using a milling machine at 600 rpm.



Figure 79. Orthopedic screws used in mechanical testing

A pullout fixture was designed in order to enable a quick and safe way to attach the mounted screw to the testing machine actuator, Figure 80. Its inner contour had a negative impression of the head of screw, while its upper portion allowed coupling to the mechanical testing machine, as seen in Figure 81.

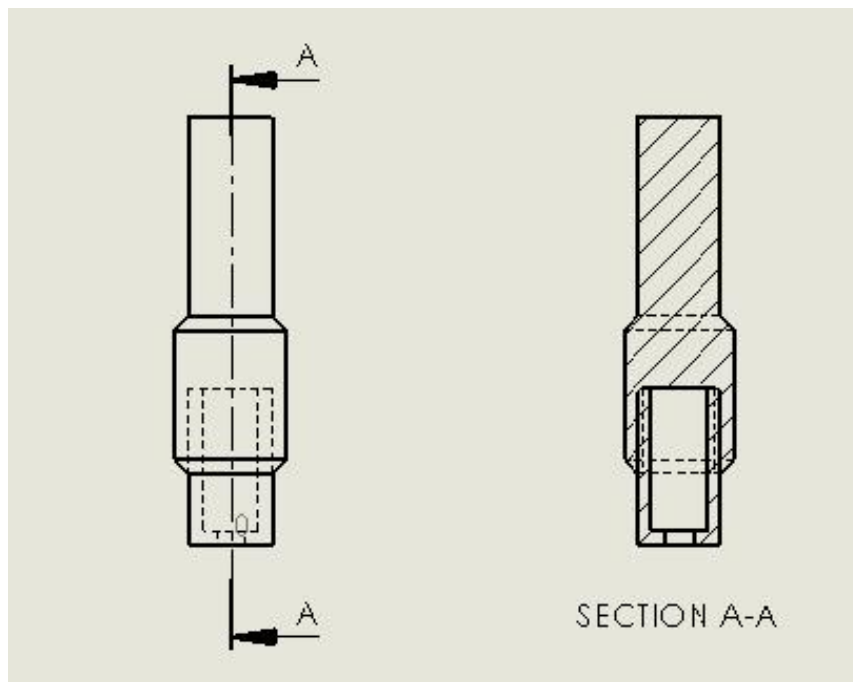


Figure 80. 2D drawing of the designed screw pullout fixture

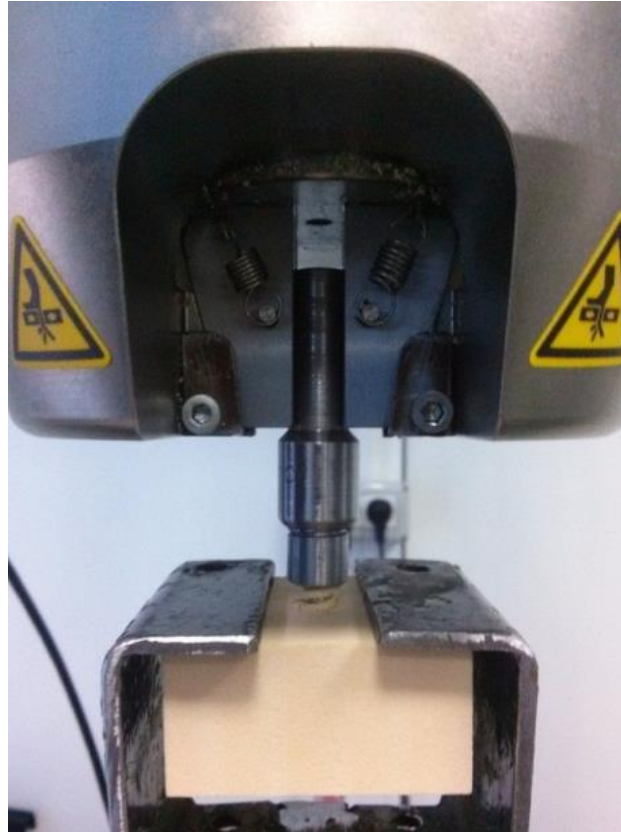


Figure 81. Test apparatus for screw pullout

A test block clamp fixed to the bottom part of the load frame was used to fix the foam blocks during testing. The block clamp was built from steel in order to be sufficiently rigid to support the required loads with minimum deformation.

Each screw was inserted with a manual orthopedic hexagonal screw driver into the foam specimens to a depth of 20 mm.

A tensile load was applied at a rate of 5mm/min until screw failure. Load and displacement values were recorded using the INSTRON data acquisition software, the pullout strength being defined as the maximum load generated prior to screw failure. Five test runs were made for each foam-screw combination.

Furthermore, load versus load fixture displacement curves were recorded on the data acquisition device in order to determine the axial pullout strength of the specimens.

Table 18. Screw pullout strength test results

Specimen	Screw pullout strength (N)	
	Grade 15	Grade 20
1	543.24	670.61
2	524.37	672.14
3	513.88	675.53
4	519.36	685.19
5	514.95	683.15
Average	523.16	677.33
Standard deviation	11.96	6.54
Coef. of variation [%]	0.02	0.01

The mean pullout force correlated with the foam density, being higher in the case of more compact material. The results satisfy the requirements of F1839 standards, 485-675 N for grade 15 foams and 670-800 N pullout strength for grade 20 foams.

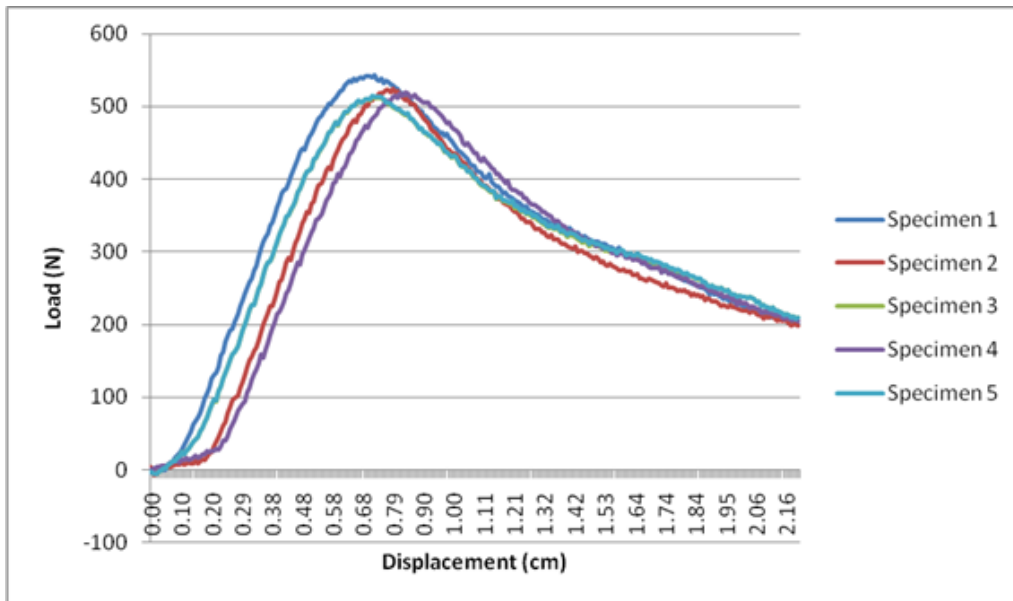


Figure 82. Representative screw pullout load-displacement curves for grade 15 foam

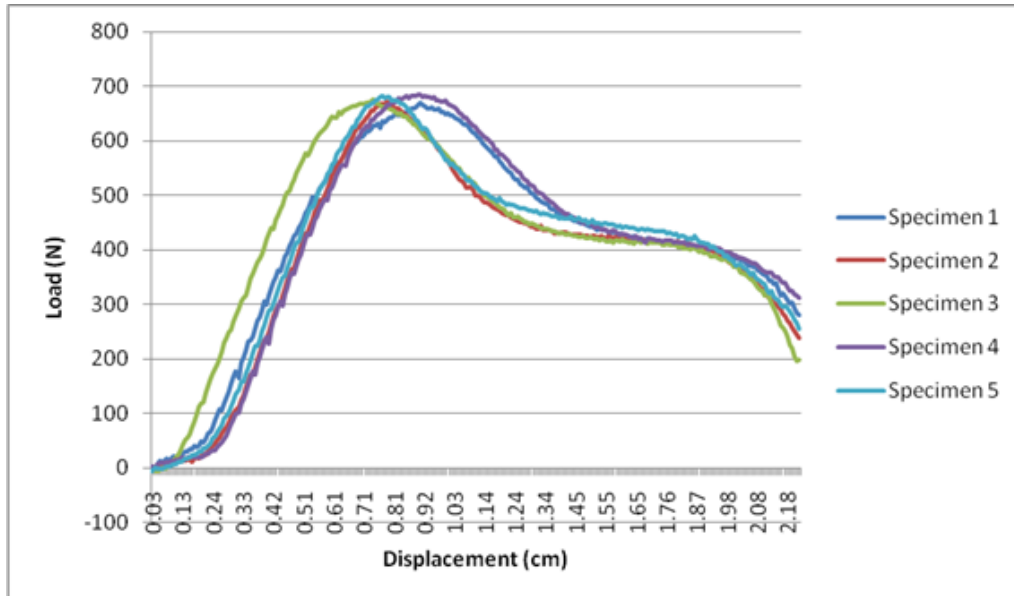


Figure 83. Representative screw pullout load-displacement curves for grade 20 foam

Failure of screw fixation, in both cortical and cancellous, was observed to be caused by the stripping of the internal screw threads within the foam.



Figure 84. Mode of failure for the medical screws

5.2.5. Concluding remarks

This study presented cellular rigid PU foams of two different densities 252 kg/m³ and 334kg/m³.

These samples were examined according to ASTM standards for apparent density, compression and screw pullout strength in order to verify if they are appropriate bone analogues for the range of normal and high quality human cancellous bone and furthermore validate their mechanical properties for their use in mechanical testing of acetabular implants.

As The ASTM F-1839-08 states that "The uniformity and consistent properties of rigid polyurethane foam make it an ideal material for comparative testing of bones screws and other medical devices and instruments.", and, based on the proof that the chosen foams passed the acceptance criteria of this standard, we may conclude that our foams represent an inexpensive substrate that may provide an alternative test medium for human cadaveric bone, providing consistent and uniform test results.

5.3. Mechanical testing of an oversized acetabular component

Even if uncemented fixation technique provides improved component stability and, subsequently, enhanced osseous ingrowth in the cup, impaction of an oversized component requires significant energy, forcing underlying bone to undergo plastic deformation leading to inadequate seating.

One of the major failure modes of cementless acetabular components is the loosening of the acetabular cup, which is mostly attributable to insufficient initial stability.

The level of interference fit during acetabular insertion is critical as insufficient press-fit may cause the acetabular component to be unstable, which leads to aseptic loosening of the implant. Even more, excessive press-fit may cause the occurrence of intra-operative fractures.

Current technique attempts to press fit 1-2 mm of a hemispherical design and only use adjunct screw fixation when necessary as it has been reported that an underreaming of 1-2 mm provides excellent stability while avoiding complications such as incomplete seating or periprosthetic fracture, which may occur during impaction of 3-4 mm oversized acetabular components [66], [69], [71], [128], [129].

Additional factors such as poor bone quality due to age or disease could have an effect on both the initial and the long-term stability of hip replacements as the deterioration of bone mechanical properties and the reduction of bone density could significantly increase the risk of fracture or loosening.

As stated above, a study was conducted to determine the necessary impaction force, and test the stability against edge loading in order to determine the effect of the two variables, amount of underreaming and bone quality and their correlation.

The aim was to determine which configuration of bone density and degree of underreaming can be used to establish a stable contact at the cup-bone interface while using a minimal impaction force.

5.3.1. Materials and methods

To use in the mechanical experiments, the acetabular component of choice was represented by the Atlas-Esop cup of FH Orthopedics, a popular cup with more than 100.000 performed implants worldwide [130].



Figure 85. The Atlas acetabular shell [130]

The ATLAS cups are made from titanium alloy with a constant 2.5 mm thickness, featuring a large central opening in the lower part as well as a slot that provides the elasticity. In addition to the press fit, the Atlas cup is fitted with four spikes that ensure primary stability and rotational resistance, while long-term fixation is accomplished through the use of a plasma-sprayed hydroxyapatite coating, allowing secondary osseointegration.



Figure 86. Radiographic image of an Atlas acetabular component [130]

According to the research of Philippe et al. [131], the Atlas acetabular component has a great survival rate with a revision rate of 90 % at 10 years and 85.5% at 15 years post-op. This cup has a successful clinical history, the implant survivorship at a maximum follow-up of 17 years showed no sign of metallosis or mobilization.

The acetabular cups had an outer diameter of 54mm while the synthetic bone substitute was represented by cylindrical blocks (height 50 and diameter 90), prepared from the above tested PU foams, Grade 15 (224.3-256.3 kg/m³) and Grade 20 (304.4-336.4 kg/m³) to represent a broad range of bone quality.

Each foam block was then reamed using a reamer mounted to a milling machine to ensure accuracy, half to a diameter of 53 and the other half to a diameter of 52, resulting in 1 mm and 2 mm underreaming. Resulted cavities were measured with vernier calipers after reaming to check the diameter.



Figure 87. Test block specimen with prepared acetabular cavity

The PU foam blocks were then secured to a on a closely fitting support base plate on the bottom part of the load frame. The purpose of the holding device is to ensure that the specimen remains stationary during loading, so as to eliminate any movements that could interfere with the motion detection at the bone-implant interface. The base plate was designed to ensure proper alignment and sufficient stability without the use of clamps or screws.

5.3.2. Impaction

The primary stability of an implant is associated with the early postoperative stage before osseointegration of the implant occurs. It is crucial for the long term success of a cementless joint replacement, and depends on factors such as implant design, bone quality and surgical technique.

Intraoperative press-fit insertion of acetabular cups translates to multiple blows applied to an impactor using a mallet until the cup is fully inserted into the prepared cavity. The acetabular shells were seated using custom threaded rod that was designed to engage with the assembly threaded hole of the shell. The assembly enables safe and quick coupling to the INSTRON 8874 load cell.

As a preliminary check, the implant was seated into the prepared cavity with manual control at different speed, in order to evaluate the testing apparatus and insertion conditions.

After preliminary testing, it was decided that a linear speed of 1mm/s was the best fit for this experiment. The displacement speed was chosen in order to ensure structural integrity of the cup, as the number of available cups was limited.

Proper component seating was checked with the use of a circular pressure sensitive sensor applied at the pole of the foam block cavity. These sensors have a low profile, and a high shock resistance, making them the best choice for this given experiment. The sensors were connected to an ohmmeter for data recording, as they work by modifying resistance with respect to load applied.

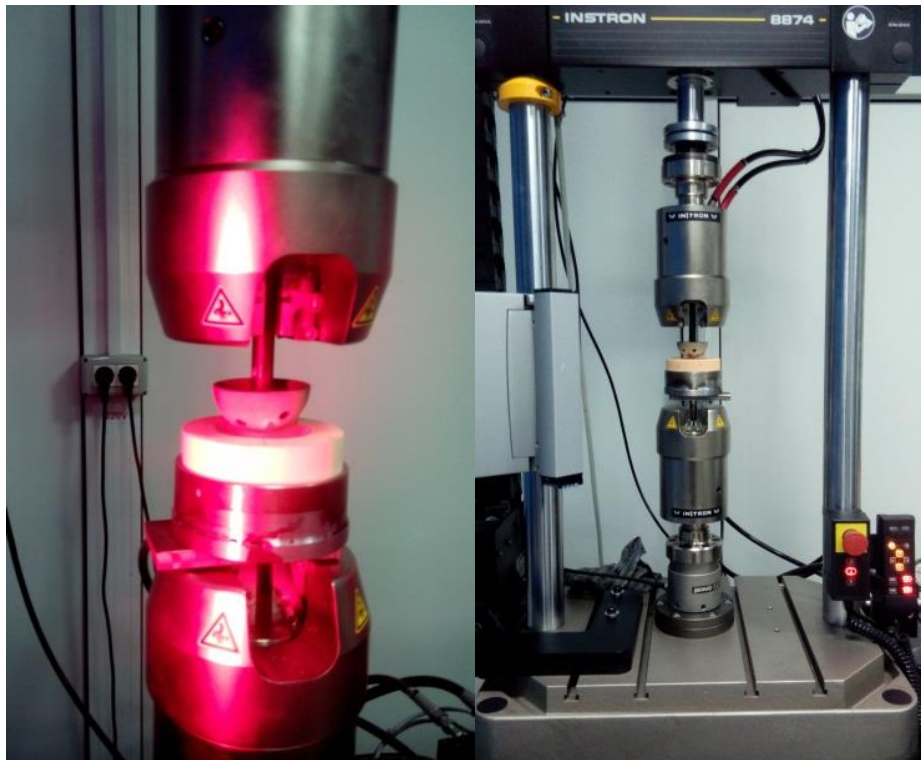


Figure 88. Experimental setup for impact testing

In addition, proper component seating was ensured by defining the start position at the distance equal to the radius of the reamed cavity and using that distance as the amount of displacement of the actuator.

There were two variables for each of the experimental setup: PU foam test block density and degree of underreaming. For each combination of foam density and degree of underreaming, the tests were repeated a minimum of three times, while the applied displacement and insertion load were continuously recorded.

Complete seating with solid fixation was achieved for each of the cups, and line to line contact at the pole of the cavity.

5.3.3. Primary stability

As already mentioned, cementless implants are mechanically stabilized in the host bone at surgery time through a press-fitting procedure. The primary mechanical stability achieved by these implants is critical for the long-term outcomes of the operation. One of the most common causes of failure due to implant dislocation or migration is due to initial instability upon implantation, as osteointegration is possible if the relative stem-bone micromotion is below a certain threshold [61], [132].

In this study, primary stability was defined as the resisting capacity of the fitted uncemented acetabular component to tangential loads, also known as the lever-out.

In order to determine the immediate post-impaction stability of the acetabular component prior to any bone ingrowth, the stability against loads that cause out of plane rotations was investigated by providing an applied load to the rim of the acetabular cup.

The lever-out test simulates the impingement forces generated by the conflict between the prosthetic neck and acetabular component rim (edge). Further motion beyond the impingement point causes subluxation of the femoral head until the joint dislocates, or failure of the acetabular bone fixation. This is resisted by a combination of friction, cup geometry and bone bed properties giving us valuable information about the degree of interference fit obtained with different amount of underreaming and influence of bone quality.



Figure 89. Test setup for rim edge loading

Thus, after complete seating was done, the impaction rod was unthreaded from the acetabular component. The base plate was specifically designed with two alignment holes for the foam clamp, in order to quickly change the setting of the assembly from impaction to lever out.

Linear perpendicular loads were applied to the rim of the acetabular component, opposite to the cup's slot, in order to cause the implant to tip. The failure load was defined by the maximum force required to cause a 3 mm displacement of the edge of the cup.

Each combination of foam density and degree of underreaming underwent the lever-out test at a rate of 3mm/min, while individual force-displacement curves were recorded.



Figure 90. Representation of cup failure (3 mm offset)

5.3.4. Results and discussions

While multiple factors are known to influence seating and stability of acetabular components, the present experiment had the goal to isolate the effect of substrate and degree of underreaming on the load necessary to achieve complete seating and primary stability.

Following mechanical testing, the acetabular cup was removed to have an understanding of the structural integrity of the cup-bone interface after impaction loading. The structural integrity of the bone was maintained in all foam specimens.

The data was evaluated statistically by an analysis of variance using the StatGraphics software. As the data of interest was the peak load in each scenario, a summary of the average peak loads is presented in Table 19. These values were then compared between each other.

Table 19. Mean peak impaction and failure loads for the different tested combinations

	Low density (Grade 15)	High density (Grade 20)
1 mm underreaming		
Impaction force [kN]	15.12	22.29
Lever-out force [kN]	3.41	5.51
2 mm underreaming		
Impaction force [kN]	16.08	24.09
Lever-out force [kN]	3.61	5.91

Increasing the diametral interference also resulted in moderate increases in the impact force. As the data shows, there was no significant difference in the mean peak impaction and failure loads with respect to the degree of underreaming, an average increase of 6.7% for impaction and 6.2% for edge loading for both high and low density foams was determined with the increase of press-fit degree.

Instead, the necessary impaction forces were found to increase significantly with the use of a denser test substrate.

In the higher density foam substrate there we noticed a more notable difference in both impaction tests, where the mean peak load increased with an average of 32.6%, and also in rim loading (38.5%).

These finds correspond to the response surface plots resulted from the statistical study, revealing that the quality of the substrate is the most influential factor in the result of both impaction and lever out test.

Additionally, using DOE response surface plots (

Figure 91), we ran an optimization design that, based on a regression model from the data recorded in vitro, reveals the optimum setting for the given test, thus minimizing the load necessary for complete seating of the cup while maximizing the edge resistance load.

The lower and upper bounds of each design variable in the optimization problem was defined, -1mm to -2mm for press fit and grade 15 to 20 for foam density. The allowable range was then discretized at different levels, from -1 to 1 for each variable, as seen on the x and y axes in

Figure 91.

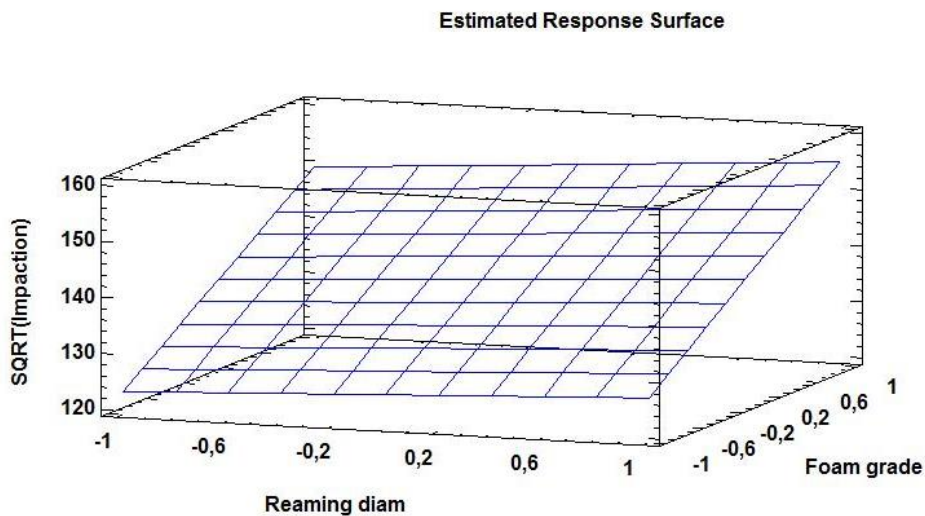


Figure 91. Response surface plot for Impaction

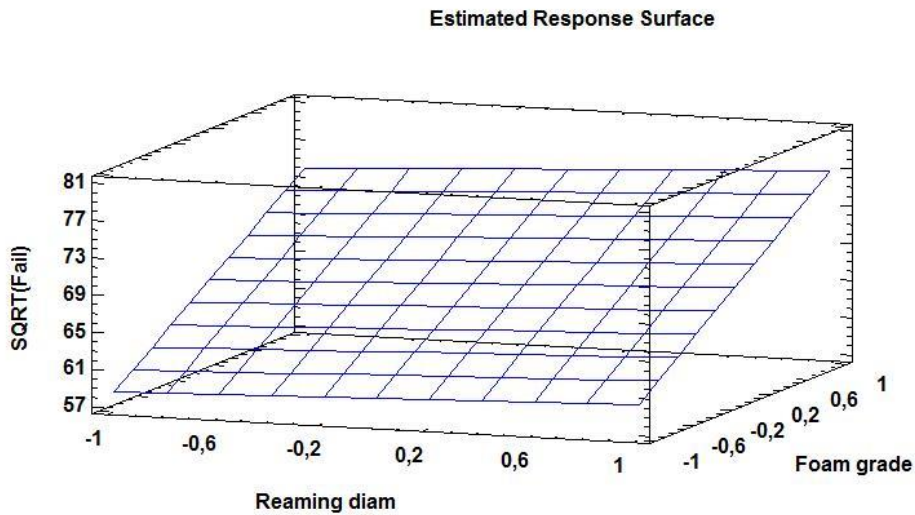


Figure 92. Response surface plot for failure

The problem in dealing with multiple responses (impaction, fail) is that there might be conflicting objectives because of the different requirements of each of the responses.

In order to find a solution that satisfies each of the requirements as much as possible, desirability plots were used, being a useful tool for interpreting the effects on overall response desirability of different combinations of levels of all pairs of independent variables.

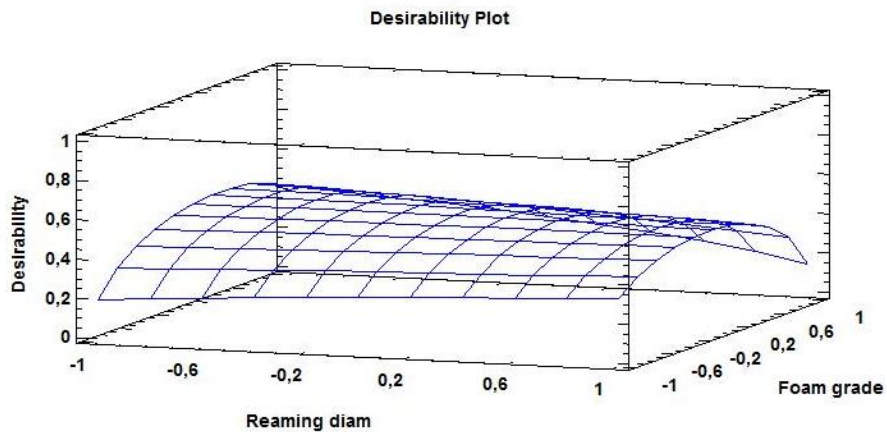


Figure 93. The surface plot graphically showing the effect of pairs of independent variables on the overall response desirability

5.3.5. Concluding remarks

The part of this study concerned the magnitude of the impaction force required to obtain complete seating of the implant and primary stability in varied bone quality substrates and amount of underreaming.

Analysis of variance showed statistically significant differences for all main effects, underreaming and material density.

As expected, the necessary impaction and failure loads were enhanced with the use of a denser substrate. Also, this revealed it to be a much more influential factor than the degree of underreaming.

Consistent with our hypothesis, the amount of underreaming proportionally influences the necessary load in order to properly seat the cup into the prepared acetabulum and component stability, respectively. This is in accordance to MacKenzie et al. and Macdonald et al., who both concluded that a 2mm oversize would be the most stable [70], [71]. An underreaming of 1mm was found to assure sufficient implant stability in high density bone. Even if by the use of a 2mm oversized cup in good quality bone would improve stability, the amount of improvement (6.7%) is lower than the increased load generated at impaction (7.5%) that may increase the risk of acetabular fractures.

The results show that both impaction force and fixation increase as a function of the amount of under-reaming, as well as artificial bone density. The average insertion force for the lower density artificial foam was approximately 15,7kN \pm 7kN, which is well above the magnitudes seen in literature.

Considering that this study assumes the cup to be in place following just one pulse of force application, while the others assumed full cup insertion following multiple pulses of increasing force, the forces needed to insert the cup predicted in this study within the same range of magnitude.

Few studies have been conducted on the peak forces resulted during cup insertion or the, Fritche et al. research found that the average impaction force needed to fully seat a press-fit acetabular cup into artificial bone was 7.5 kN when inserted with a standard 1.2kg surgical hammer [133]. The difference in magnitude of the impaction force may be explained by the use of different density bone substrate; hence the above mentioned study used artificial bone models that simulated osteoporotic and sclerotic bone. Moreover, the use of a continuous load may have amplified the loads compared to impaction using blows applied to a hammer, and the rigid frame may prohibit bone deformations.

In conclusion, the amount of oversizing of the acetabular component is beneficial for the primary stability as long as the quality of the bony substrate is not optimal and the increase of primary fixation overcomes the risks implied by the increase load necessary for proper seating. From a clinical point of view, this experimental results obtained confirm the potential concerns associated with oversizing the acetabular component in relation to the reamed acetabular surface as the use of an oversized cup may need impaction forces difficult to achieve manually, leading to improper seating and increased risk of bone damage.

Thus, the amount of underreaming should be adjusted according to the bone quality of each individual patient.

The study is subject to some limitations. The proposed test substrate was represented by a synthetic bone substitute in order to achieve more uniform results, while loading type was chosen different from other studies in order to protect the limited number of components available.

It is possible that the reuse of components may have led to deformation and subsequently have affected the results. However, these limitations would not affect the conclusion of the study, that bone quality and amount of underreaming affect the impaction and also the primary fixation of the acetabular component.

Furthermore, with the use of an oversized cup, load transfer is expected to be limited to the periphery of the acetabulum, which may ultimately affect the overall implant stability, the ingrowth of bone, the long term load transfer to the bone and bone remodeling process.

Periprosthetic fractures are expected to become a more common mode of failure, as the increase in younger patients undergoing THR results in superior bone quality and the need for extended periods of implant survivorship.

6. CONCLUSIONS AND FUTURE RESEARCH

The research activity carried out during the three years of PhD course in Biomedical engineering was motivated by a great interest in the orthopedic field, a great will to work for providing the surgeons with reliable tools that could make a difference in prosthetic survivorship and a great curiosity to assess the combined effect of variability of the geometrical parameters that would aid to the design of an optimal acetabular implant.

The biomechanics of the hip joint has been of great interest to researchers and clinicians since the early days of anatomical studies as the understanding of biomechanics of Total Hip Replacement (THA) is important since all joint parameters have an influence: joint center, neck angle, offset, lever arms, and the range of motion until impingement. Range of motion and joint stability are decisive issues, especially in younger patients with high expectations on their quality of life after THA.

Clinical success of a primary total joint arthroplasty depends upon developing adequate initial fixation and maintaining the fixation over the long term. Although the clinical results of total joint arthroplasty are usually excellent, some implants develop loosening and require revision.

As the primary stability of cementless acetabular cups depends on different parameters such as component seating, implant design, implant orientation and the bone quality of the patient, the aim of the present thesis was to assess the primary stability of a cementless acetabular component employing computational and experimental methods. Maintaining initial mechanical fixation depends in part on maintaining local bone mass and minimizing bone remodeling.

Adequate primary stability is achieved when mechanical stability of an implant assures low magnitudes of interface micro-motions that can be obtained using oversized acetabular components. However, excessive impaction loads can lead to bone fractures during insertion of the cup.

Thus, a balance should be found between achieving an adequate stability and preventing bone damage.

Although good primary and secondary stability of cementless implants are directly related, altered load distribution can cause bone tissue will be stress-shielded and adapt to the new mechanical conditions, leading to implant failure.

In the present context, the PhD thesis entitled "Prospective study on geometrical parameters of hip prostheses" aims to bring contributions to improve functional characteristics of the acetabular component of THR by studying the characteristic variables of geometrical variables of the hip joint and implant through experimental biomechanical analysis of gait, 3D reconstruction, design, simulation and experimental testing of acetabular components. Among the many factors that may lead to implant failure, the research was focused on the variables that directly involve the development of peri-prosthetic aseptic loosening.

6.1. Conclusions and personal contributions

The overall aim of the PhD research was to computationally and experimentally assess the performance of a uncemented total hip replacement. The project presented methodologies to evaluate implant performance when various geometrical parameters are subjected to uncertainties. While designing the methodologies, limitations of current research have been identified and discussed in each of the chapters.

The **Introduction** chapter supports the topicality and importance of research on hip joint replacement by reviewing the data offered by the national register of arthroplasty. Furthermore, it summarizes the objectives and content of the thesis and briefly describes the research methodology addressed to achieve those objectives.

Chapter 1: Aspects of hip joint structure, pathology and function presents literature review on anatomical and biomechanical aspects of the hip joint. This chapter is consisted on three main goals:

- Provide an overview of the hip joint structure and function, with the focus on bone structure as well as ligaments and muscles involved in hip joint statics and dynamics;
- Conduct a review focused on the description of the main pathological and classification of traumatic disorders causing the necessity of replacing the hip joint;
- Achieve a bibliographic summary on the fundamental concepts of the biomechanical system of the hip joint with the focus on hip joint mobility and gait parameters that may be useful in experimental gait analysis.

Chapter 2: Total hip replacement overview represents a study of the evolution of hip replacement surgery.

It describes the most frequent types of prosthesis classified based on fixation modes as well as the most common alternatives, such as hemiarthroplasty and resurfacing .

A description and classification of the contact bearing materials was realized in order to better understand the advantages and disadvantages of each couple based on frictional and mechanical properties.

The proposed research addressed the clinically relevant issue of implant failure following total hip replacement, as the main post-operative failure reasons are listed in this section along and a review of the literature related to their incidence.

The main focus was on the uncemented THR implants and the event of failure caused by aseptic loosening. Stress shielding caused by the mismatch of elastic modulus between the implant and bone stood out as the most influential factor in the occurrence of component loosening.

Chapter 3: Reliability of gait parameters in gait analysis investigated the effect of anatomic landmarks estimation methods on the angular parameters during three-dimensional gait analysis.

The hip joint center was found to be a fundamental landmark in the identification of lower limb mechanical axis, being the point with respect to which

hip joint moments are calculated. Thus, errors in its location may lead to substantial inaccuracies in both joint reconstruction and gait analysis.

The study describes the methods used for determination of hip joint center, the apparatus and methodology employed in the three-dimensional kinematical analysis.

To accomplish this, the default apparatus method was compared with two other estimation methods: the greater trochanter method that places the HJC at one quarter of the distance from the ipsilateral to the contralateral greater trochanter and the radiographic method.

Using ultrasound based experimental motion analysis methods, angular variation for each flexion-extension, adduction-abduction and rotation of the hip were determined in order to identify those influenced by the HJC location.

Further data analysis consisted of descriptive statistics such as mean and standard deviation (SD) used to characterize the gait cycle, while analysis of variance (ANOVA), data intraclass correlation coefficients (ICCs), Pearson product-moment correlations (r), and Bland and Altman methods were used as estimates of reliability of hip joint center estimation methods.

It was concluded that the most accurate method of locating the hip center was by radiographic measurement.

In order to develop and validate a statistical model, one healthy young volunteer has been involved in the study.

From the resulted data, a straightforward statistical method was developed to correct the initial gait data in order to allow for a better estimation using non-invasive methods. The results of this preliminary study suggest that even though the differences between the three scenarios were not statistically high, there is still room for improvement using simple statistical regression. To assess the accuracy of the resulted method, a new set of data were generated using yielding, in average, an approximately 8% increase of the ICC (0.8-28%), while the mean differences were minimized.

The study provides a brief description of the kinematic analysis protocol and statistical models that may be useful in clinical assessment of joint movements of daily activities. The statistical method provides a non-invasive optimization method for a more accurate estimation of the hip joint center.

Chapter 4: Computational studies on the effect of geometrical parameters on implant performance describes the materials used and the methodology employed for the computational studies.

A three dimensional model of the human hemipelvis was reconstructed from Computer Tomography (CT) scans. The discrete two dimensional images have been converted into 3D volumes using the tools provided by Mimics 10.01 image-processing software.

The model obtained will serve to achieve virtual functional assemblies with various geometrical parameters that will be subject to numerical Finite Element analysis.

The study explains the steps used to generate and validate finite element models suitable for patient specific analysis in order to understand the behavior at the cup-bone interface following total hip acetabular replacement.

The goals of this study were two-fold, to have a complete understanding of the effect of acetabular component orientation during THR, and also asses the influence of acetabular liner design in contact stress pattern and magnitudes.

The first study employed FE simulation to analyze stress patterns and contact pressure distribution within the reconstructed and prepared acetabular cavity under loads that mimic those seen in normal walking.

In addition to 3D reconstruction and FE simulation, the study employs experimental design (DOE) in order to identify the most significant factors for acetabular component behavior and predict the best configuration of acetabular spatial orientation angles within the constraints of the Lewinnek's safe zone in order to minimize peak contact pressures.

Data analysis by response surface method revealed that the magnitude of periacetabular pressures was significantly reduced by the anteversion angle at its lowest value as well as the abduction angle located at the central point value, which corresponded to a 40° abduction and 5° anteversion of cup orientation.

Additionally, a novel mathematical method of implant orientation optimization was developed allowing for ideal acetabular cup positioning to be determined for the specific reconstructed patients joint.

In the second part of the computational study, periacetabular pressures produced by different acetabular liner geometries were analyzed using Finite Element Method. The cup models consist of hemispherical metal shells fitted with normal and different chamfered polyethylene liner geometries, with the same degree of femoral head coverage. Von Mises equivalent stress and contact pressures of at the bone-implant interface were analyzed assessing the effect three different loading scenarios to highlighting the changes caused by implanting in their pattern and magnitude.

The biomechanical role of the chamfer geometry of the acetabular liner was described using a three-dimensional mathematical model. The cup models were loaded to simulate periacetabular pressures during routine activities. It shows that the increase of the chamfer angle contributes to a more uniform articular contact stress distribution and a consequent decrease in the peak contact stress. Based on the results it is suggested that the characteristic chamfered design of acetabular liners optimizes the contact stress distribution in the hip joint.

The results of this study provide information useful for pre-clinical testing of total hip prostheses. In particular, it is of clinical interest to have an understanding of the distribution and magnitude of stresses at the cup-bone interface as a result of varying component orientation, as well as effect of liner design. Adaptive periprosthetic bone remodelling in the acetabular area after uncemented total hip arthroplasty could be reduced using an appropriate component orientation and design.

Future development of the methodology created in this work could be the increase of the refinement of the thresholding used for material segmentation of material properties considered. The model could further be improved through the introduction of anisotropic properties.

Future work will involve use of the technique with different cup designs and spatial orientations, and comparison of these designs with conventional, full hemispherical designs, and also development of a dynamic simulation in order to achieve more realistic loading scenarios.

Chapter 5: Mechanical testing of acetabular implants presented experimental methodologies to evaluate implant performance the role of various parameters on the behavior and stability of the cup. The aim of this experimental study was to assess the most suitable degree of underreaming of the acetabulum in

the implantation of uncemented components, which would generate sufficient fixation without increasing the risk of intra-operative fractures.

Factors such as poor bone quality due to age or disease could influence both the initial and the long-term stability of THA. In such cases, the deterioration and reduction in bone-tissue properties could significantly increase the risk of fracture or loosening.

The aim of the studies presented in this chapter was to develop intra-operative tools that could help the surgeon evaluate the amount of impaction force needed and degree of primary stability achieved by press-fitting of the acetabular component during total hip replacement surgery considering the variability of bone quality.

Therefore, the development of a synthetic bone model replicating the human cancellous bone tissue was highly demanded to provide an easy to get uniform test base. Bone substitutes, composed of Polyurethane foams were tested for two different densities in this study in order to validate their use as analogous to cancellous bone porous structure for mechanical testing. The methodology followed the guidelines of ASTM standards: apparent density, compressive strength and screw pull-out test were conducted.

The results indicated that PU foams of 0.25g-0.34 g/cm³ density, simulating normal and high quality cancellous bone, had fulfilled the desired mechanical properties for the use in testing orthopedic devices and instruments.

In the second part of the study, the material and methodology for the impaction of an oversized acetabular component was described.

Commercially available Atlas acetabular cups were seated with 1 and 2mm of interference fit in reamed polyurethane foam specimens of two different densities. The acetabular shells were seated using a custom threaded rod that was designed to engage with the assembly threaded hole of the shell.

The forces necessary for impaction of the cup to a complete seating were investigated under uniaxial compression test and analyzed to define the effects of degree of underreaming and bone quality.

Subsequently, primary stability of each of the previously fitted implants was investigated by measuring the peak failure load in a tangential lever-out test method as a measure of stability against loads that cause out of plane rotations.

Analysis of variance showed statistically significant differences for all main effects, underreaming and material density.

The results of this chapter suggest that the amount of oversizing of the acetabular component is beneficial for the primary stability as long as the quality of the bony substrate is not optimal and the increase of primary fixation overcomes the risks implied by the increase load necessary for proper seating.

From a clinical point of view, this experimental results obtained confirm the potential concerns associated with oversizing the acetabular component in relation to the reamed acetabular surface as the use of an oversized cup may need impaction forces difficult to achieve manually, leading to improper seating and increased risk of bone damage.

Thus, the amount of underreaming should be adjusted according to the bone quality of each individual patient.

Additionally, using DOE response surface plots, we run an optimization design that, based on a regression model from the data recorded in vitro, reveal the optimum setting for the given test, thus minimize the load necessary for complete seating of the cup while maximizing the edge resistance load.

The degree of under-reaming and bone quality play a significant role in the amount of surface contact and micromotion of the cup at the interface. Increased bone density shows a positive correlation with increasing levels of under-reaming, as well as increasing force needed for cup insertion. This phenomenon is visible throughout loading, and is more pronounced in the case of 2 mm of under-reaming. However, it is interesting to note that approximately the same amount of fixation can be achieved with only 1 mm of under-reaming in conjunction to a more dense bone.

An optimization of the amount of reaming needed can be used clinically giving a better understanding of the reaming characteristics which provide a stable fixation of the acetabular cup while reducing the risk of fractures caused by high impaction forces.

The research presents four main novelties:

- The use of statistical regression technique to develop a correction model for a better definition of anatomical landmarks in three-dimensional gait analysis when using non-invasive estimation methods;
- The thesis focused on both design related, i.e. chamfer degree and amount of component oversize, and non-design parameters such as component orientation and quality of surrounding bone. All of the studied geometrical parameters proved to have a specific influence on implant performance, thus they can be optimized;
- The employment of a full factorial design that allowed the study the effect of each orientation parameter on the response variable, i.e. periprosthetic stress, as well as the effects of interactions between the factors. Furthermore, this method also aided in the reduction of experimental trials and, alongside ANOVA and regression analysis, enabled for prediction and optimization of acetabular component orientation;
- The methodology presented in **Chapter 5** proved to have a great capability to improve the preclinical prediction of implant survival. A combined analysis of the influence of two studied parameters, bone quality and interference fit on primary stability of acetabular components using uniform bone analogues and servo-hydraulic testing machine is unique to biomedical field. If validated, the experimental design proposed could be used to predict the risk of intra-operative bone damage for THR of known bone quality, allowing the surgeon to adjust the degree of component oversizing so that the optimal intraoperative stability is reached and therefore prolong the life of the prosthesis.

6.2. Future development

The aim of the PhD project was to computationally and experimentally assess the performance of cementless acetabular components. The results obtained by the simulations provide details for application in the design considerations that are expected to improve the implant's biomechanical performance, with the aim of achieving more stable fixations.

While the promising qualitative correlations observed experimentally are encouraging, the experimental techniques developed in this study were limited in number due to time and expense considerations. We believe that future improvements to implant performance prediction future studies would benefit from

more elaborate methodologies and extensive mechanical testing in order to increase confidence in the computational findings.

Having performed this specific biomechanical study, there are a number of improvements that can be made to increase the accuracy and relevance of the results:

- Growing of the kinematic data base, including patients of both genders and all ages, and, using non-invasive methods, generate a mathematical formula that would help the examiner to better estimate the position of the joint center;
- Using Finite Element Analysis, the developed model could include various cup designs and spatial orientations and can be subjected to a number of loading conditions that are closer to the physiological state such as dynamic simulations and fatigue tests in order to achieve more realistic loading scenarios;
- As the present research provides a theoretical basis for further optimization of cup geometry, testing of different size and shape implants in order to gain additional biomechanical information on the influence of geometric parameter, knowledge that will prove useful in designing an optimized model.

6.3. Valorisation of research results

The research conducted during the doctoral internship led to the publication of scientific papers in proceedings of international conferences and volumes of journals.

The list of published works by the author of the thesis is:

- [1] **M. Krepelka**, M. Toth-Tascau, "Optimization of acetabular component orientation", AIP Conference Proceedings, vol. 1479, pp. 1091-1094, September 2012.
- [2] M. Toth-Tascau, F. Balanean, **M. Krepelka**, "Assessment and prediction of of inter-joint upper limb movement correlations based on kinematic analysis and statistical regression", AIP Conference Proceedings, vol. 1558, pp. 1648-1651, October 2013.
- [3] M. Toth-Tascau, F. Balanean, **M. Krepelka**, L. Rusu, C. Toader-Pasti, "Computing simulation of the influence of plate design, material, and screw positioning on biomechanical behavior of ulna bone plates", Key Engineering Materials, vol. 583, pp. 115-118, September 2013.
- [4] **M. Krepelka**, M. Toth-Tascau, "Influence of acetabular liner design on periprosthetic pressures during daily activities", Key Engineering Materials, vol. 601, pp. 159-162, March 2014.
- [5] **M. Krepelka**, M. Toth-Tascau, D.I. Stoia, "Reliability of gait parameters depending on HJC estimation method", IFMBE Proceedings, vol. 44, pp. 321-324, 2014.
- [6] M. Toth-Tascau, **M. Krepelka**, "Comparative analysis of deformation field in three customized hip prostheses", 12th International Conference „Research

and Development in Mechanical Industry” Proceedings, Serbia, vol. 1, pp. 7-15, September 2012.

The 6 scientific papers published by the author of the thesis can be summarized as follows:

- 4 papers published in the proceedings of international conferences - ISI Proceedings;
- 1 published papers in proceedings of international conferences - under Springer;
- 1 paper published in the proceedings of international conferences abroad, with review committee without quotation.

REFERENCES

- [1] Romanian Arthroplasty Register. (Online). Accessed 03 21, 2013, at www.rne.ro.
- [2] J Stolk, J., Dormans, K. W., Sluimer, J., Van Reitberger, B., Geesink, R. G., & Huiskes, R. (2004). Is Early Bone Resorption around Non-Cemented THA Cups Related to Stress Shielding? *50th Annual meeting of the Orthopaedic Research Society*. San Francisco.
- [3] Pitto, R. P., Bhargava, A., Pandit, S., & Munro, J. T. (2008). Retroacetabular Stress-shielding in THA. *Clinical Orthopaedics and Related Research*, 353-358.
- [4] Del Schutte, H., Lipman, A. J., Bannar, S. M., Livermore, J. T., Ilstrup, D., & Morrey, B. F. (1998). Effects of acetabular abduction on cup wear rates in total hip arthroplasty. *The Journal of Arthroplasty*, 13(6), 621-626.
- [5] Kennedy, J. G., Rogers, W. B., Soffe, K. E., Sullivan, R. J., Griffen, D. G., & Sheehan, L. J. (1998). Effect of acetabular component orientation on recurrent dislocation, pelvic osteolysis, polyethylene wear, and component migration. *The Journal of Arthroplasty*, 13(5), 530-534.
- [6] D'Lima, D. D., Chen, P. C., & Colwell, C. W. (2001, November). Optimizing Acetabular Component Position to Minimize Impingement and Reduce Contact Stress. *The Journal of bone and joint surgery*, 83(2), 87-91.
- [7] Magee, D. J. (2007). *Orthopaedic physical assessment*. Saunders Elsevier.
- [8] Murray, D. W. (1993). The definition and measurement of acetabular orientation. *The Journal of Bone and Joint Surgery*, 75(2), 228-232.
- [9] Lubowsky, O., Wright, D., Hardisty, M., Kiss, A., Kreder, H., & Whyne, C. (2012). Acetabular orientation: anatomical and functional measurement. *International Journal of Computer Assisted Radiology and Surgery* 7(2), 233-240.
- [10] Shepherd, D. E., & Seedhom, B. B. (1999). Thickness of human articular cartilage in joints of the lower limb. *Annals of the rheumatic diseases*, 58(1), 27-34.
- [11] Drake, R., Vogl, W. A., & Mitchell, A. A. (2005). *Gray's anatomy for students*. Toronto: Elsevier.
- [12] Alter, M. J. (2004). *Science of flexibility-3rd edition*. Human kinetics.
- [13] Johnson, D. H., & Pedowitz, R. A. (2006). *Practical Orthopaedic Sports Medicine and Arthroscopy*. Lippincott Williams & Wilkins.
- [14] Callaghan, J. J., Rosenberg, A. G., & Rubash, H. E. (2006). *The adult hip* (Second ed., Vol. 1). Lippincott Williams & Wilkins.
- [15] Martini, F. H. (2002). *Fundamentals of Anatomy and Physiology* (Fifth ed.). Benjamin-Cummings Publishing Company.
- [16] Nordorthopaedics Clinic. (Online). Accessed 04 09, 2013, at

www.nordorthopaedics.com

- [17] Ito, K., Minka-II, M. A., Leunig, M., Werlen, S., & Ganz, R. (2001). Femoroacetabular impingement and the cam-effect. A MRI-based quantitative anatomical study of the femoral head-neck offset. *The Journal of bone and joint surgery*. British volume, 83(2), 171-176.
- [18] Clinical Sports Medicine. (Online). Accessed 04 09, 2013, at www.clinicalsportsmedicine.com
- [19] Greenspan, S. L., Myers, E. R., Maitland, L. A., Kido, T. H., Krasnow, M. B., & Hayes, W. C. (1994). Trochanteric bone mineral density is associate with type of hip fracture in the elderly. *Journal of bone and mineral research*, 9(12), 1889-1894.
- [20] Cummings, S. R., Kelsey, J., Nevitt, M. C., & O'Dowd, K. J. (1985). Epidemiology of Osteoporosis and Osteoporotic Fractures. *Epidemiologic reviews*, 7(1), 178-208.
- [21] Muller, M. E. (2006). *Müller AO Classification of Fractures. Long bones*. AO Publishing.
- [22] Zuckerman, J. D. (1996). Hip fracture. *The New England Journal of Medicine*, 334, 1519-1525.
- [23] Pagenkopf, E., Grose, A., Partal, G., & Helfet, D. L. (2006). Acetabular Fractures in the Elderly: Treatment Recommendations. *HSS*, 2(2), 161-171.
- [24] Judet, R., Judet, J., & Letournel, E. (1964). Fractures of the acetabulum: Classification and surgical approaches for open reduction. *The Journal of Bone and Joint Surgery*, 46, 1615-1675.
- [25] AO foundation (Online). Accessed 08 12, 2013, at www2.aofoundation.org.
- [26] Berryman Reese, N., & Bandy, W. D. (2009). *Joint Range of Motion and Muscle Length Testing*. Saunders Elsevier.
- [27] Greene, W. B., & Heckman, J. D. (1994). *The clinical measurement of joint motion*. American Academy of Orthopaedic Surgeons.
- [28] Clarkson, H. M. (2005). *Joint Motion And Function Assessment: A Research-based Practical Guide*. Lippincott Williams & Wilkins.
- [29] Pasparakis, D., & Darras, N. (2009). Normal walking Principles, basic concepts, terminology. *EEXOT*, 60(4), 183-194.
- [30] Murray, P. M., Drought, B. A., & Kory, R. C. (1964). Walking Patterns of Normal Men. *The Journal of Bone and Joint Surgery*, 46(2), 335-360.
- [31] Bergmann, G., Deuretzbacher, G., Heller, M., Graichen, F., Rohlmann, A., Strauss, J., et al. (2001). Hip contact forces and gait patterns from routine activities. *Journal of Biomechanics*, 34(7), 859-871.
- [32] Evert Smith (Online). Accessed 10 26, 2014, at www.evertsmith.com.
- [33] Duwelius, P. J., Hartzband, M. A., Burkhart, R., Carnahan, C., Blair, S., Wu, Y., et al. (2010). Clinical results of a modular neck hip system: hitting the "bull's-eye" more accurately. *American journal of orthopedics*, 39(10), 2-6.
- [34] Jones, R. E. (2004). Modular revision stems in total hip arthroplasty. *Clinical orthopaedics and related research*, 420, 142-147.
- [35] Hunter, G., & Long, M. (2000). Abrasive wear of oxidized Zr-2.5Nb, CoCrMo, and Ti-6Al-4V against bone cement. *Sixth World Biomaterials Congress*, (p. 835).

124 References

- [36] Smith & Nephew (Online). Accessed 03 27, 2013, at www.smith-nephew.com.
- [37] Charnley, J. (1960). Anchorage of the femoral head prosthesis to the shaft of the femur. *The Journal of Bone and Joint Surgery*, 42-B, 28-30.
- [38] Majkowski, R. S., Miles, A. W., Bannister, G. C., Perkins, J., & Taylor, G. J. (1993). Bone surface preparation in cemented joint replacement. *The Journal of bone and joint surgery*, 75(3), 459-463.
- [39] Gouldson, S. L., Coathup, M. J., Blun, G. W., & Sood, M. (2006). The effect of cement penetration into bone of lavage with different solutions. *The Journal of bone and joint surgery*, 88-B(Supp III), 368.
- [40] Garellick, G., Malchau, H., & Herberts, P. (2000). Survival of hip replacements. A comparison of a randomized trial and a registry. *Clinical Orthopaedics and Related Research*, 375, 157-167.
- [41] Baumer Orthopedics. (Online). Accessed 06 12, 2013, at www.baumer.com.br.
- [42] DePuy Synthes. (Online). Accessed 10 19, 2012, at www.depuy.com.
- [43] Oh, I., Santer, T. W., & Treharne, R. W. (1985). Total hip acetabular flange design and its effect on cement fixation. *Clinical Orthopaedics and Related Research*, 195, 304-309.
- [44] Shelley, P., & Wroblewski, B. M. (1988). Socket design and cement pressurisation in the Charnley low-friction arthroplasty. *The Journal of bone and joint surgery*, 70, 358-363.
- [45] Parsch, D., Diehm, C., Schneider, S., New, A., & Breusch, S. J. (2004). Acetabular cementing technique in THA—flanged versus unflanged cups, cadaver experiments. *Acta Orthopædica Scandinavica*, 75(3), 269–275.
- [46] Bhattacharya, R., Attar, F. G., Green, S., & Port, A. (2012). Comparison of cement pressurisation in flanged and unflanged acetabular cups. *Journal of Orthopaedic Surgery and Research*, 7(5).
- [47] Huiskes, R., Verdonschot, N., & Nivbrant, B. (1998). Migration, stem shape, and surface finish in cemented total hip arthroplasty. *Clinical Orthopaedics and Related Research*, 335, 103-112.
- [48] Shen, G. (1998). Topic for debate. Femoral stem fixation. *The Journal of bone and joint surgery.Br.*, 80(5), 754-756.
- [49] Stryker. (Online). Accessed 11 12, 2012, at www.stryker.com.
- [50] Zimmer. (Online). Accessed 03 26, 2013, at www.zimmer.com
- [51] Hank, C., Schneider, M., Achary, C., Smith, L., & Breusch, S. (2010). Anatomic stem design reduces risk of thin cement mantles in primary hip replacement. *Archives of orthopaedic and trauma surgery*, 130(1), 17-22.
- [52] Biomet. (Online). Accessed 03 26, 2013, at www.biomet.de.
- [53] Kedgley, A. E., Takaki, S. E., Lang, P., & Dunning, C. E. (2007). The Effect of Cross-Sectional Stem Shape on the Torsional Stability of Cemented Implant Components. *Journal of biomechanical engineering*, 129(3), 310-314.
- [54] Scheerlinck T, C. P. (2006). The design features of cemented femoral hip implants. *The Journal of bone and joint surgery Br.*, 88(11), 1409-1418.
- [55] Dorr, L., Lockett, M., & Conaty, J. (1990). Total hip arthroplasties in patients younger than 45 years. *Clinical Orthopaedics and Related Research*, 260, 215-219.

- [56] Joshi, A., Porter, M., Trail, I., Hunt, L., Murphy, J., & Hardinge, K. (1993). Long-term results of Charnley low-friction arthroplasty in young patients. *The Journal of Bone and Joint Surgery Br.*, 75(4), 616-623.
- [57] Daras M, M. W. (2009). Total hip arthroplasty in young patients with osteoarthritis. *American Journal of Orthopedics*, 38(3), 125-129.
- [58] Rothman, R., & Cohn, J. (1990). Cemented versus cementless total hip arthroplasty. A critical review. *Clinical Orthopaedics and Related Research*, 254, 153-169.
- [59] Albrektsson, T., Brånemark, P., Hansson, H., & Lindström, J. (1981). Osseointegrated titanium implants. Requirements for ensuring a long-lasting, direct bone-to-implant anchorage in man. *Acta Orthopædica Scandinavica*, 52(2), 155-170.
- [60] Pilliar, R. M., Lee, J. M., & Maniopoulos, C. D. (1986). Observations on the Effect of Movement on Bone Ingrowth into Porous-Surfaced Implants. *Clinical Orthopaedics and Related Research*, 208, 108-113.
- [61] Engh, C., O'Connor, D., Jasty, M., McGovern, T., Bobyn, J., & Harris, W. (1992). Quantification of implant micromotion, strain shielding, and bone resorption with porous-coated anatomic medullary locking femoral prostheses. *Clinical Orthopaedics and Related Research*, 285, 13-29.
- [62] MacDonald, S. J., McCalden, R. W., Bourne, R. B., & Barrack, R. L. (2010). Proximally Versus Fully Porous-coated Femoral Stems. A Multicenter Randomized Trial. *Clinical Orthopaedics and Related Research*, 468, 424-432.
- [63] Khanuja, H. S., Vakil, J. J., Goddard, M. S., & Mont, M. A. (2011). Cementless Femoral Fixation in Total Hip Arthroplasty. *The Journal of Bone and Joint Surgery Am.*, 93, 500-509.
- [64] Engh, C., & Massin, P. (1989). Cementless total hip arthroplasty using the Anatomic. *Clinical Orthopaedics and Related Research*, 249, 141-158.
- [65] Whiteside, L., & Easley, J. (1989). The effect of collar and distal stem fixation on. *Clinical Orthopaedics and Related Research*, 239, 145-153.
- [66] Adler, E., Stuchin, S., & Kummer, F. (1992). Stability of press-fit acetabular cups. *Journal of Arthroplasty*, 7(3), 295-301.
- [67] Perona, P., Lawrence, J., Paprosky, W., Patwardhan, A., & Sartori, M. (1992). Acetabular micromotion as a measure of initial implant stability in primary hip arthroplasty. An in vitro comparison of different methods of initial acetabular component fixation. *Journal of Arthroplasty*, 7(4), 537-547.
- [68] Zilkens, C., Djalali, S., Bittersohl, B., Kälicke, T., Kraft, C., Krauspe, R., et al. (2011). Migration pattern of cementless press fit cups in the presence of stabilizing screws in total hip arthroplasty. *European Journal of Medical Research*, 16(3), 127-132.
- [69] Curtis, M., Jinnah, R., Wilson, V., & Hungerford, D. (1992). The initial stability of uncemented acetabular components. *The Journal of Bone and Joint Surgery Br*, 74(3), 372-376.
- [70] Macdonald, W., Carlsson, L., Charnley, G., & Jacobsson, C. (1999). Press-fit acetabular cup fixation: principles and testing. *Proceedings of the Institution of Mechanical Engineers*, Part H, 213(1), 33-39.
- [71] MacKenzie, J., Callaghan, J., Pedersen, D., & Brown, T. (1994). Areas of contact and extent of gaps with implantation of oversized acetabular

- components in total hip arthroplasty. *Clinical Orthopaedics and Related Research*, 298, 127-136.
- [72] Ries, M., Salehi, A., & Shea, J. (1999). Photoelastic analysis of stresses produced by different acetabular cups. *Clinical Orthopaedics and Related Research*, 369, 165-174.
- [73] Smith, S., & Harris, W. (1997). Total hip arthroplasty performed with insertion of the femoral component with cement and the acetabular component without cement: ten- to thirteen-year results. *The Journal of Bone and Joint Surgery Am.*, 79(12), 1827-1833.
- [74] Noble, P., Paravic, V., & Ismaily, S. (2002). Are big heads the solution to dislocation after total hip replacement? *48th Annual Meeting of the Orthopaedic Research Society*.
- [75] Levine, B. R., Meere, P. A., Di Cesare, P. E., & Zucherman, J. D. (2007). *Hip Fractures Treated by Arthroplasty*. In J. J. Callaghan, A. G. Rosenberg, & H. E. Rubash (Eds.), *The Adult Hip* (2nd ed.). Lippincott Williams & Wilkins.
- [76] Blackley, H. R., Davis, A. M., Hutchison, C. R., & Gross, A. E. (2001). Proximal femoral allografts for reconstruction of bone stock in revision arthroplasty of the hip. A nine to fifteen-year follow-up. *The Journal of Bone and Joint Surgery Am.*, 83(3), 346-354.
- [77] Malchau, H., & Herberts, P. (1996). *Prognosis of Total Hip Replacement*. American Academy of Orthopedic Surgeons. Atlanta.
- [78] Furnes, O., Lie, S. A., Espehaug, B., & Vollset, S. A. (2001). Hip disease and the prognosis of total hip replacements. A review of 53,698 primary total hip replacements reported to the Norwegian Arthroplasty Register. *The Journal of Bone and Joint Surgery*, 83(4), 579-586.
- [79] Tillmann, B. (1978). A contribution to the functional morphology of articular surfaces. *Normale und pathologische anatomie*, 34, 1-50.
- [80] Huiskes, R., Weinans, H., & Dalstra, M. (1989). Adaptive bone remodeling and biomechanical design considerations for noncemented total hip arthroplasty. *Orthopedics*, 1255-1267.
- [81] Manley, M. T., Ong, K. L., & Kurtz, S. M. (2006). The Potential for Bone Loss in Acetabular Structures Following THA. *Clinical orthopaedics and related research*, 246-253.
- [82] DeLisa, J. A. (1998). *Gait Analysis in the Science of Rehabilitation*. U.S. Department of Veterans Affairs, Veterans Health Administration, *Rehabilitation Research and Development Service*.
- [83] Oberg, T., Karsznia, A., & Oberg, K. (1994). Joint angle parameters in gait : Reference data for normal subjects: 10-79 years of age. *Journal of Rehabilitation Research and Development*, 31(3), 199-213.
- [84] Kirtley, C. (2006). *Clinical Gait Analysis, Theory and Practice*.
- [85] Benoit, D. L., Ramsey, D. K., Lamontagne, M., Xu, L., Wretenberg, P., & Renstrom, P. (2006). Effect of skin movement artifact on knee kinematics during gait and cutting motions measured in vivo. *Gait & Posture*, 24(2), 152-164.
- [86] Leardini, A., Chiari, L., Della, C. U., & Cappozzo, A. (2004). *Human movement analysis using stereophotogrammetry* Part 3. Soft tissue artifact assessment and compensation. *Gait & Posture*, 21(2), 212-225.

- [87] Loudon, J. K. (Online). Accessed 04 15, 2014, at <http://pdfmanual4.com>
- [88] Seidel, G. K., Marchinda, D. M., Dijkers, M., & Soutas-Little, R. W. (1995). Hip joint center location from palpable bony landmarks- a cadaver study. *Journal of Biomechanics*, 28(8), 995-998.
- [89] Kirkwood, R. N., Culham, E. G., & Costigan, P. (1999). Radiographic and non-invasive determination of the hip joint center location: effect on hip joint moments. *Clinical Biomechanics*, 14(4), 227-235.
- [90] Bell, A. L., Pedersen, D. R., & Brand, R. A. (1990). A comparison of the accuracy of several hip center location prediction methods. *Journal of Biomechanics*, 23(6), 617-621.
- [91] O'Connor, K. M., & Weinhandl, J. T. (2010). Hip joint movements using a greater trochanter method of locating the hip joint center. *Conference Proceedings of the Annual Meeting of the American Society*, (pp. 252-253).
- [92] Zebris CMS-HS: Operating Instructions.
- [93] RadiAnt. (Online). Retrieved from www.radiantviewer.com.
- [94] Shrout, P. E., & Fleiss, J. L. (1979). Intraclass correlations: uses in assessing rater reliability. *Psychological Bulletin*, 36, 420-428.
- [95] Bland, M. J., & Altman, D. G. (1986). Statistical methods for assessing agreement between two methods of clinical measurement. *The Lancet*, 327(8476), 307-310.
- [96] McGraw, K. O., & Wong, S. P. (1996). Forming inferences about some intraclass correlation coefficients. *Psychological Methods*, 1(1), 30-46.
- [97] Dutch Arthroplasty Register. Accessed 4 22, 2014 at www.lroi.nl.
- [98] Wright, J. M., Pellicci, P. M., Salvati, E. A., Ghelman, B., Roberts, M. M., & Koh, J. L. (2001). Bone Density Adjacent to Press-Fit Acetabular Components: A prospective analysis with quantitative computed tomography. *The Journal of Bone and Joint Surgery*, 529-536.
- [99] Schmidt, R., Muller, L., Kress, A., Hirschfelder, H., Ablas, A., & Pitto, R. P. (2002). A computer tomography assessment of femoral and acetabular bone changes after total hip arthroplasty. *International Orthopaedics*, 26, 299-302.
- [100] Schmidt, R., Kress, A. M., Nowak, M., Forst, R., Nowak, T. E., & Mueller, L. A. (2012). Periacetabular cortical and cancellous bone mineral density loss after press-fit cup fixation: a prospective 7-year followup. *The Journal of Arthroplasty*, 27(7), 1358-1363.
- [101] Krepelka, M., & Toth-Taşcău, M. (2012). Optimization of acetabular component orientation using DOE . *AIP Conference Proceedings*, 1479, 1091-1094.
- [102] Krepelka, M., & Toth-Taşcau, M. (2013). Influence of acetabular liner design on periprosthetic pressures during daily activities. *14th Symposium on Experimental Stress Analysis and Materials Testing*. Timisoara.
- [103] Gondi, G., Robertson, J. R., Ganey, T. M., Shahriari, A., & Hutton, W. C. (1997). Impingement After Total Hip Arthroplasty Related to Prosthetic component Selection and Range of Motion. *Journal of the Southern Orthopaedic Association*, 6(4), 266-272.
- [104] Zvartele, R. E., Olsthoorn, P. G., Poll, R. G., Brand, R., & Doets, H. C. (2008). Primary total hip arthroplasty with a flattened press-fit acetabular component

128 References

- in osteoarthritis and inflammatory arthritis: a prospective study on 416 hips with 6–10 years follow-up. *Archives of Orthopaedic and Trauma Surgery*, 128(12), 1379-1386.
- [105] Lewinnek, G. E., Lewis, J. L., Tarr, R., Compere, C. L., & Zimmerman, J. R. (1978). Dislocations after total hip replacement arthroplasties. *The Journal of Bone and Joint Surgery Am.* 60, 217-220.
- [106] Kirk, R. (2009). *Experimental design*. In The Sage handbook of quantitative methods in psychology (pp. 23-46). London: SAGE Publications.
- [107] Bergmann, G., Graichen, F., Rohlmann, A., Bender, A., Heinlein, B., Duda, G. N., et al. (2010). Realistic loads for testing hip implants. *Bio-medical Materials and Engineering* 20(2), 65-75.
- [108] Cilingir, A. C., Ucar, V., & Kazan, R. (2007). Three-Dimensional Anatomic Finite Element Modelling of Hemi-Arthroplasty. *Trends in Biomaterials and Artificial Organs*, 21(1), 63-72.
- [109] Box, G., & Wilson, K. (1951). On the Experimental Attainment of Optimum Conditions. *Journal of the Royal Statistical Society*, B13(1), 1-45.
- [110] Hayes, W. C., & Bouxsein, M. L. (1997). *Biomechanics of cortical and trabecular bone: Implications for assesment of fracture risk*. In Basic Orthopaedic Biomechanics (2 ed.). Philadelphia: Lippincott-Raven.
- [111] Hodge, W. A., Fijan, R. S., Carlson, K. L., Burgess, R. G., Harris, W. H., & Mann, R. W. (1986). Contact pressures in the human hip joint measured in vivo. *Proceedings of the National Academy of Sciences*, 83, pp. 2879-2883.
- [112] McCollum, D. E., & Gray, W. J. (1990). Dislocation after total hip arthroplasty. Causes and prevention. *Clinical Orthopaedics and Related Research*, 261, 159-170.
- [113] Krushell, R. J., Burke, D. W., & Harris, W. H. (1991). Elevated-rim acetabular components. Effect on range of motion and stability in total hip arthroplasty. *The Journal of Arthroplasty*, 6, 53-58.
- [114] Cobb, T. K., Morrey, B. F., & Ilstrup, D. M. (1996). The elevated-rim acetabular liner in total hip arthroplasty: Relationship to Postoperative Dislocation. *The Journal of Bone and Joint Surgery*, 78(1), 80-86.
- [115] Steele, G. D., Fehring, T. K., Odun, S. M., Dennon, A. C., & Nadaud, M. C. (2011). Early Failure of Articular Surface Replacement XL Total Hip Arthroplasty. *The Journal of Arthroplasty*, 14-18.
- [116] Olory, B., Havet, E., Gabrion, A., Vernois, J., & Mertl, P. (2004). Comparative in vitro assessment of the primary stability of cementless press-fit acetabular cups. *Acta Orthopaedica Belgica*, 70, 31-37.
- [117] Ries, M. D., & Harbaugh, M. (1997). Acetabular strains produced by oversized press fit cups. *Clinical Othopaedics and Related Research*, 334, 276-281.
- [118] Antoniadou, G., Smith, A. J., Deakin, A. H., Wearing, S. C., & Sarungi, M. (2013). Primary stability of two uncemented acetabular components of different geometry: hemispherical or peripherally enhanced?. *Bone & Joint Research*, 2(12), 264-269.
- [119] Patel, P. S., Sheperd, D. E., & Hkins, D. W. (2008). Compressive properties of commercially available polyurethane foams as mechanical models for osteoporotic human cancelous bone. *BMC Musculoskeletal Disorders*(9), 137.

- [120] Mehmanparast, H. N., Mac-Thiong, J. M., & Petit, Y. (2012). Compressive Properties of a Synthetic Bone Substitute for Vertebral Cancellous Bone. *International Journal of Medical and Biological Sciences*, 6, 287-290.
- [121] Calgar, Y. S., Torum, F., Pait, T. G., Hogue, W., Bozkurt, M., & Ozgen, S. (2005). Biomechanical comparison of inside-outside screws, cables, and regular screws, using a sawbone model. *Neurosurgical review*, 28(1), 53-58.
- [122] Shim, V., Boheme, J., Josten, C., & Anderson, I. (2012). *Use of Polyurethane Foam in Orthopaedic Biomechanical Experimentation and Simulation*. (D. F. Zafa, Ed.)
- [123] ASTM F1839 – 08. (2012). *Standard specification for rigid polyurethane foam for use as a standard material for testing orthopedic devices and instruments*.
- [124] SikaBlock M440 model board technical data sheet (2012).
- [125] SikaBlock M330 model board technical data sheet (2010).
- [126] Instron. (Online). Accessed 05 15, 2014, at www.instron.com/en.
- [127] ASTM F543-02. (2002). *Standard Specification and Test Methods for Metallic Medical Bone Screws*.
- [128] Kim, Y. S., Callaghan, J. J., Ahn, P. B., & Brown, T. D. (1995). Fracture of the acetabulum during insertion of an oversized hemispherical component. *The Journal of Bone and Joint Surgery*, 77(1), 111-117.
- [129] Sharkley, P. F., Hozak, W. J., Callaghan, J. J., Kim, Y. S., Berry, D. J., Hanssen, A. D., et al. (1999). Acetabular fracture associated with cementless acetabular component insertion: a report of 13 cases. *The Journal of Arthroplasty*, 14(4), 426-431.
- [130] Fournitures Hospitalieres. (Online). Accessed 01 24, 2014, at www.fhorthopedics.com.
- [131] Philippe, M., & Ameil, M. (2007). Survival analysis at 10 years of a cohort of 297 atlas total hip prostheses. *European Journal of Orthopaedic Surgery & Traumatology*, 17(6), 573-578.
- [132] Soballe, K. (1993). Hydroxyapatite ceramic coating for bone implant fixation: Mechanical and. *Acta Orthopaedica Scandinavica*, 255, 1-58.
- [133] Fritsche, A., Zeitz, C., Teufel, S., Kolp, S., Tokar, I., Mauch, C., et al. (2011). In-vitro and in-vivo investigations of the impaction and pull-out behavior of metal backed acetabular cups. *The Journal of Bone and Joint Surgery Br.*, 93, 406.
- [134] DePuy Synthes. (Online). Accessed 06 12, 2013, at <http://www.depuy.com/uk>.